

Imaging and Analysis Of The Immunological Synapse Formed
Between CD4⁺ T Lymphocytes And Antigen Presenting Cells

by

Scott Allen Wetzel

A DISSERTATION

Presented to the Department of Molecular Microbiology and Immunology

and the Oregon Health Sciences University

School of Medicine

in partial fulfillment of

the requirements for the degree of

Doctor of Philosophy

December 2001

Imaging and Analysis Of The Immunological Synapse Formed
Between CD4⁺ T Lymphocytes And Antigen Presenting Cells

by

Scott Allen Wetzel

A DISSERTATION

Presented to the Department of Molecular Microbiology and Immunology

and the Oregon Health Sciences University

School of Medicine

in partial fulfillment of

the requirements for the degree of

Doctor of Philosophy

December 2001

School of Medicine
Oregon Health & Science University

CERTIFICATE OF APPROVAL


This is to certify that the Ph.D. thesis of

Scott Allen Wetzel


has been approved



Dr. David J. Hinrichs, Ph.D., Committee Chair



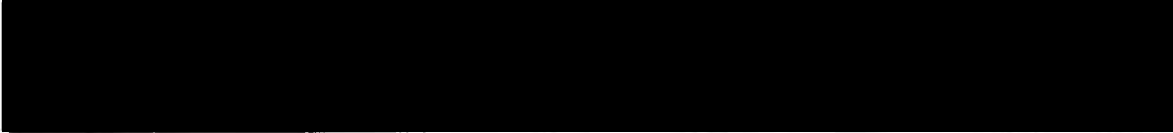
Dr. Ann B. Hill, M.D., Ph.D.



Dr. Michael P. Davey, M.D., Ph.D.



Dr. David C. Parker, Thesis Advisor



Dr. Rich A. Maurer, Ph.D., Associate Dean of Graduate Studies

Table of Contents

Table of Contents	i
Acknowledgements	v
Abstract	vi
CHAPTER 1: INTRODUCTION	1
T Cell Activation: T Cell Receptor Triggering	1
<i>TCR Mediated Intracellular Signaling</i>	1
TCR Triggering	3
<i>TCR Triggering: Conformational Change Model</i>	4
<i>Receptor Aggregation Models: Serial Triggering</i>	4
<i>Receptor Aggregation Models: Topology</i>	5
<i>Receptor Aggregation Models: Kinetic Proofreading</i>	6
Costimulation	6
<i>Anergy</i>	7
<i>Costimulation Via B7/CD28 Interactions</i>	9
<i>CD28-Mediated Intracellular Signaling</i>	10
<i>CD28 And The Actin Cytoskeleton</i>	11
<i>ICAM-1 Costimulation</i>	12
<i>Costimulatory Requirements Of Naive And Effector T Cells</i>	13
Microscopy of T Cell – Antigen Presenting Cell Interactions	14
<i>T Cell Morphological Changes Up-On Antigen Recognition</i>	14

<i>Supramolecular Activation Complexes (SMACS) And The Immunological Synapse</i>	14
<i>Formation Of The Immunological Synapse</i>	17
<i>Topology Model</i>	17
<i>Lipid Raft Accumulation</i>	18
<i>Costimulation And The Immunological Synapse</i>	18
Rationale	20
CHAPTER 2: MATERIALS AND METHODS	22
Animals	22
Antibodies	23
Antigen Presenting Cell Generation	23
<i>Cells</i>	23
<i>Plasmids</i>	24
<i>Transfections</i>	25
<i>In Vitro</i> T Cell Priming	26
Fura-2 Loading	27
Anergy Induction	27
Measurement Of T Cell Proliferation	28
Measurement Of T Cell Activation By Flow Cytometry	28
MICROSCOPY	29
<i>Signaling Inhibitors</i>	29
<i>Cytoskeletal Inhibitors</i>	29
<i>Live Cell Microscopy</i>	29
<i>Fixed Conjugate Microscopy</i>	30
CHAPTER 3: RESULTS	33
APC Characterization	33
Synapse Formation Is A Dynamic Process	40
The Role Of The Cytoskeleton In Synapse Formation	46
Movement Of The Synapse With T Cell Migration	48

MHC Capture From The Synapse	50
Stoichiometry Of T:APC Interactions	58
Signaling And The Synapse	61
Peptide Specificity	69
Effect Of Costimulation Blockade On Synapse Formation	75
Anergic T Cell Synapses	88
CHAPTER 4: DISCUSSION	100
Synapse Formation Is A Dynamic Process	105
T Cell Movement Across APC And MHC Transfer	109
Stoichiometry Of T-APC Interactions	115
Intracellular Signaling And Synapse Formation	116
Peptide Specificity Of The Immunological Synapse	120
The Role Of Costimulation In Synapse Formation	124
Anergic T Cell Synapses	130
CHAPTER 5: SUMMARY AND FUTURE DIRECTIONS	135
References	140

MHC:peptide is unclear, but there is preferential survival of these T cells in culture.

I have used this system to examine several additional facets of immunological synapse formation. Using antibodies to block ICAM-1/LFA-1 interactions or soluble CTLA-4Ig to block CD28/B7-1 (CD80) interactions, I have shown that costimulation is essential in the formation of a mature immunological synapse. When costimulation is blocked, the morphology of the clustered MHC is altered and the amount of MHC:peptide complexes, as well as the size of the MHC:peptide clusters, is significantly reduced. These reductions correlate with reductions in T cell proliferation seen under the same blocking conditions. Interestingly, when T cells are rendered anergic by stimulation through the TCR in the absence of costimulation, they subsequently form mature immunological synapses with normal MHC accumulation, ICAM-1 and PKC θ distribution. However, at anergic synapses there is preferential accumulation of c-Cbl, a known negative regulator of TCR signaling.

Finally, I have examined the peptide specificity of the MHC:peptide complexes accumulated within the mature immunological synapse. Unlabeled wild type MHC molecules on the surface of the APC were exogenously loaded with a second antigenic peptide. T cells specific for this peptide, which do not recognize the peptide covalently attached to the GFP-tagged MHC molecules, do not accumulate the GFP-tagged MHC molecules within the immunological synapse suggesting that there is accumulation of only the T cell's cognate peptide.

Acknowledgements

David Parker – For his guidance and giving me the opportunity to pursue my own research interests. This freedom has made me a better scientist.

Timothy W. McKeithan – A great collaborator who is always supportive and supplied me with the necessary DNA constructs essential to this thesis.

Aurelie Snyder – For amazing technical assistance and support with the microscopy. Without her expertise, this project would not have been possible.

Thesis Committee Members (David Hinrichs, Ann Hill and Michael Davey) for important suggestions and tremendous support during this process.

Dean Evans – For his friendship and moral support.

Stan Barter – For his assistance in preparing the APC used in this study along with his friendship.

Current and Former Members of the Parker Lab: For helpful discussions, friendship, and moral support when things weren't going as well as hoped.

My wife Michelle: For her amazing support and love. Her understanding of late nights, early mornings and working weekends made my success possible.

Abstract

In this thesis, I report the generation of a novel cellular reagent that has allowed for the examination of immunological synapse formation using live CD4⁺ T cells and antigen presenting cells (APC). This system relies on a fibroblast cell line transfected with a GFP-tagged MHC molecule with covalently attached antigenic peptide. This system has major advantages over previously reported systems in that movement of specific MHC:peptide complexes can be followed at all stages of the interaction of T cells and APCs during the formation of the immunological synapse. Using this system, I have shown that within 30 seconds of contact with the APC, there is a rapid increase in intracellular Ca⁺⁺ concentration and subsequent large-scale morphological changes of the T cell leading a flattening against the APC, which significantly increases the surface area between the two cells. Within 1 minute of T-APC contact, multiple small spots of redistributed MHC:peptide complexes appear at the interface which intensify and coalesce into a single large cluster approximately 5.5 minutes after initial contact. Based upon the prototypical distribution of ICAM-1 and PKC θ , this structure is characterized as a “mature” immunological synapse. After synapse formation, a fraction of the T cells re-initiate locomotion across the surface of the APC and the synapse moves along with the T cell. During the process of synapse formation, as well as during the process of cellular dissociation, MHC:peptide complexes are captured by the T cells and are retained on their surface for up to 96 hours. The function of this captured

Chapter 1

Introduction

T Cell Activation: T Cell Receptor Triggering

The activation of T lymphocytes is a key event in the generation of an immune response. Since the early 1980's, it has been known that the clonally distributed TCR recognizes peptide fragments presented in the context of polymorphic MHC molecules on the surface of antigen presenting cells (1-3). The interaction of the TCR with cognate MHC:peptide complexes initiates a series of intracellular signaling events which, depending upon the environment (other signals) and state of differentiation of the T cell, ultimately leads to effector functions such as cytokine production, proliferation of naive or memory T cells, positive or negative selection in the thymus, cell death, or anergy.

TCR Mediated Intracellular Signaling

Signaling from the TCR is a complicated affair, involving numerous kinases and adaptor proteins in the transduction of signals from the TCR to the nucleus (Figure 1). The TCR-CD3 complex contains no intrinsic enzymatic activity and, thus, relies on the recruitment of cytoplasmic and membrane-bound molecules to potentiate downstream signaling. The earliest detectable signaling event after TCR antigen recognition is phosphorylation of tyrosine residues in immunoreceptor tyrosine activation motifs (ITAM) found on CD3 γ , δ , ϵ and ζ molecules (4). ITAM phosphorylation is predominantly carried out by the co-receptor associated Src- family kinase p56^{Lck} (5). The phosphorylated ITAMs on

CD3 ζ act as a docking site for ZAP-70, which interacts via its Src-homology 2 (SH2) domains (6, 7). ZAP-70 is a Syk-family kinase that also contains ITAMs and is itself phosphorylated and activated by Lck (8, 9). In turn, the activated ZAP-70 phosphorylates several important adapter proteins including SLP-76 and LAT (10). These adapters are involved in the activation of several downstream signaling cascades including the Ras-activated extracellular regulated kinase (ERK) pathway, the Janus kinase (JNK) pathway, and PLC γ 1 dependent signaling pathways (10, 11, 12, 13). These pathways converge in the nucleus to transactivate transcription of effector cytokines such as IL-2 and IFN γ . TCR signaling has also been linked to controlling cytoskeletal rearrangements within the T cell. Activated ZAP-70 can phosphorylate Vav1, a guanine exchange factor that activates, among other targets, members of the Rho-family of GTPases. The activity of Rho-family members in controlling cytoskeletal rearrangements is discussed in greater detail below.

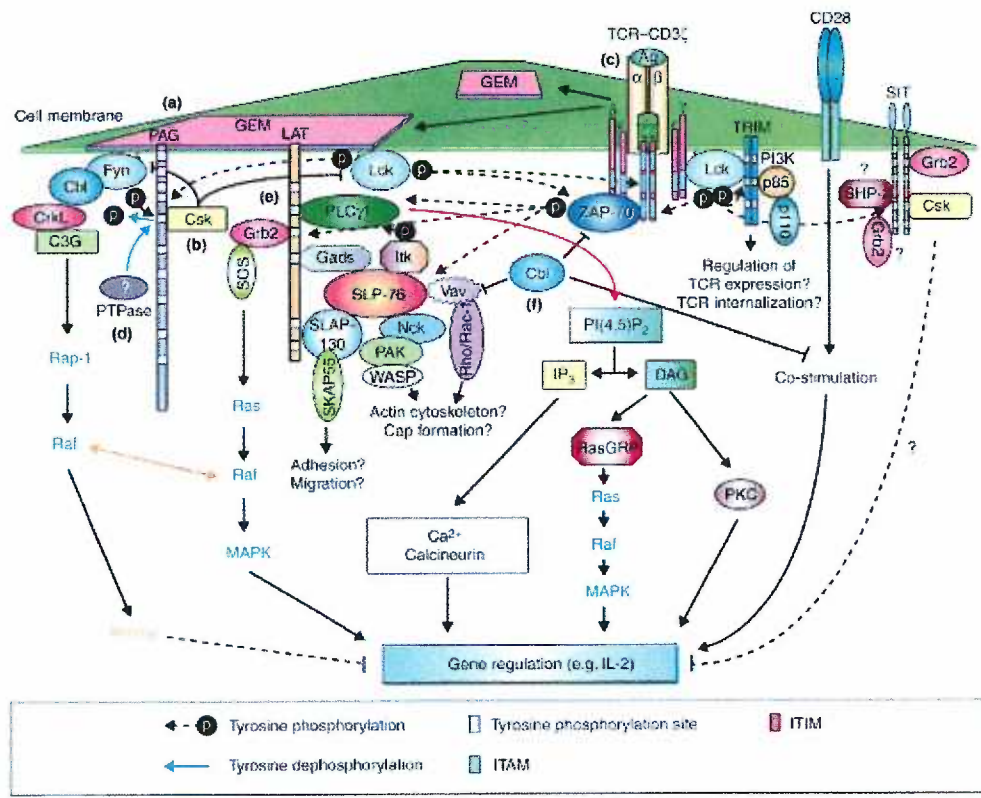


Figure 1. Overview of TCR-induced intracellular signaling pathways. Reproduced from (227).

TCR Triggering

While our understanding of the details of intracellular signaling events initiated by TCR triggering is increasing, and we understand much about the physical interactions between the TCR and its MHC:peptide ligand from X-ray crystallography studies, the mechanism by which TCR ligation initiates the intracellular signaling is still unknown. Several different models have been proposed to explain TCR triggering that involve at their core either a

conformational change or aggregation/oligomerization of the receptor upon ligand binding.

TCR Triggering: Conformational Change Model

In the TCR triggering model championed by Janeway and colleagues, MHC:peptide binding induces a conformational change within the receptor, initiating signaling (14). One of the strongest supports for a conformational change model came from measurements of interactions of purified TCR and MHC:peptide molecules by plasmon surface resonance (BIAcore), which showed that at 37°C, TCR intrinsically formed dimers with agonist complexes. This was interpreted as a TCR conformational change, which facilitated interactions between ligand, bound and unbound receptors, favoring subsequent ligand interactions with the recruited receptor (15). However, these experiments were repeated and with contradictory results (16). Significant technical difficulties in the first report lead to erroneous conclusions, and it appears that the conformational changes inferred by the BIAcore data does not occur (16). This finding, combined with a lack of any observed large-scale conformational change in TCR/MHC:peptide crystals (17) has left this theory of TCR triggering in disfavor.

Receptor Aggregation Models: Serial Triggering

There are three basic TCR triggering models that incorporate TCR aggregation/oligomerization as a key component. In the serial triggering model proposed by Lanzavecchia (18-21), a single MHC:peptide complex can serially engage and trigger as many as 180 TCR molecules (18). The triggered TCR are

internalized and their intracellular accumulation is “counted” by an unknown mechanism. When a critical threshold of internalized receptors is reached, the T cell becomes activated. According to Lanzavecchia, individual TCR complexes are recruited to membrane microdomains enriched in signaling molecules (lipid rafts) (20). In these rafts, the engaged TCR aggregate with signaling intermediates or with each other and trigger their activation. This model is supported by evidence that TCR do move into lipid rafts upon ligation and that these rafts are necessary for T cell activation (22-24).

Receptor Aggregation Models: Topology

The second receptor aggregation model, which is based upon membrane topology, is the kinetic segregation model of Shaw and van der Merwe (25, 26, 27). In this model, the 2D affinity of molecules on the surface is considered as well as their lateral mobility and physical size. The TCR-CD3 complex is held in a zone of close membrane contact where tyrosine phosphorylation can occur (26). This model invokes the physical segregation of the TCR-CD3 complex away from phosphatases such as CD45 based largely upon the size of the extracellular domains of these molecules. Only molecules of the approximate size as the TCR-MHC ligand pair, such as CD2/CD48 and B7-1/CD28, are associated with the TCR, while larger molecules such as CD45 are segregated away from the TCR. This teleologically pleasing model is supported chiefly by studies showing that CD2 molecules with different large extracellular domains inhibit T cell activation, rather than providing costimulation (27).

Receptor Aggregation Models: Kinetic Proofreading

The final aggregation model is the kinetic proofreading model proposed by our collaborator Tim McKeithan (28) and later refined by Rabinowitz *et al.* (29). In this model, TCR engagement initiates a multi-step program, which leads to T cell activation. Each step takes a certain amount of time to complete and if the TCR/MHC:peptide interaction ends before completion of the program, incomplete signaling from the TCRs can result in a partially active state in which the T cell may become non-responsive to further stimulation (i.e., antagonized). By requiring a sustained TCR/MHC:peptide interaction, this model explains how the T cell can distinguish between cognate and non-cognate peptides as well as distinguishing between peptides containing only minor sequence differences (altered peptide ligands) based upon affinity. It is supported by the demonstration that MHC: altered peptide ligands have higher dissociation rates (30) and by the finding that antagonists induce partial phosphorylation of CD3 ζ , and this partial phosphorylation pattern results in inactivation of the T cell (9, 31).

Costimulation

One of the fundamental paradigms that underlies cellular immunology is the concept of self – nonself discrimination. In 1970, Bretscher and Cohn proposed a model for B cell activation that required two distinct signals – one through the antigen receptor and a second “help” signal provided by another cell also responding to antigen (32). A few years later, Lafferty and Cunningham

modified this theory and applied it to T cell activation. Their model required 2 distinct signals to activate a T cell; one involving antigen recognition, the other a “costimulatory” signal provided by the antigen presenting cell (33). This model was later modified to include the concept that antigen recognition (signal 1) in the absence of costimulation (signal 2) would lead to inactivation of the cell (34). Formal demonstration of the need for costimulation came a decade later with the work of Ron Schwartz and colleagues. They showed that fixed antigen presenting cells or planar lipid bilayers containing only MHC molecules did not induce T cell activation, but instead rendered the T cells hyporesponsive (35, 36). This hyporesponsive state, termed anergy, was prevented by the inclusion of B7-1 molecules in the bilayers (37).

Anergy

Since the initial descriptions of anergy in the late 1980's, a major effort has been undertaken to understand this phenomenon. While much has been learned about the signaling defects and the phenotype of anergic cells, the mechanism driving anergy induction remains unknown. Anergy is actually quite heterogeneous and can be divided into forms that are rescued by IL-2 addition and those that are not (38). Induction of IL-2 responsive anergy requires a signal through the TCR in the absence of costimulation (39).

On the molecular level, anergic T cells display altered CD3 phosphorylation patterns (40, 41), which may be related to reductions in the Src-family kinases p56^{Lck} and p59^{Fyn} (42). Anergic T cells have severely reduced levels of the AP-1 transcription factor and c-fos/c-jun containing NFAT (43). In

addition, the composition of NF- κ B in anergic cells is altered; it is a p50-homodimer rather than the p50-p65 heterodimer normally found in activated T cells (43). As outlined below, these transcription factors (AP-1, NFAT, NF- κ B) are involved in regulating IL-2 secretion (43, 44). Anergic T cells are incapable of producing sufficient IL-2 to maintain cell proliferation (35, 45, 46) and remain in the G1 phase of the cell cycle (47).

This lack of IL-2 and subsequent inability of anergic T cells to progress through the cell cycle has been attributed to continued presence of p27^{Kip1}, a cyclin-dependent kinase inhibitor (47, 48). With non-anergic T cells, IL-2 receptor signaling or costimulatory signals through CD28 cause p27^{Kip1} degradation and the cells transcribe AP-1 allowing for IL-2 transcription as well as progression through the cell cycle (47, 48).

The precise events leading to the altered signaling I have described above are less well understood. It is unknown how CD28 signals result in Kip1 downregulation or how this is related to the other signaling defects found in anergic T cells. The IL-2 gene serves as a coincidence detector, requiring both a signal through the TCR and costimulatory molecules for transcription to occur. The nature of that costimulatory signal is unclear, because as described below, the exact nature of costimulation is unknown. With the description of a macromolecular signaling complex formed at the interface of a T cell and APC (the immunological synapse-see below) (49, 50), it is tempting to envision that differential recruitment of signaling molecules to anergic and non-anergic immunological synapses could account for the differences in downstream signaling observed and could account for the maintenance of the anergic state,

once established. To date, however, no rigorous studies of the molecular components of anergic immunological synapse have been published.

Costimulation Via B7/CD28 Interactions

One of the first costimulatory interactions described, and the best characterized, involves B7 family members, B7-1 (CD80) or B7-2 (CD86), on the antigen presenting cell and their receptor on T cells, CD28. B7 molecules can also bind an inhibitory receptor on T cells, CTLA-4 (CD152) (51). Early studies showed that B7-1/CD28 interactions increased T cell proliferation, accumulation of IL-2 mRNA and the subsequent secretion of IL-2 protein (52, 53, 54). Antibody blockade of B7-1 results in significant reductions in antigen-specific T cell proliferation (55). Combined with Schwartz et al.'s data using the planar lipid bilayers (36, 37), results showing B7 blockade with a soluble CTLA-4-Ig fusion protein (56) reduced IFN γ production and proliferation of T_H1 cells *in vitro* (57, 58), lead to the conclusion that B7/CD28 interactions are sufficient to provide costimulation.

This costimulatory function of B7/CD28 interactions may play a role in T cell activation *in vivo* as well. It has been proposed that the lack of costimulatory molecules on normal somatic tissues plays a role in peripheral tolerance to self. Without costimulation, potentially self-reactive T cells encountering antigen are rendered anergic, rather than being activated and inducing an autoimmune response (48). This theory is supported by evidence that abnormal expression of B7 molecules plays a role in the pathology of experimental autoimmune encephalomyelitis (59, 60) and experimental autoimmune anterior uveitis (61).

CTLA-4Ig blocks diabetes induction in non-obese diabetic (NOD) mice (62). Human rheumatoid synovial T cells express B7-1, and it is thought that this allows them to present antigen to each other to facilitate disease (63).

CD28-Mediated Intracellular Signaling

While CD28 initiates intracellular signaling and controls actin filament rearrangements, the exact mechanism by which costimulation through CD28 prevents anergy is not yet fully understood. CD28 ligation induces a series of intracellular signaling events that synergize with signals from the TCR and enhance early TCR signaling pathways (64). These CD28 and TCR signals integrate at the IL-2 gene to promote IL-2 production (65). CD28 ligation induces phosphorylation of LAT (66), activation of Lck and TEC kinases (67), increased expression of the anti-apoptotic gene Bcl-X_L (68), and is linked to increases in intracellular Ca⁺⁺ concentration (69). The IL-2 promoter (along with IL-3, GM-CSF, and IFN γ) contains a region which is responsive to signals generated by CD28 ligation, the so-called CD28 responsive element (CD28RE) (70). The CD28RE has an NF- κ B binding site and a non-consensus AP-1 binding site (65, 70). This is consistent with the finding that CD28 activates AP-1 by inducing c-jun phosphorylation along with enhancing NF- κ B nuclear translocation (71) through activation of protein kinase C- θ (PKC θ) (72, 73). It is not yet clear whether the signals generated by CD28 ligation induce complementary parallel pathways, or whether they function to augment TCR signaling cascades (65). Recent unpublished evidence from John Riley at the University of Pennsylvania presented at the 2002 Keystone Symposia on T Lymphocyte Activation using

gene array analysis showed that CD28 signals quantitatively alter signals from the TCR, but do not appear to qualitatively affect gene expression. Signals through CD28 alone only induce <12 genes out of 18,000 tested (TCR alone alters expression of ~2,700).

CD28 and the Actin Cytoskeleton

The other main function of CD28 ligation is the control of actin cytoskeleton dynamics (74). CD28 signals induce the hyperphosphorylation and activation of Vav (75) presumably via CD28's ability to activate Lck (67, 76). Vav is a guanine exchange factor that activates members of the Rho family of GTPases (77-79). One member of the Rho family, Cdc42, controls actin polymerization by controlling the activity of the Wiskott-Aldrich syndrome protein (N-WASP) (80). In combination with PIP₂, another downstream result of CD28 ligation (78), N-WASP regulates nucleation of actin polymerization by controlling the activity of Arp 2/3 (81). In response to antigen, even in the presence of optimal costimulation, Vav1^{-/-} T cells have reduced proliferation and cytokine production; phenotypically resembling T cells activated in the absence of costimulation (82-85). Blocking actin cytoskeletal rearrangements with pharmacological agents, such as cytochalasin D or *C. botulinum* C3 exotoxin, results in a significant reduction in T cell proliferation and cytokine production similar to costimulation blockade (84-87) demonstrating the importance of cytoskeletal alterations in T cell activation.

ICAM-1 Costimulation

While CD28 is important, it is not unique in its ability to provide costimulation. CD28^{-/-} mice have been generated, and although CD28^{-/-} T cell responses are reduced, they are not rendered uniformly anergic by exposure to antigen and APC as would be predicted if CD28 was the only costimulatory molecule (88). Studies have shown that intercellular adhesion molecule-1 (ICAM-1) binding to its receptor LFA-1 is the dominant costimulatory interaction in CD28^{-/-} mice (88). ICAM-1 is an integrin originally classified as an adhesion molecule, but it clearly possesses costimulatory functions as well (89). CD8⁺ cells appear to be most sensitive to ICAM-1 costimulation, but CD4⁺ cells are also responsive (54, 89, 90). On transfected fibroblast APC, ICAM-1 expression increases T cell sensitivity to antigen by 10 – 100 fold versus ICAM-1⁻ fibroblasts (91). This shift in the dose-response is not simply a result of increased adhesion because anti-LFA-1 antibodies mediate adhesion without affecting the dose response curve (91, 92). Inclusion of ICAM-1 protein on beads coated with anti-CD3 also increases CD25 expression (92) and T cell proliferation (91-93). This effect requires that the ICAM-1 and anti-CD3 be present on the same surface, because unlike B7/CD28 (52), ICAM-1/LFA-1 interactions cannot provide costimulation *in trans* (91, 93). ICAM-1 functions to augment TCR signaling (86) and is implicated in prolonging inositol phosphate production (93) maintaining PIP₂ hydrolysis, and sustaining higher Ca⁺⁺ plateaus several hours after initial T-APC interactions (93, 94).

The costimulatory activity of CD28 and ICAM-1 can synergize to provide optimal costimulation for the activation of T cells. With transfected fibroblasts, T

cell proliferation is 10 fold higher on ICAM-1⁺ B7-1⁺ APC compared to ICAM-1⁺ B7-1⁻ or ICAM-1⁻ B7-1⁺ APC (58). ICAM-1 and B7 molecules also synergize to stabilize IL-2 mRNA for several hours compared to less than 30 minutes in their absence (95).

Costimulatory Requirements of Naive and Effector T cells

The requirement for costimulation in the activation of T cells depends upon both the activation state of the T cells in question, and the response being measured. Dubey *et al.* showed that naive T cells are strictly dependent upon costimulation for proliferation and cytokine production (58, 96). These findings have been confirmed by several other labs (54, 57, 92, 93, 97, 98). The requirement for costimulation on activated or effector T cells is widely thought to be minimal, if at all. This is primarily the result of the work again by Dubey *et al.* which suggested that these T cells were costimulation independent (96); however, the preponderance of evidence suggests that while these cells are less dependent upon costimulation, they still require B7/CD28, LFA-1/ICAM-1, or both to achieve full activation (54, 57, 99, 100). Recently activated T cells require B7-1/CD28 interactions; they become anergic in their absence (100). These differences probably result from differential dependence on costimulation of different effector functions. IL-2 and IL-5 production along with proliferation are very costimulation dependent, while IL-4 production is largely costimulation independent in effector cells (57, 96).

Microscopy of T Cell – Antigen Presenting Cell Interactions

T Cell Morphological Changes Upon Antigen Recognition

When the leading edge of a polarized T cell, which is more sensitive to antigen than the trailing edge (101, 102), contacts an APC displaying appropriate MHC:peptide complexes, TCR ligation rapidly induces a flurry of signaling events including protein phosphorylation and increases in cytoplasmic Ca^{++} concentrations. Initiation of signaling stops T cell migration (103, 104), and the T cells undergo a program of Ca^{++} -dependent, (102, 105, 106) cytoskeleton- driven morphological changes (107, 108) resulting in the formation of a tight T-APC conjugate with dramatically increased surface contact. These morphological changes are antigen-specific (107) and require protein tyrosine kinase activity (85, 108). The T cells continue to display active membrane ruffling at the contact zone after tight conjugate formation (108).

Supramolecular Activation Complexes (SMACs) and the Immunological Synapse

Pioneering work done largely by Kupfer and colleagues has shown that a variety of molecules accumulate at antigen-specific T-APC interfaces including: TCR and CD4 (109), talin, LFA-1/ICAM-1, and PKC θ (110). In addition, the microtubule organizing center (MTOC) migrates from the uropod of polarized cells to an area adjacent to the engaged TCR (111). In a ground breaking study, Monks *et al.* (50) observed that rather than just random clustering at the T-APC interface, molecules were spatially segregated into distinct structures termed supramolecular activation complexes (“SMACs”). The central region (c-SMAC)

contains TCR/MHC:peptide complexes, B7-1 (CD80)/CD28, PKC θ , Lck and Fyn (50, 112). Surrounding the c-SMAC is a peripheral ring containing ICAM-1/LFA-1, Talin, and CD2/CD48 called the p-SMAC (50, 112). Recently, Freiberg described the formation of a third region outside the p-SMAC called the distal SMAC or d-SMAC (113). The phosphatase CD45 is found in the d-SMAC, as are p56^{Lck} and CD4 by 15 and 23 minutes after initial contact, respectively (113).

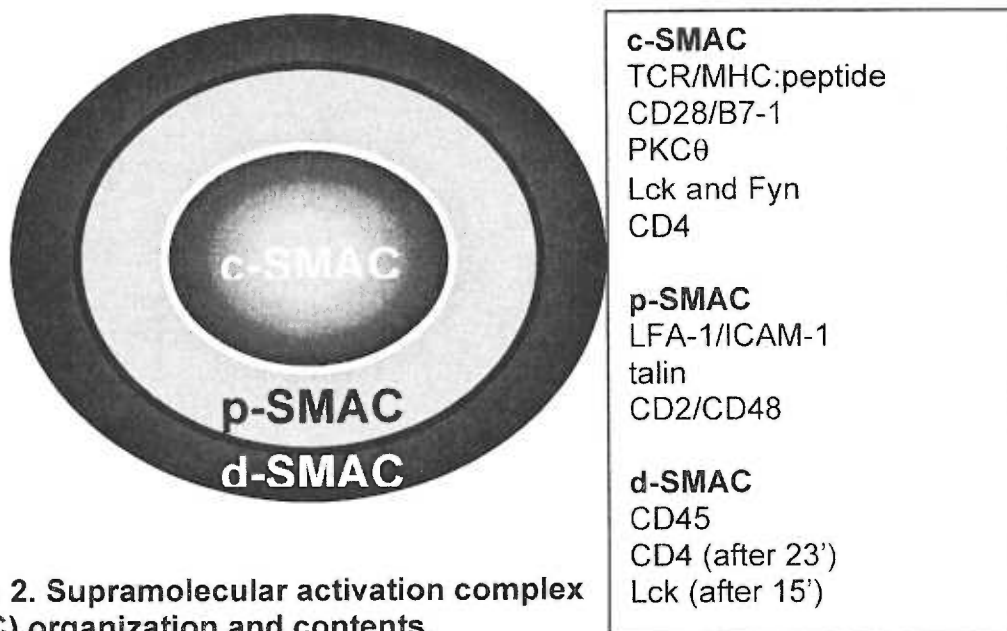


Figure 2. Supramolecular activation complex (SMAC) organization and contents.

An elegant live cell imaging study by Grakoui *et al.* (49) using fluoresceinated proteins suspended in a planar lipid bilayer described the molecular rearrangements leading to the formation of this ordered structure. Their bilayers contained only MHC:peptide complexes and ICAM-1 molecules. As seen in figure 3, the green-labeled MHC molecules originally surrounded the red-labeled ICAM-1 molecules. Over the period of 5 minutes, these molecules

change position and the ICAM-1 ends up surrounding the MHC molecules. Over the next 55 minutes, this structure continues to evolve so that by 1 hour, the arrangement of ICAM-1 and MHC molecules resembles the SMACs described by Monks *et al.* (50). Because the molecular accumulation and the directed secretion of cytokines (114) and cytolytic granules (115, 116) at the T-APC interface resembles a neuronal synapse, this structure is also called an immunological synapse (117).

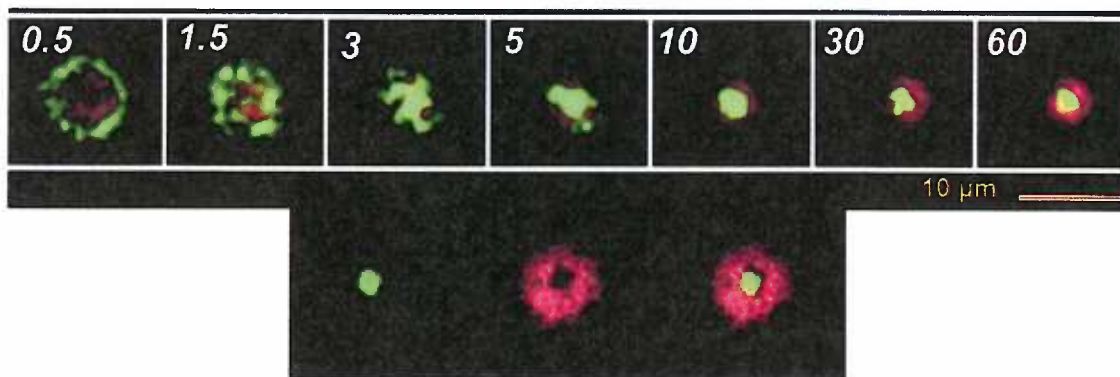


Figure 3. Formation of the immunological synapse. (Top) Time lapse imaging of molecular rearrangements of MHC (green) and ICAM-1 (red) during the interaction of T cells with proteins embedded in planar lipid bilayers. Times are given in minutes after initial contact. (Bottom) Synapse after 60 minutes clearly showing the mutually exclusive segregation of MHC to the c-SMAC and ICAM-1 to the p-SMAC. From Grakoui *et al.* (49).

It is hypothesized that the immunological synapse stabilizes the interaction between the T cell and APC serving as a signaling platform where various signaling molecules are recruited and maintained (118, 119), which allows for signaling of sufficient duration to activate T cells (120). Consistent with this model, many molecular species associated with T cell signaling are accumulated in the synapse including: PKC ζ 9 (110), activated Lck (113), CD45 (113), CD3 (69), Fyn, CD28, and CD4 (118). The formation of the synapse is

thought to represent a checkpoint for full T cell activation (78, 112, 118, 121), because only T-APC interactions involving antigen recognition will be of sufficient duration to allow for synapse formation.

Formation of the Immunological Synapse

The precise molecular events leading to the formation of the immunological synapse are unknown. Immunological synapse formation requires T cell cytoskeletal rearrangements (74, 94) but, as seen in Figure 3, it does not form until several minutes after the initiation of intracellular signaling. There are several theories that have been proposed to explain how antigen-recognition could result in the spatial segregation of molecules seen within the immunological synapse.

Topology Model

The first model to be considered is the topology model of van der Merwe described above (26, 112). This model relies on the segregation of different sized molecules interacting at the T-APC interface. The TCR-MHC interaction is predicted to span approximately 15 nm between the membranes (25). This model predicts that molecules of similar size (CD2/CD48, B7/CD28) would have to segregate from larger molecules such as CD43 and CD45 for efficient interaction (25, 26). This segregation is occurring on a submicroscopic level with microclusters of just a few engaged molecules at the earliest time points. As time progresses, these microclusters aggregate, forming the visible immunological synapse. It conveniently explains the segregation of molecules with very large extracellular domains (CD43 and CD45) from the c- and p-SMAC structures (27,

122, 123). A potential problem with this model is that while it can explain the aggregation of molecules at the T-APC interface, it does not adequately explain the segregation of similar sized molecules such as B7-1/CD28 and CD2/CD48 into different regions of the immunological synapse (49).

Lipid Raft Accumulation Model

The second model predicts that the engagement of the TCR with cognate MHC:peptide complexes induces the aggregation of membrane microdomains (124) (lipid rafts) at the T-APC interface (125). This aggregation would bring together a variety of signaling molecules and their substrates that are found constitutively associated with rafts along with the recruitment of other proteins to the rafts, forming a large signaling complex (22-24, 126-129). This model is supported by the findings of Viola et al. (130) showing that CD28 crosslinking results in raft aggregation. Currently there is little other evidence in support of, or against, this model. This model has the same shortcomings as the topology model, in addition to the fact that rafts have not previously been shown to accumulate at the synapse (129).

Costimulation and the Immunological Synapse

The role of costimulation in the formation of the immunological synapse is unclear. As described above, synapse formation is driven by the T cell actin cytoskeleton (74, 94) and costimulation is involved in controlling actin cytoskeletal rearrangements. The localization of B7-1/CD28 to the c-SMAC and ICAM-1/LFA-1 to the p-SMAC combined with the circumstantial evidence

surrounding actin filament control is suggestive of a role for these molecules in organizing the synapse. However the evidence for costimulation involvement in the control of synapse formation is contradictory. The work of Wülfing and Davis suggests that costimulation through CD28 and/or ICAM-1 is crucial for synapse formation (74, 94, 131, 132). Blockade of costimulation in their system results in formation of defective synapses with only transient clustering of CD3 ζ in the c-SMAC (69).

By contrast, inclusion of B7-1 in planar lipid bilayers used by Dustin and colleagues has no effect on synapse formation (49, 121). With CD28^{-/-} T cells, PKC θ and LAT are accumulated at the T-APC interface; although they are uniformly distributed rather than accumulating in the c-SMAC (113). CD28^{-/-} T cells also show redistribution of the TCR toward the APC *in vivo* (133).

The apparent discrepancy in the role of costimulation from these different groups most likely is due to differences in their experimental systems. The approach of Dustin and colleagues utilizes a completely artificial system, replacing living APC with a glass supported planar lipid bilayer into which GPI-tethered proteins have been embedded. While this system is optimal for imaging studies and allows for the assessment of defined arrays of protein components in synapse formation, the bilayers lack the full complement of surface proteins found on a living APC, as well as extracellular matrix components, which are implicated in controlling T cell activation (134). This has the potential to generate erroneous results because on a living APC, these proteins are not in isolation and may function cooperatively with proteins not included in the planar bilayer. It is

important not to over-interpret results from this system and any finding should be confirmed with more physiologically relevant systems.

There are problems with the systems employed by Wülfing and Davis as well. They are capturing images at a very high frame rate, which is critical for generating 4D data sets, but it comes at the cost of optical and spatial resolution. Their optical sectioning in the z-axis is in 1 μ m steps, requiring interpolation of data in between actual data points. This limits their ability to precisely quantify areas or density of molecules.

Rationale

In this thesis I describe the generation of an imaging system that improves on the currently used systems in several ways, and allows for the examination of several key issues surrounding immunological synapse formation. My system employs living fibroblasts transfected with an MHC class II molecule containing covalently attached antigenic peptide and tagged with green fluorescence protein (GFP) on the cytoplasmic tail. With these APC, I can follow the redistribution of a specific MHC:peptide complex during antigen recognition by T cells. While not a physiological APC, it is an improvement over the completely artificial lipid bilayer system. Our state-of-the-art wide-field deconvolution imaging system is capable of generating superb high-resolution images of fixed T-APC conjugates, with superior spatial resolution that can be accurately quantified.

There are several important questions that I have addressed with this system. First, I have examined the dynamics of synapse formation using live cells

as APC. With the aforementioned advantages over previous systems, I analyzed the early steps in synapse formation, correlating early MHC:peptide redistribution to mature synapse formation. My results have added to our understanding of the early events in synapse formation.

Another area that I addressed was the relationship between the immunological synapse and intracellular signaling. By using pharmacological inhibitors of intracellular signaling pathways, I have begun to define the signaling events that are important in synapse formation. In agreement with previous reports, I show that increases in intracellular Ca^{++} concentrations are necessary for TCR-driven morphological changes upon antigen encounter. When the Ca^{++} flux is prevented, T cells do not efficiently interact with the APC and do not form immunological synapses. Inhibition of Src kinases (Lck and Fyn) also inhibits efficient immunological synapse formation. In contrast, the MAPK pathway does not appear to be necessary for formation of the synapse, but it is required for continual T-APC interactions.

In addition to examining the formation of the immunological synapse, I have addressed three major questions in my thesis research:

1. Do the MHC:peptide molecules accumulated in the immunological synapse contain a mixture of cognate and non-cognate peptides, or is the synapse peptide-specific?
2. What is the role of costimulation through CD28 or LFA-1 on the formation and maintenance of the immunological synapse?
3. Do anergic T cells form synapses? Do they differ from synapses formed by non-anergic T cells?

Chapter 2

Materials and Methods

Animals

Heterozygous AD10 TCR transgenic mice on a B10.BR (H-2K) background, specific for pigeon cytochrome C (PCC) fragment 88-104 (135) and reactive against moth cytochrome C (MCC) fragment 88-103, were kindly provided by Steve Hedrick (UCSD, San Diego, CA) by way of Philippa Marrack (National Jewish Medical Center, Denver, CO). Homozygous 3.L2 TCR transgenic mice, specific for peptide 64-76 of murine hemoglobin (Hb) d allele, were kindly provided by Paul Allen (Washington University, St. Louis, MO) (136). The mice were bred and maintained in specific pathogen-free conditions in the OHSU animal care facility. For the PCR identification of the AD10 transgenic mice, small pieces were collected from the tip of the tail and digested overnight in digestion buffer (10mM Tris, pH 8.4, 5 mM KCl, 100 µg/ml gelatin, 0.45% NP-40, 0.45% Tween-20) supplemented with proteinase K (0.2 mg/ml) at 55°C. After heating at 95°C for 15 minutes to destroy proteinase K activity, 2 µl of the digestion reaction was used as a template in a PCR reaction. To detect the AD10 TCR β chain transgene, a 5' primer specific for Vβ3 (GACTCCAAGATATCTGGTG) and a 3' primer (TGAGCCGAAGGTGTAGTC) specific for the J region of the transgene were used. Samples were amplified using a Stratagene Robocycler Gradient 96 (La Jolla, CA) following this amplification procedure: one cycle using 94° for 5 minutes, 55° for 1 minute, 72°

for 1 minute followed by 35 cycles using 94° for 1 minute, 72° for 1 minute, and 55 ° for 1 minute. PCR products were separated by electrophoresis on 1% agarose/TBE gels.

Antibodies

The following antibodies were purchased from PharMingen (BD Biosciences, San Diego, CA): anti-I-E^k (17-3-3), anti-I-E^k (14-4-4s), anti-B7-1 (16-10A1), anti-ICAM-1 (3E2), anti-CD69 (H1.2F3), anti-Vβ3 (KJ25), anti-Vβ8.3 (1B3.3), anti-CD25 (3C7), anti-Vα11 (RR8-1), anti-TCRβ (H57). Polyclonal goat anti-nPKCθ (C18-G) and polyclonal goat anti-c-Cbl (C15-G) were purchased from Santa Cruz Biotechnology (Santa Cruz, CA). An anti-mouse IgG-PE secondary antibody was purchased from Southern Biotechnology (Birmingham, AL). Streptavidin Texas Red and Texas-Red conjugated donkey anti-goat were purchased from Jackson ImmunoResearch (West Grove, PA). Biotinylated Cholera Toxin B (CTxB) subunit was purchased from Sigma (St. Louis, MO). CTLA-4/Ig was purified from supernatants from a hybridoma kindly provided by Peter Lane (University of Birmingham, UK) (56).

Antigen Presenting Cell Generation

Cells

Ltk⁻ fibroblasts obtained from the ATCC (Rockville, MD) displayed a broad range of endogenous B7-1 expression. To generate B7-1^{hi} fibroblasts used in transfections, Ltk⁻ cells were stained with anti-B7-1 FITC, and brightly stained cells were sorted on a FACSCalibur (BD Biosciences, Palo Alto, CA). Sorted cells

were cloned at limiting dilution and the resulting clones were analyzed by flow cytometry. A high B7-1 expressing clone (Ltk^{B7-1^{hi}}) with levels similar to B10.BR splenocytes was used as the parental cell in the transfections. Cells were maintained in DMEM (Gibco, Bethesda, MD) containing 10 % FBS (Hyclone, Logan, UT.) and supplemented with 1 mM L-glutamine, 100 mg/ml sodium pyruvate, 5×10^{-5} M 2-ME, essential and non-essential amino acids (Gibco, Bethesda, MD), 100U/ml penicillin G, 100 U/ml streptomycin and 50 μ g/ml gentamycin.

Plasmids

To generate the GFP-tagged I-E^k β chain with covalent antigenic peptide used in this study, the MCC:I-E^k β chain (137) was cut out of the ph β A-pr1-neo vector (138) with Alu and EcoRI. This fragment was ligated into a shuttle vector containing a c-myc epitope tag, in frame. This plasmid was cut with EcoRV and BsiWI to generate a C-terminal fragment of I-E^k with a c-myc tag. The ph β A-pr1-neo vector (138) containing the covalent MCC:I-E^k β chain was digested with BamHI and BsiWI and the c-terminal c-myc fragment was ligated in. This generated a full length I-E^k β chain with covalently attached MCC peptide and a C-terminal c-myc tag.

To generate an EGFP fragment, the Clontech EGFP-N3 plasmid (Clontech Laboratories Inc., Palo Alto, CA) was digested with BglIII and BamHI and religated to delete much of the polylinker region. The EGFP fragment was then cut out with AflIII (filled in to form a blunt end) and NheI, then ligated into the MCC:I-E^k β :C-myc plasmid digested with BamHI (also filled in to form a blunt

end) and XbaI. This generated the MCC:I-E^kβ:c-myc-EGFP construct used in this study.

To prepare the wild type I-E^k construct, a fragment containing the entire wild type I-E^k β chain was cut out of the PLXSN retroviral plasmid vector (a gift of Hans Fischer and John Kappler) with BamHI and EcoRI. This fragment was ligated into a shuttle vector, bluescript sk. It was then cut out of bluescript sk with ApaII and BamHI and ligated into pcDNA3.1 (-) Hygro (Promega, Madison, WI) which carries a hygromycin resistance gene.

Transfections

Ltk⁻ B7-1^{hi} cells were transfected with 2 μg of the MCC:I-E^k GFP construct, 30 μg of I-E^k α chain in the pEVX-3 plasmid, kindly provided by Ronald Germain (NAIAD, Bethesda, MD) (139), and 2 μg of ICAM-1 in the phβA-pr-1-neo plasmid, obtained from Dr. A. Brian (91), with lipofectin (Gibco, Bethesda, MD) according to manufacturer's directions. Briefly, 10⁶ Ltk⁻ B7-1^{hi} cells were plated into a 6 well plate and cultured overnight. The plasmid DNA was mixed and incubated for 1 hour with a 1:4 dilution of Lipofectin in serum free Opti-MEM media (Gibco, Bethesda, MD), then added drop-wise to the cells, also in Opti-MEM. After 24 hours, an equal volume of DMEM containing 10% FBS was added to the plates and they were incubated for an additional 24 hours. The cells were split equally into 2 - 24 well plates and placed on drug selection for 3 weeks with 500 μg/ml G418 active drug. Drug resistant cells were screened for GFP expression and I-E^k surface expression by flow cytometry. Positive cells were sorted on a FACSCalibur (BD Biosciences, Palo Alto, CA) based upon GFP

expression level, and cloned by limiting dilution. MCC Clone A was chosen because its GFP expression was the highest of the tested clones.

To better mimic physiologic conditions where the cognate ligand is found in a sea of non-cognate ligands, the MCC Clone A cells were super-transfected with 2 µg wild-type I-E^k β chain cDNA in pcDNA3.1(-) Hygro and 30 µg I-E^k α chain plasmid. After selection with 350 µg/ml of hygromycin, the surviving cells were analyzed by FACS for significant increases of I-E^k expression compared to the MCC Clone A cells. Positive populations were FACS sorted and cloned by limiting dilution. One clone (MCC:GFP) was selected because it expressed the highest level of wild type I-E^k with minimal increases in GFP expression. These transfectants were cycled on selecting drugs for 2 – 3 weeks every 3 months, and maintain stable expression levels of the transfected molecules.

In Vitro T Cell Priming

Single cell splenocyte suspensions from 6 – 12 week old AD10 or 3.L2 TCR transgenic mice were depleted of erythrocytes by hypotonic lysis with Gey's solution and resuspended in RPMI 1640 (Gibco, Bethesda, MD) containing 10 % FBS (Hyclone, Logan, UT) and supplemented with 1 mM L-glutamine, 100 mg/ml sodium pyruvate, 5×10^{-5} M 2-ME, essential and non-essential amino acids, 100U/ml penicillin G, 100 U/ml streptomycin and 50 µg/ml gentamycin. Cells were primed *in vitro* with 2.5 µM peptide (PCC₈₈₋₁₀₄ for AD10, Hb₆₄₋₇₆ for 3.L2) for 6 days with no addition of exogenous IL-2. Lymphocytes were isolated from the primed cultures by density centrifugation using Lympholyte M (Cedarlane, Hornby, Ontario) with a resulting purity of CD4⁺ cells > 75 %. T cells

were resuspended at 5×10^6 /ml in phenol red-free, bicarbonate-free RPMI-10 for use in microscopy. To measure intracellular Ca^{++} concentration, T cells were labeled with $1\mu\text{M}$ Fura-2 as described below.

Fura-2 Loading

For measuring Ca^{++} flux, *in vitro* primed T cells were resuspended at 2×10^6 /ml in PBS containing 10 % FBS, 1 mM Ca^{++} and 0.5 mM MgCl_2 . The cells were incubated with $1\mu\text{M}$ Fura-2 AM (Molecular Probes, Eugene, OR) for 30 minutes at 37°C in the dark. After washing in PBS, cells were resuspended at 10^7 /ml in PBS containing 1mM Ca^{++} and 0.5 mM Mg^{++} and incubated at room temperature in the dark for 15 minutes to allow for AM hydrolysis. Cells were stored on ice until use.

Anergy Induction

AD10 T cells were *in vitro* activated for 4 – 6 days in the presence of $2.5 \mu\text{M}$ PCC peptide. Lymphocytes were isolated from the primed cultures by density centrifugation using Lympholyte M (Cedarlane, Hornby, Ontario). Cell concentration was adjusted to 5×10^6 /ml. 5 ml of the cell suspension was added to 100 mm petri plates precoated with $10 \mu\text{g}/\text{ml}$ anti-TCR β (H57) in PBS. Control cells were incubated on petri plates precoated with PBS only. After an 18 hour incubation at 37°C , cells were removed from the plates by gentle scraping, washed twice and resuspended at 5×10^6 /ml. The cells were incubated an additional 2 days in the absence of antigen or IL-2 before use.

Measurement of T Cell Proliferation

Proliferation of the AD10 T cells in response to MCC:GFP cells was measured by a standard 72-hour [^3H] thymidine incorporation assay. Naive AD10 T cells were purified by T Collect column (Cytovax, Edmonton, AB). For APC titration experiments, 2.5×10^4 responders were co-cultured with increasing numbers of the MCC:GFP cells and pulsed with 1 μCi [^3H] thymidine (2Ci/mmol specific activity) during the last 12 hours of a 72 hour assay. In costimulation blocking experiments, 10^4 MCC:GFP cells were pre-incubated with blocking reagents for 1 hour prior to the addition of 2.5×10^4 primed AD10 T cells. The proliferative response of 3.L2 T cells to the MCC:GFP cells was measured similarly. For maximal loading of Hb peptide, MCC:GFP cells were treated for 20 minutes in 100 mM citrate buffer, pH 5.3 in PBS to strip weakly binding peptides from the wild type I-E^k. These cells were then exogenously loaded with 20 μM Hb peptide by overnight incubation.

Measurement of T Cell Activation by Flow Cytometry

2.5×10^6 T cells and 2.5×10^5 MCC:GFP cells were incubated overnight (12 – 16 hours) in 2 ml total volume. Cells were stained for the activation markers CD25 and CD69, along with anti-V β antibodies (anti-V β 3 for AD10, anti-V β 8 for 3.L2) to measure TCR down-modulation.

Microscopy

Signaling Inhibitors

To study the role of intracellular signaling cascades in the formation and maintenance of the immunological synapse, cells were preincubated with 50 μM PD98058 (140) (Sigma, St. Louis, MO) a specific MEK inhibitor, 5 μM PP2 (141) (Sigma, St. Louis, MO), a specific Src kinase inhibitor, or 20 μM BAPTA-AM (Molecular Probes, Eugene, OR), a Ca^{++} Chelator for 30 minutes before imaging began.

Cytoskeletal Inhibitors

To examine the role of cytoskeletal rearrangements in the formation of the synapse, T cells or APC were pretreated for 1 hour with 10 μM colchicine (Sigma, St. Louis, MO) to block microtubule polymerization or 10 μM cytochalasin D (Sigma, St. Louis, MO) to block actin filament polymerization. Both of these reagents were suspended in DMSO and were added at a final DMSO concentration of 0.5 % to the T cell or APC cultures. They were diluted 1:20 when added to the imaging dishes. The final concentration of these inhibitors in the imaging dish did not have any observable effect on the population of untreated cells.

Live Cell Microscopy

For live cell microscopy, 2.5×10^5 APC were seeded into 0.15 mm Delta T dishes (BiopTechs, Butler, PA) 1 day prior to the experiment in DMEM culture medium. In the 3.L2 experiments, the MCC:GFP cells were acid stripped and loaded with

20 μM Hb peptide as described above. The acid stripping did not alter the AD10 response to the MCC:GFP cells, indicating that the covalent MCC peptide was not being displaced. Blocking reagents were added to the APC 1 hour prior to imaging. Just prior to microscopy, DMEM culture medium was removed from the plate and replaced with 1ml phenol red- and bicarbonate-free RPMI culture medium. Dishes were fitted into a BiopTechs ΔTC3 heating collar and maintained at 37°C for the duration of the imaging. After adding 2.5×10^5 AD10 T cells to the dish, alternating 400 or 600X green fluorescent (528 nm) and differential interference contrast (DIC) images (500 nm) were taken every 8 – 10 seconds for 45 minutes with the Applied Precision Instruments (API) DeltaVision[®] image restoration system (Issaquah, WA). This includes the API chassis with precision motorized XYZ stage, a Nikon TE200 inverted fluorescent microscope with standard filter sets, halogen illumination with API light homogenizer, a CH350L camera (500 kHz, 12-bit, 2 Megapixel, liquid cooled), and DeltaVision[®] software. Images were obtained at 512×512 pixels, with binning of 2. For Fura-2 analysis 600X images with excitation at 340 nm and 380 nm and emission at 510 nm were captured in addition to fluorescent and DIC. Image analysis was performed on a Silicon Graphics Octane workstation using the API SoftWorx software package.

Fixed Conjugate Microscopy

For analysis of fixed conjugates, 5×10^4 APC were placed into a LabTek II 8 chambered 0.15 mm cover glass. After overnight incubation at 37°C , any blocking reagents were added to the APC at least 1 hour prior to addition of T

cells. 2.5×10^5 *in vitro* primed AD10 T cells were added to the wells in a total volume of 100 μ l and the chambers were centrifuged for 30 seconds to facilitate T-APC interactions before being incubated for 30 minutes at 37°C. Media was then removed and the conjugates were fixed for 30 minutes at room temperature with 4 % paraformaldehyde containing 0.5% glutaraldehyde in PBS.

For extracellular staining, the cells were incubated for 2 hours at 37°C with 0.5 μ g/ml PE-conjugated anti-ICAM-1 antibody or 5 μ g/ml biotinylated Cholera Toxin B subunit (CTxB) (to stain lipid rafts). After washing 3 times with PBS, the CTxB stained cells were incubated with streptavidin-texas red to detect the biotinylated CTxB.

For intracellular staining, cells were permeabilized with 1% Triton X-100 in PBS for 5 minutes at room temperature before 3 washes with PBS. After blocking for 24 hours with 1% BSA/0.1% NaN_3 in PBS, cells were stained with anti-PKC θ at 10 μ g/ml in blocking buffer for 2 hours at room temperature in a humidified chamber. Following 4 washes of 5 minutes with PBS, cells were incubated with 5 μ g/ml Texas-Red conjugated donkey anti-goat IgG for 2 hours at room temperature. After 3 more washes with PBS, Anti-Fade reagent (Molecular Probes, Eugene, OR) was added to the wells and chambers were stored at 4° in the dark until imaged.

Conjugates were chosen based upon the characteristic flattened morphology in DIC image. A stack of 50 – 90 fluorescent images spaced 0.2 μ m apart in the z-axis was obtained at 1000X on the API system and were deconvolved using the constrained iterative algorithm of Sedat and Agard (142, 143). Deconvolution, three dimensional reconstructions, and measurements of synapse area and fluorescence intensity within the synapse were performed on

an SGI Octane workstation using the API SoftWorx software package. For quantification of the GFP at the T-APC interface, the background fluorescence was determined by use of the built-in data inspector feature on an area on the APC adjacent to the synapse. Using the autopolygon feature of the SoftWoRx program, pixels with a GFP intensity at least 2 fold above background were selected. To determine the total area of the accumulated GFP, areas with GFP intensity twice background were summed. After subtraction of background, the integrated intensity, an indication of the amount of accumulated MHC within in the synapse, was summed for areas with GFP intensity twice that of background.

Statistics

Determination of statistical significance was performed with student's t test.

Chapter 3

Results

APC Characterization

The precise spatial and temporal resolution of molecular rearrangements leading to the formation of the immunological synapse during the interaction of living T cells and antigen presenting cells (APC) have not previously been examined. Previous studies examining immunological synapse formation have used T cells interacting with surrogate APC consisting of fluoresceinated proteins embedded in planar lipid bilayers (49), examined paraformaldehyde fixed T - B cell conjugates after antibody staining (50, 109, 111, 144), or used living T cells and APC but have displayed the results as manipulated grayscale intensity images which limits useful detailed spatial and/or temporal information (69, 131). As a part of my thesis research, I have developed a system involving APC expressing a GFP-tagged MHC molecule containing covalently attached antigenic peptide. With these cells, I have been able to follow the redistribution of specific MHC:peptide complexes on the surface of the APC during T cell antigen recognition and subsequent immunological synapse formation.

To produce the antigen presenting cells used in these studies, an MHC Class II negative murine fibroblast cell line (Ltk⁻) was obtained from the ATCC. In initial screening, it was observed that there was a broad range of B7-1 (CD80) surface expression on these cells, while they were B7-2 (CD86) and ICAM-1

(CD54) negative (Figure 4). From our previous studies, we knew that even high levels of expression of the covalent MHC:peptide complexes on the surface of an APC in the absence of ICAM-1 and B7 proteins was not sufficient to induce activation of T cells (data not shown). To generate an Ltk⁻ clone with uniformly high expression of B7-1, the cells were FACS sorted based upon their B7-1 expression level and were cloned by limiting dilution. One of the clones (B7-1^{hi} Ltk⁻) expressed levels of B7-1 similar to B10.BR splenocytes (Figure 4E) and this clone was used as the parental cell line for all transfections. These cells have maintained their B7-1 levels for over 3 years in continuous culture.

The B7-1^{hi} Ltk⁻ cells were co-transfected with the moth cytochrome C (MCC):I-E^k β chain:GFP construct (Figure 4A), I-E^k α chain, and ICAM-1 plasmids. The resulting MCC Clone A cells showed a 7.7 fold increase in GFP fluorescence above autofluorescence background (Figure 4C) and expressed levels of I-E^k 17.6 fold above the I-E^k negative parental cells (Figure 4B). They also expressed high levels of B7-1 and intermediate levels of ICAM-1 (data not shown). These cells were found to induce proliferation of naive, antigen-specific T cells from the AD10 TCR transgenic mouse in a dose-dependent manner (data not shown).

All of the MHC on these fibroblasts contained the covalently attached MCC₈₈₋₁₀₃ peptide. To better mimic physiologic conditions in which specific MHC:peptide ligands are found in a sea of non-cognate ligands, MCC Clone A cells were super-transfected with plasmids encoding wild type I-E^k β chain and additional I-E^k α chain. One of the resulting clones, MCC:GFP, expresses 2 fold more I-E^k than the MCC Clone A cells and 32.2 fold more than the parental cells

(Figure 4B). I-E^k expression on the MCC:GFP cells is similar to B10.BR splenocytes (Figure 4B). These cells express slightly elevated levels of GFP compared to MCC Clone A, perhaps a function of additional I-E^k α chain (Figure 4B). Because the increase in I-E^k staining is greater than the increase in GFP levels, we deduced that the wild type I-E^k β chain is expressed. The MCC:GFP cells also expressed intermediate levels of ICAM-1 (Figure 4E) and high levels of B7-1 (Figure 4D) but remain B7-2 negative (data not shown). As seen in Figure 4F, surface expression of the MCC:I-E^k β chain:GFP fusion proteins are fairly uniform on the surface of the MCC:GFP cells (bright green spot and black regions are artifacts due to the contours of cell surface). This is an important characteristic, since I will be looking at redistribution of these molecules upon T cell engagement.

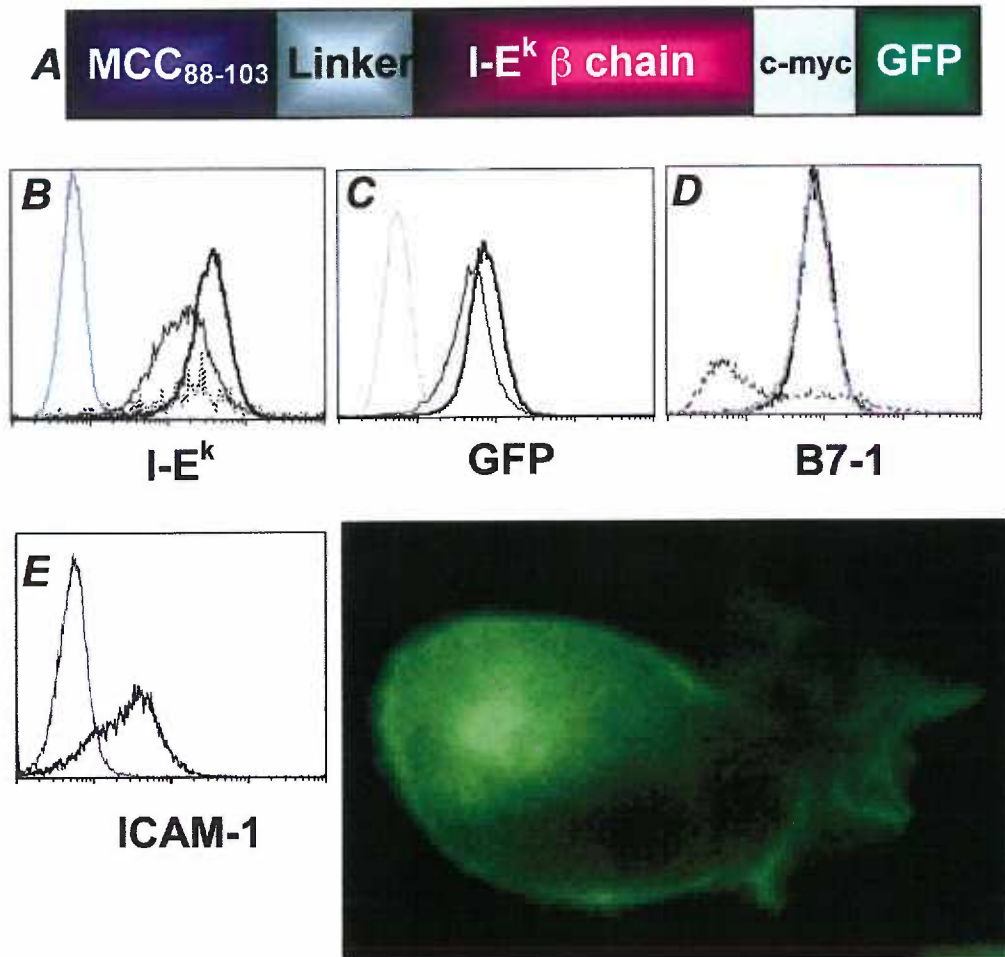


Figure 4. Surface Phenotype of Transfected Fibroblast APC.

(A) Schematic of the MCC:I-E^k:GFP construct used to transfect fibroblasts. (B) I-E^k expression on B7-1^{hi} Ltk⁻ (gray line) compared to MCC Clone A cells (thin line). To better mimic physiologic conditions, MCC clone A cells were super-transfected with wild type I-E^k generating MCC:GFP cells (bold line). I-E^k expression on B10.BR splenocytes (dotted line) is shown for comparison. The isotype control is shaded. (C) Expression of GFP by MCC Clone A (thin line) and MCC:GFP (bold line) cells compared to B7-1^{hi} Ltk⁻ (gray line) parental cells. (D) B7-1 expression on parental Ltk⁻ (dotted line), B7-1^{hi} Ltk⁻ clone (gray line), and MCC:GFP cells (bold line). The isotype control is shaded (E) ICAM-1 expression on MCC:GFP (bold line) compared to B7-1^{hi} Ltk⁻ (gray line). Isotype control is shaded (F) GFP-tagged MCC:I-E^k is uniformly distributed on the surface of the MCC:GFP cells.

The ability of the MCC:GFP cells to activate T cells was also assessed. Since the amount of MCC – loaded I-E^k on the cells is fixed, the number of antigen presenting cells per well was titrated to generate a dose response curve. Using a standard 72 hour ³H-thymidine incorporation assay, the MCC:GFP cells induced proliferation of naive AD10 T cells in a dose dependent manner (Figure 5D). The expression of cell surface phenotypic markers of T cell activation as well as intracellular cytokine levels was assessed by flow cytometry. For these studies, the AD10 T cells were activated *in vitro* for 6 – 8 days prior to the initiation of the 18 hour experiments. The T cells incubated with the MCC:GFP cells for 18 hours showed increased expression of CD69 (Figure 5A) along with down-modulation of the TCR (Figure 5B), both hallmarks of T cell activation. These cells also showed increases in intracellular effector cytokines such as TNF- α (Figure 5C), IL-2 and IFN γ (data not shown).

The FACS data suggested that the MCC:GFP cells express unlabelled wild type I-E^k in addition to the MCC:I-E^k:GFP fusion protein. To assess the ability of the wild type I-E^k to present antigen, the cells were exogenously loaded with 20 μ M Hb₆₄₋₇₆ peptide and used to present antigen to Hb:I-E^k specific T cells from the 3.L2 TCR transgenic mouse. These Hb-loaded MCC:GFP cells were capable of inducing down-modulation of the 3.L2 TCR (Figure 6B) as well as inducing the dose-dependent proliferation of naive 3.L2 T cells (Figure 6A). This response is antigen-specific, as the MCC:GFP cells induce TCR down modulation on the Hb-specific 3.L2 T cells only when Hb peptide is present (Figure 6B).

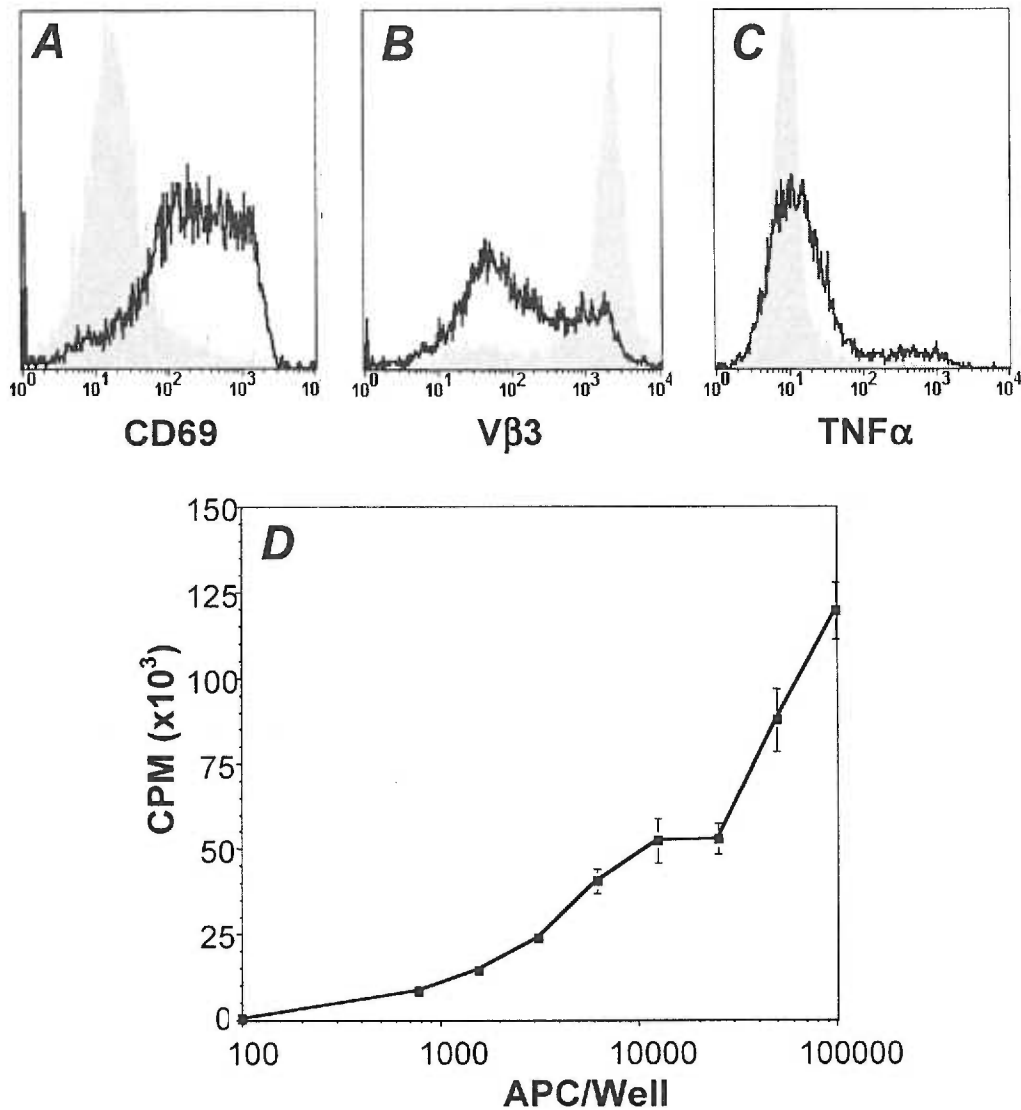


Figure 5. MCC:GFP cells induce full activation of AD10 T cells.

(A - C) *In vitro* activated AD10 T cells were cultured for 16 hours with MCC:GFP cells before staining with anti-CD69 (A), anti-Vβ3 to measure TCR down-modulation (B), or intracellular anti-TNFα (C) Line indicates cells incubated with APC, shaded histograms are unstimulated controls. (D) Results of 72 hour ³H-thymidine incorporation assay showing MCC:GFP cells induce proliferation of primary AD10 T cells in a dose-dependent manner.

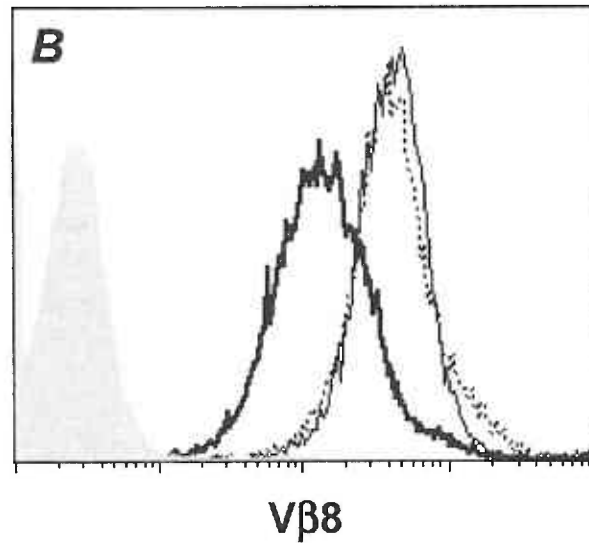
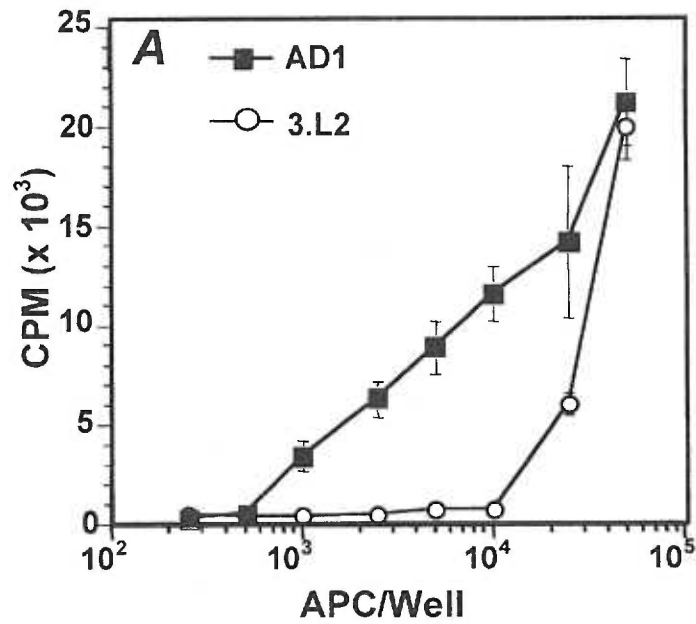


Figure 6. MCC:GFP Cells pulsed with Hb peptide stimulate 3.L2 T cells.

(A) Proliferative response of AD10 T cells to MCC:GFP cells (■) and 3.L2 T cells to 20 μ M Hb peptide-pulsed MCC:GFP cells (○) as measured in a 72 hour [³H] thymidine incorporation assay. (B) TCR down modulation on 3.L2 T cells after a 16 hour incubation with MCC:GFP cells alone (dotted line) or 20 μ M Hb-peptide pulsed MCC:GFP cells (bold line). Unstimulated cells (thin line) are shown for comparison. The isotype control is shaded.

Synapse Formation is a Dynamic Process

Having established that the MCC:GFP cells induce full activation of AD10 T cells, we went on to characterize the interaction of the T cells and MCC:GFP cells and to determine whether an observable immunological synapse forms during that interaction. To assess the potential redistribution of the GFP-tagged MHC:peptide complexes and monitor the morphology of T-APC interactions, alternating fluorescent and differential interference contrast (DIC) images were obtained using the API DeltaVision wide field microscopy system.

The interactions of the T cell and the APC are complex and dynamic but from observing more than 500 interactions, a consistent pattern emerged. First, T cell migration usually ceases after the T cell makes initial contact with the APC. This initial interaction of the T cell and the APC is generally mediated by a slender membrane projection from the leading edge of the T cell that interacts with the membrane of the APC (Figure 7). This is followed by distinct morphological changes of the T cell resulting in tight adherence and flattening against the APC, dramatically increasing the contact area. This typical flattened appearance served as the basis for selecting fixed T-APC conjugates for further examination of potential immunological synapses. When a 3D reconstruction of the interface of the T cell and the APC is made, we often observed that a peripheral ring on the T cell appeared to be pushing against the APC membrane resulting in a bulging out or “blistered” appearance of the APC membrane within this ring (Figure 8). This appearance is consistent with a model of immunological synapse formation predicted by Dustin and colleagues (49, 118, 119) (Figure 8D), which proposed that the T cell actin cytoskeleton would

generate a “protrusive” force against the APC membrane, and the observed formation of a polymerizing actin ring at the periphery of a T cell interacting with anti-CD3 on a glass coverslip (85).

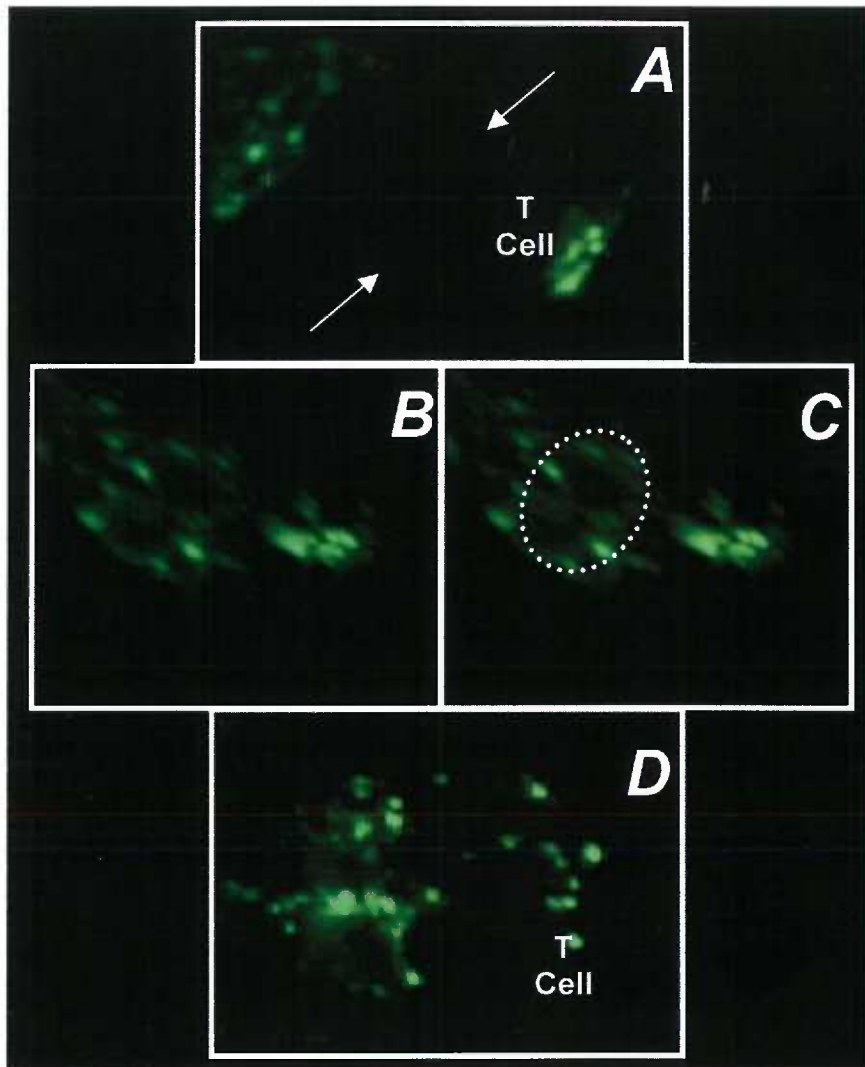


Figure 7. Fixation catches early events in the process of synapse formation.

AD10 T cells and MCC:GFP were incubated for 30 minutes at 37° before fixation. (A) Very early interaction between T and APC shows faint GFP “strings” projecting from the APC to the T cell. The accumulation of MHC opposite the interface is a common feature. (B-C) The same interaction rotated 45° to show the ring of small MHC clusters at the interface. The dotted line in (C) delineates this ring. (D) A second interaction showing a large triangular membrane flap from the APC covering a portion of the T cell. At various points along where the APC and T cell are interacting, small GFP clusters are visible.

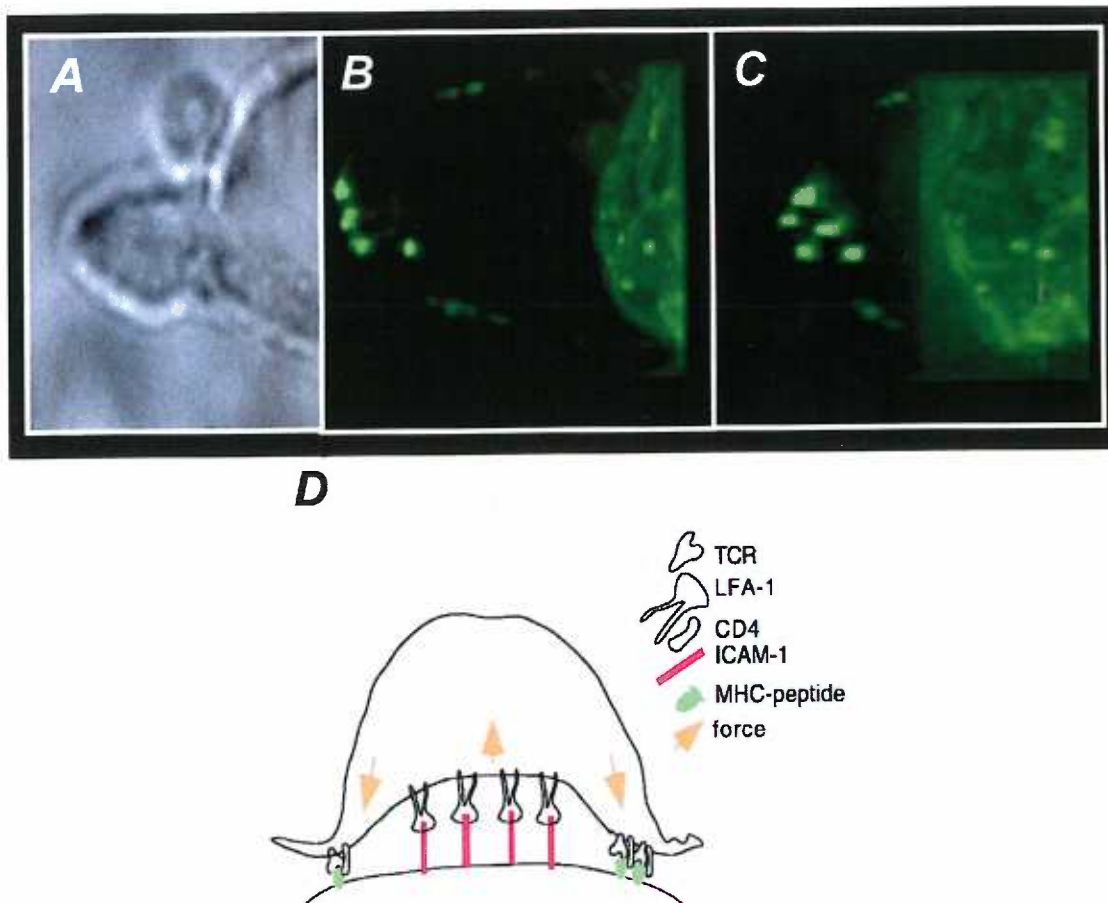


Figure 8. T cell induced deformation of the APC membrane during initial T-APC interactions.

(A) DIC image of a T cell interacting with an APC. (B and C) Fluorescent images of the T-APC interaction showing bulging of APC membrane under the T cell. This interaction is in the early stages because there is essentially no MHC redistribution at the interface (white arrow). The “blistered” region of the APC membrane lies within the periphery of the T cell interface. Note the GFP clusters found on the backside of the T cell, even at this early time point of the interaction (yellow arrow). (D) These images confirm a model of early interaction predicted by Grakoui *et al.* (49).

Within approximately 0.5 – 1 minute of the first contact, and concomitant with the morphological changes of the T cell, small spots with increased GFP fluorescence become visible at several locations along the T-APC interface (Figure 9). The appearance of these MHC clusters is antigen specific because no similar structures are observed when the Hb-specific 3.L2 T cells encounter these same APC (see below, Figure 23). Over the next several minutes, these small clusters intensify, indicating the accumulation of specific MHC molecules. In fixed T-APC conjugates, these small clusters form at multiple sites along the interacting regions of the T cell and the APC (Figure 7). These spots ultimately coalesce into a very bright (Figure 9), stable, compact structure with significantly increased MHC density that co-localizes with PKC- θ (Figure 24I), characteristic of a mature immunological synapse. On average, this process takes 5.5 minutes from first contact to mature synapse formation (range is 3 – 20 minutes).

An example of the dynamic nature of T-APC interactions and synapse formation is seen in Figure 10. In this set of images, a polarized T cell with a highly active leading edge approaches an APC and over a 2.5-minute period appears to sample or “scrub” the surface of the APC without forming a tight conjugate. At 2:37 after initial contact, a small MHC cluster appears within the T cell’s highly active leading edge (indicated by an arrow). As the T cell continues to scrub the APC surface, this small spot intensifies and migrates toward the center of the T- APC interface. At the interface, this cluster intensifies and eventually forms a mature synapse. For the duration of the imaging, the T cell membrane at the interface with the APC continues to be highly active as previously described (108). This scrubbing morphology is commonly exhibited even after the formation of the mature synapse and clearly demonstrates the

dynamic nature of the early interactions between T cells and APC not visible with fixed conjugates, planar lipid bilayers, or reports utilizing manipulated grayscale intensities of GFP rather than raw images.

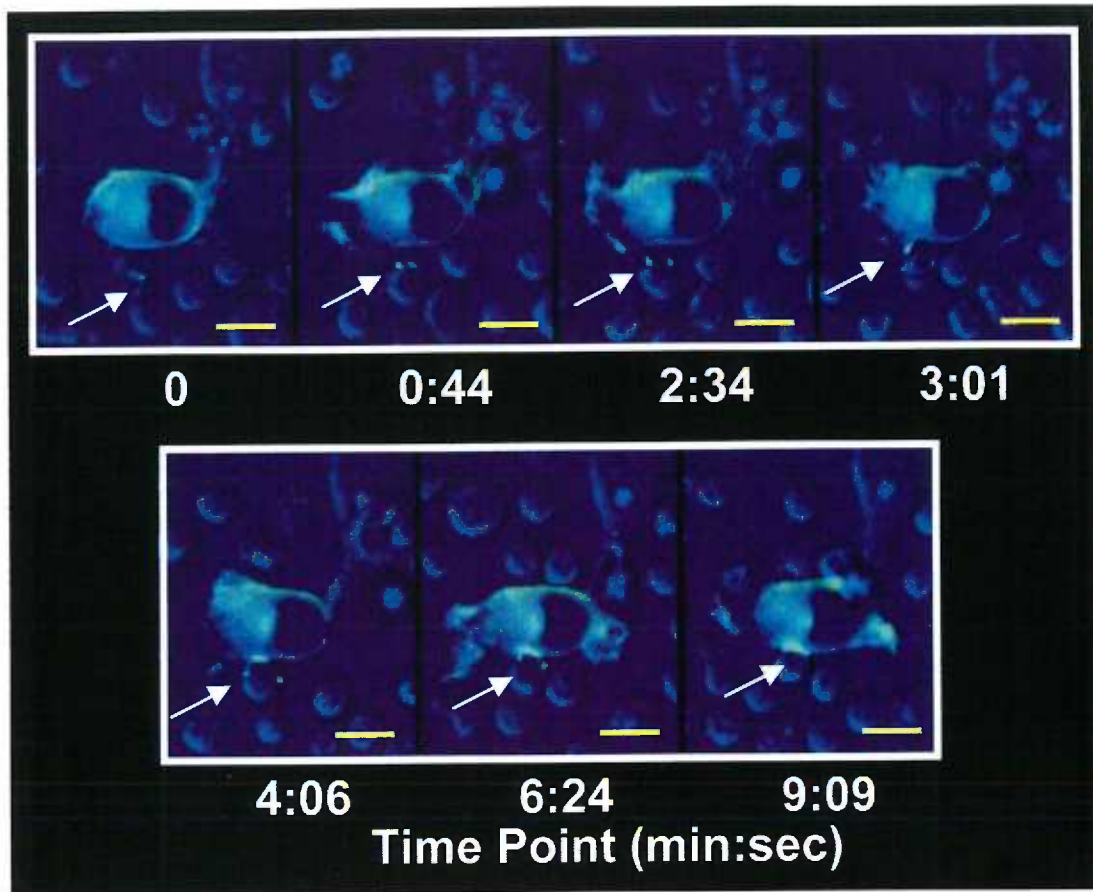


Figure 9. Small clusters of redistributed MCC:I-E^k:GFP form at T-APC interface that coalesce into mature immunological synapse.

To follow the interaction of *in vitro* activated AD10 T cells and MCC:GFP cells resulting in synapse formation, alternating GFP and DIC images were captured with an image capture frequency of 12 seconds. Images contain a composite overlay of GFP images (green) with DIC images (pseudocolored blue). Small MHC clusters appear at the T-APC interface soon after interaction that intensify and ultimately coalesce to form a mature immunological synapse. Images obtained at 400X, Bar = 10 μ m.

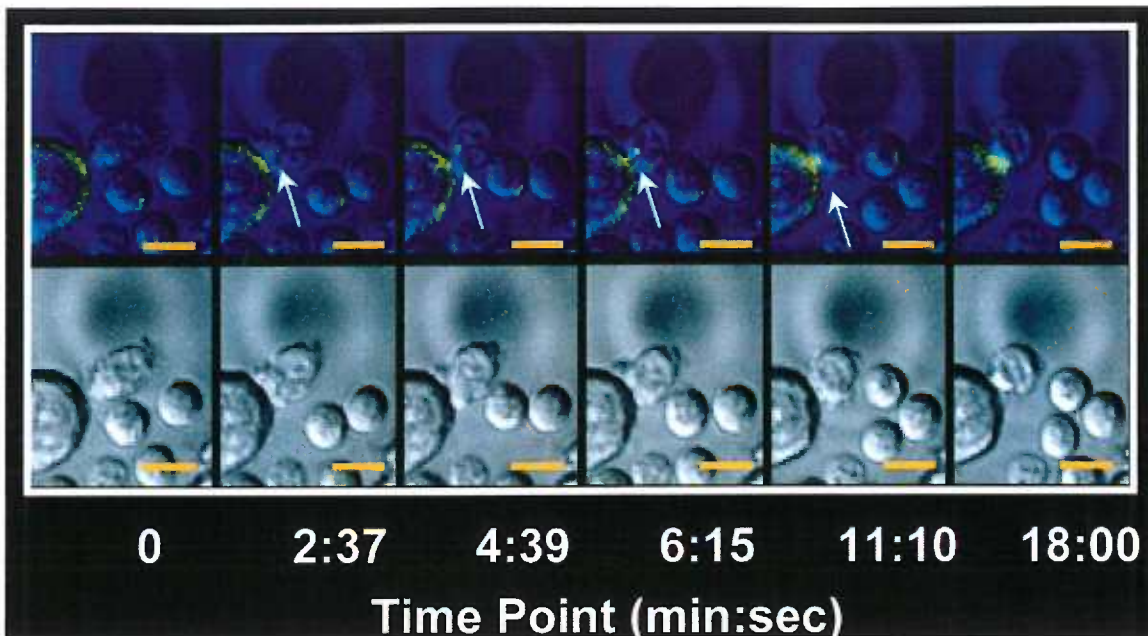


Figure 10. Formation of the Immunological Synapse is a dynamic process.

The approaching *in vitro* activated AD10 T cell has very active leading edge that makes contact with APC. The nascent synapse is visible within the highly active lamellipodia of the T cell after initial contact (arrow). The leading edge of the T cell maintains a high degree of activity for the duration of observation which in real time displays “scrubbing” morphology (See movie 10 on CD). Lower images are DIC only pictures showing morphologic changes during T-APC interactions. Images obtained at 400X, Bar = 10 μ m.

The Role of the Cytoskeleton in Synapse Formation

The dynamic T cell morphological alterations exhibited upon T – APC interactions clearly displayed in the scrubbing morphology images suggests that active cytoskeletal rearrangements are involved in the process of immunological synapse formation. Using pharmacological inhibitors or T cells from *Vav*^{-/-} mice, Wülfing and colleagues have shown that the bulk flow of membrane proteins across the T cell surface to the T-APC interface and subsequent normal accumulation of MHC molecules in the synapse requires rearrangement of the actin cytoskeleton driven by members of the myosin II protein family (94, 131). To confirm the previous reports and show that synapse formation in my system is also dependent upon actin-cytoskeleton rearrangements, the T cells were pretreated with colchicine to inhibit microtubule rearrangements or I pretreated the T cells or the APC with cytochalasin D to block actin polymerization. The data shows that when the APC was pretreated with cytochalasin a normal synapse formed (Figure 11 B), but when actin rearrangements were blocked in the T cell, small, stable spots appeared that never accumulated more MHC (Figure 11D). Colchicine treatment of the T cells had little or no effect on synapse formation (Figure 11C). Thus, while the formation of the small synapse precursor clusters appears to be independent of the cytoskeleton, the aggregation of these clusters to form a mature immunological synapse is driven by the active rearrangements of the T cell actin cytoskeleton. The microtubule network within the T cell and the actin cytoskeleton within the APC are not necessary for synapse formation. The formation of the small spots when the T cells were cytochalasin D treated is in agreement with Dustin's hypothesis that early in the

process of synapse formation, the formation of small ligand-bound TCR clusters may be independent of the T cell cytoskeleton (119).

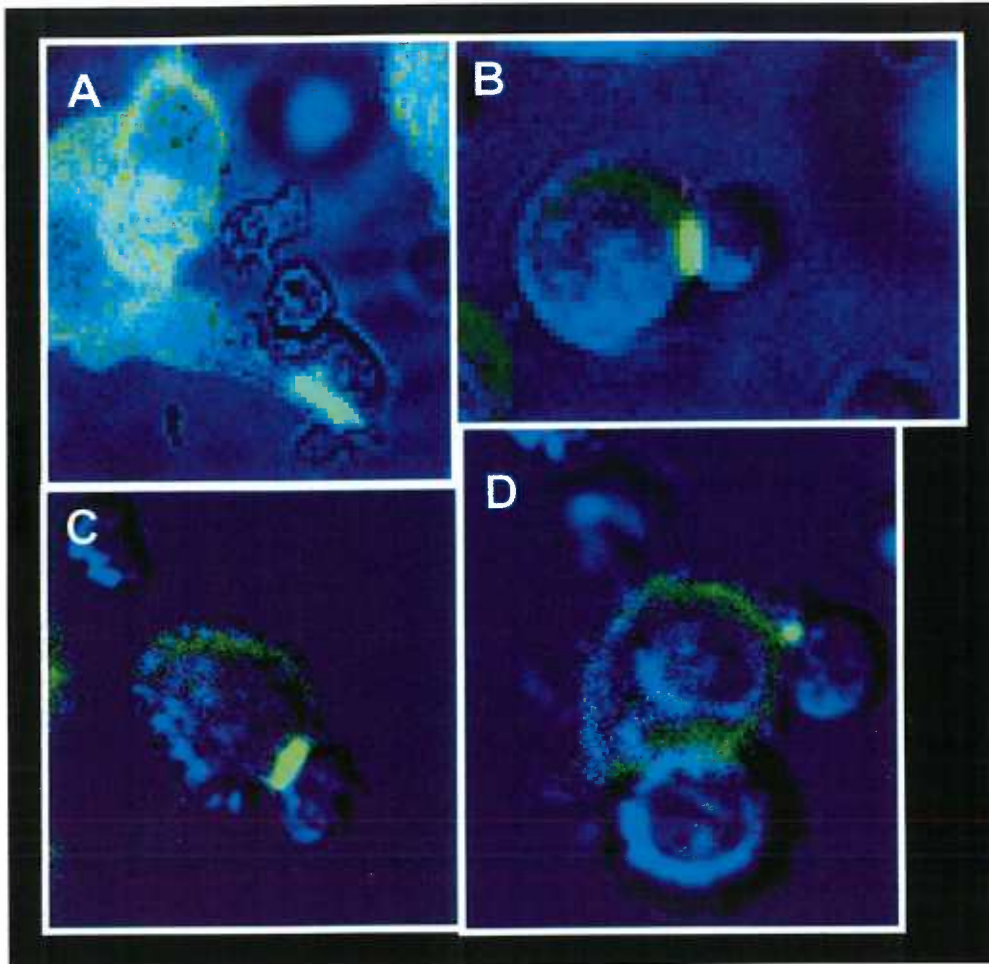


Figure 11. Synapse formation involves actin cytoskeleton rearrangement within T cells.

When compared to the control (A), treatment of AD10 T cells with 20 μM cytochalasin D (D) alters synapse size, intensity and morphology while 20 μM colchicine treatment of T cells (C) does not significantly alter synapse formation. 20 μM Cytochalasin D treatment of APC (B) has no effect on synapse formation.

Movement of the Synapse With T cell Migration and Class II Transfer to T cells

While many of the T-APC interactions were static for more than 45 minutes (the duration of imaging), in 25 – 30 % of the conjugates movement of the T cell across the APC resumes after synapse formation. Similar movements have been previously described (145, 146) but these studies did not examine the fate of the immunological synapse. I followed the movement and status of the immunological synapse during this T cell migration and observed that as the T cell migrates across the surface of the APC, the synapse moves along with it. For example, in Figure 12A the T cell interacts with the APC and forms a mature synapse after approximately 5 minutes. At that point (labeled time 0), the T cell re-initiates locomotion across the APC and the synapse itself moves along with the T cell; more than 24 μm over a period of 13 minutes and 48 seconds period. This is the first demonstration that migration of T cells across an APC includes the attendant movement of a mature immunological synapse.

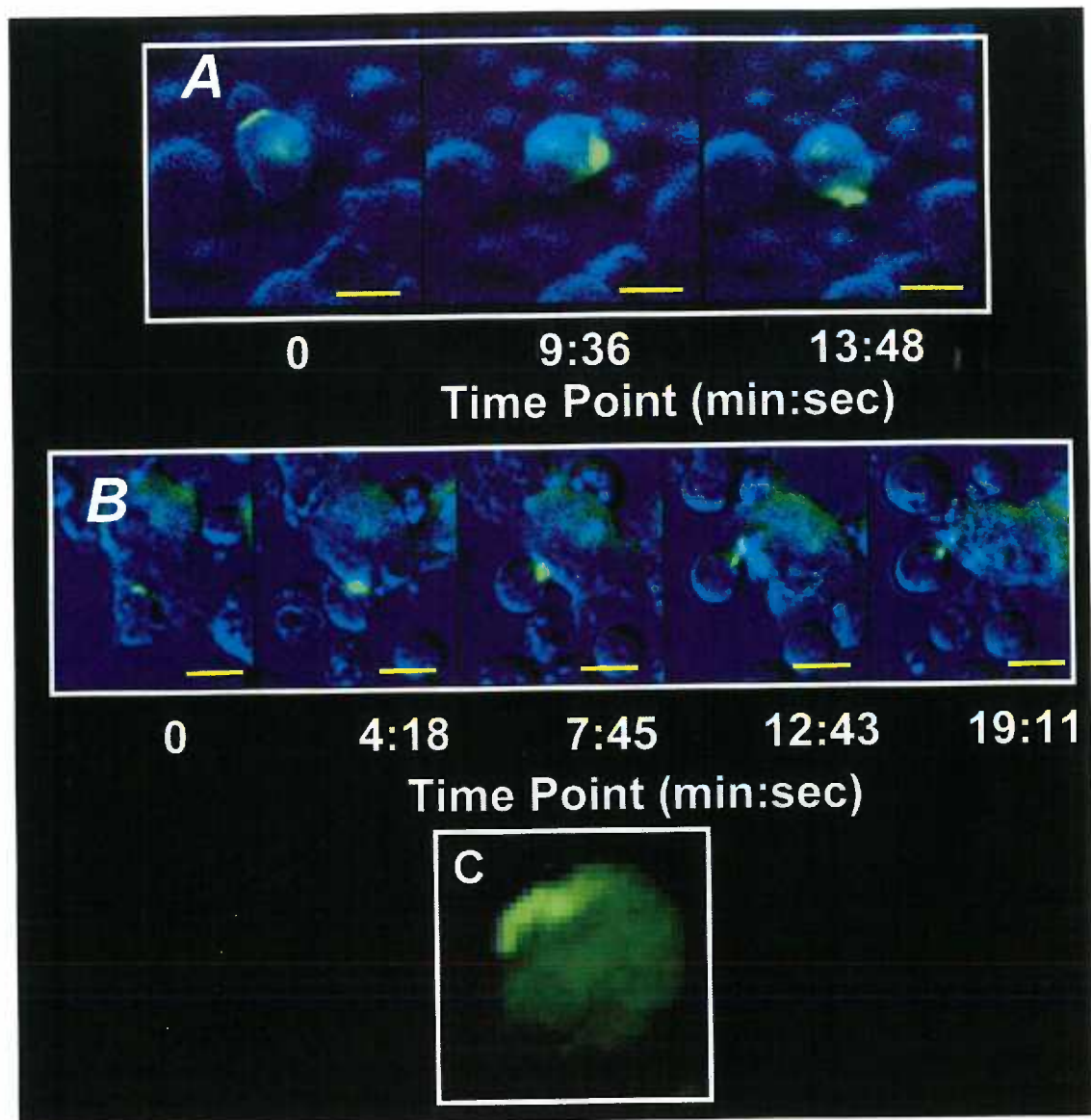


Figure 12. The Immunological Synapse moves with T cells as they migrate across APC and dissociating T cells capture MHC from the synapse.

(A) Movement of the T cell across the surface of the APC is associated with the movement of the mature immunological synapse. GFP (green) image is overlaid on DIC (blue) image. In 13 minutes, the synapse has moved a total of 24 μm . (B) The T cell and associated synapse migrate 8.6 μm across the APC. The T cell then dissociates from the APC and captures MHC:peptide complexes directly from the immunological synapse. The spot on the APC diminishes significantly while the MHC spot transferred to the T cell remains unchanged. (C) Transferred GFP-tagged MHC is present on the surface of T cell 4 hours after removal of MCC:GFP cells. Images obtained at 400X, Bar = 10 μm .

MHC Capture from the Synapse

During the 45 minute imaging period, T cells dissociate from the APC in approximately 10% of interactions. When this occurs, transfer of MCC:I-E^k:GFP molecules from the synapse to the T cell is commonly observed (Figure 12B). The series of images in Figure 12B illustrates such a “life cycle” of an immunological synapse. By 4 minutes and 18 seconds after contact, a mature immunological synapse has formed and the T cell begins migrating across the APC dragging the synapse with it. When the T cell stops migrating and dissociates from the APC at 12:43, the synapse itself has moved a total of 8.6 μm . There is clearly a spot of GFP on the T cell captured directly from the immunological synapse. Over the next 7 minutes, the spot on the T cell remains unchanged in size and intensity, but the spot remaining on the APC dramatically diminishes in intensity. This is consistent with the fact that immunological synapse formation is driven by the T cell and that the APC plays a “passive” role, as shown by the differential effects of cytochalasin D treatment of T cells and APC (Figures 11B and 11D and (74). Acquisition of MHC by T cells during antigen recognition has been detected previously (147-150), but this is the first time transfer of specific MHC:peptide complexes from an immunological synapse to a CD4⁺ T cell has been observed directly.

The fate of the MHC:peptide complexes captured by the T cells was examined. Hwang and Sprent showed that transferred MHC class I molecules were internalized and degraded in the T cell within 1 hour of capture (150). However, Schlom and colleagues have demonstrated that the transfer of B7-1 to T cells after incubation with APC results in the ability of these T cells to present

antigen to other T cells up to 24 hours later (151). While they did not directly assess the transfer of MHC molecules or the potential fate of these molecules, the fact that these T cells could present antigen to fresh T cells without addition of exogenous antigenic peptide implied that they captured preformed MHC:peptide complexes from the APC and that they were still present on the surface of the T cells 24 hours later. To address the fate of the transferred MCC:I-E^k:GFP complexes, I incubated AD10 blasts with the MCC:GFP cells for 18 hours. After isolation, I cultured the T cells for an additional 96 hours and at various time points, I examined them for the presence of the transferred GFP tag by flow cytometry as an indication of transferred MHC. The cells were also stained with antibodies against I-E^k to detect surface-associated transferred MHC still on the cell surface and for the activation marker CD69.

As seen in Figure 13, the T cells continued to express detectable levels of surface I-E^k for up to 96 hours after they were removed from the APC. In parallel experiments with the non-specific 3.L2 T cells, there is no detectable transfer of GFP, indicating that the GFP transfer is due to antigen-specific recognition of the GFP-tagged MCC:I-E^k complexes on the APC (data not shown). At the earliest time points (0 and 1 hour) the amount of I-E^k on the surface of the T cells is relatively high and it drops by 2 hours to a plateau level approximately 37% lower than the initial time point (Figure 16). This suggests that some of the T cells are internalizing MHC early in the culture, but a significant and FACS-detectable level remains on the cells surface. A picture showing continued surface expression of the transferred MCC:I-E^k:GFP 4 hours after T cells were removed from the APC is shown in Figure 12C.

The I-E^k FACS profiles of the AD10 T cells pre-incubated with the MCC:GFP cells are bimodal, while the no APC control histograms are not (Figure 13). The GFP mean fluorescence intensity values for the whole population steadily increase on the cells initially cultured with MCC:GFP cells after 12 hours, even though there is no source of additional MCC:I-E^k:GFP present. This increase correlates with a relative time-dependent decrease in the numbers of I-E^{lo} cells and an increase in the I-E^{hi} population (Figure 13). The I-E^{khi} cells are also CD69⁺, indicating that they have been activated in the overnight culture (Figure 17). This general pattern was observed in 3 independent experiments and suggested that the GFP^{lo} T cells were dying during the extended culture period, while the GFP^{hi} cells were surviving. The relative shift in the population from equal numbers of GFP^{lo} and GFP^{hi} cells to a population dominated by the GFP^{hi} cells explains the increase in the MFI. To examine this possibility, in a single preliminary experiment Fas-mediated activation induced cell death was prevented by inclusion of a blocking anti-FasL antibody to the extended cultures. In those cultures, there was a bimodal distribution, but the relative sizes of the GFP^{hi} and GFP^{lo} populations were not significantly different over time (Figure 14). The relative percentage of the GFP^{hi} cells was 2 fold higher than the MCC:GFP preincubated cultures without the anti-FasL or the first 48 hours, thereafter dropping precipitously by 96 hours (Figure 15). During this same time frame, the I-E^k MFI also drops from its peak at 48 hours (Figure 15, 16). This data suggests that the shift in the GFP and I-E^k MFI over time is due to the selective death of the GFP^{lo} cells in the cultures. The cause of this phenomenon is unknown, but it clearly involves the Fas-mediated apoptosis of the GFP^{lo} cells.

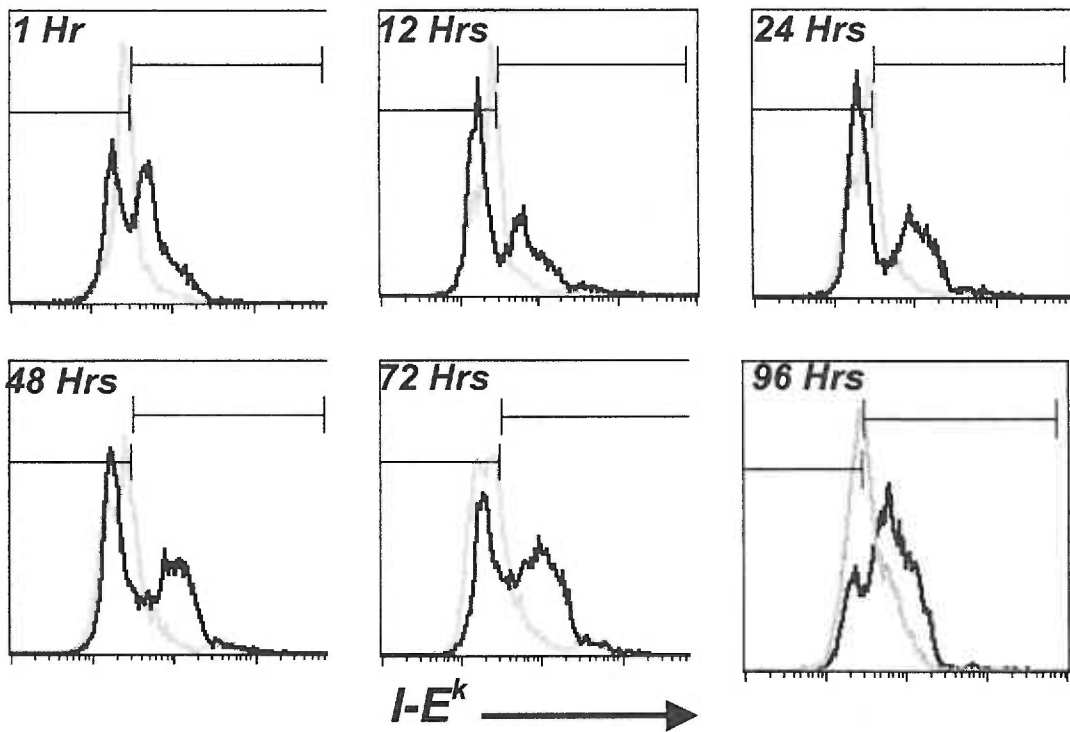


Figure 13. Transferred MHC:peptide complexes remain on the surface of T cells for up to 96 hours.

AD10 T cells were incubated with (black lines) or without (gray lines) MCC:GFP cells for 18 hours and before being isolated. They were cultured for an additional 96 hours and at the indicated time points, samples were stained for surface I-E^k expression. The transferred MHC is present on the cell surface for up to 96 hours. Note the I-E^{hi} and I-E^{lo} populations when the T cells were incubated with MCC:GFP cells. The I-E^{lo} cells over time, there is a gradual shift in the relative frequencies of these two populations.

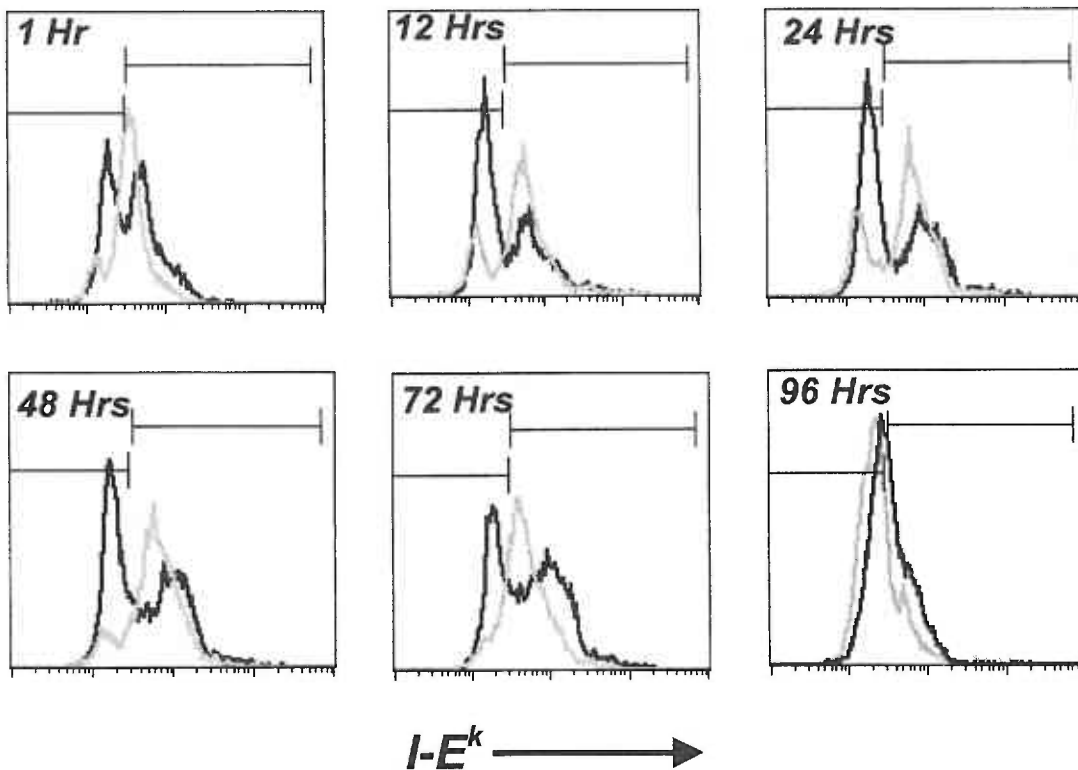


Figure 14. Blocking Fas engagement prevents loss of I-E^{lo} T cells.

Experiment is as described for figure 13 except that after removing T cells from MCC:GFP cells, T cells were cultured with (Gray lines) or without (black lines) blocking anti-FasL antibodies. In the untreated cultures, the I-E^{lo} cells are gradually lost over time, but they are maintained in the anti-FasL treated cultures.

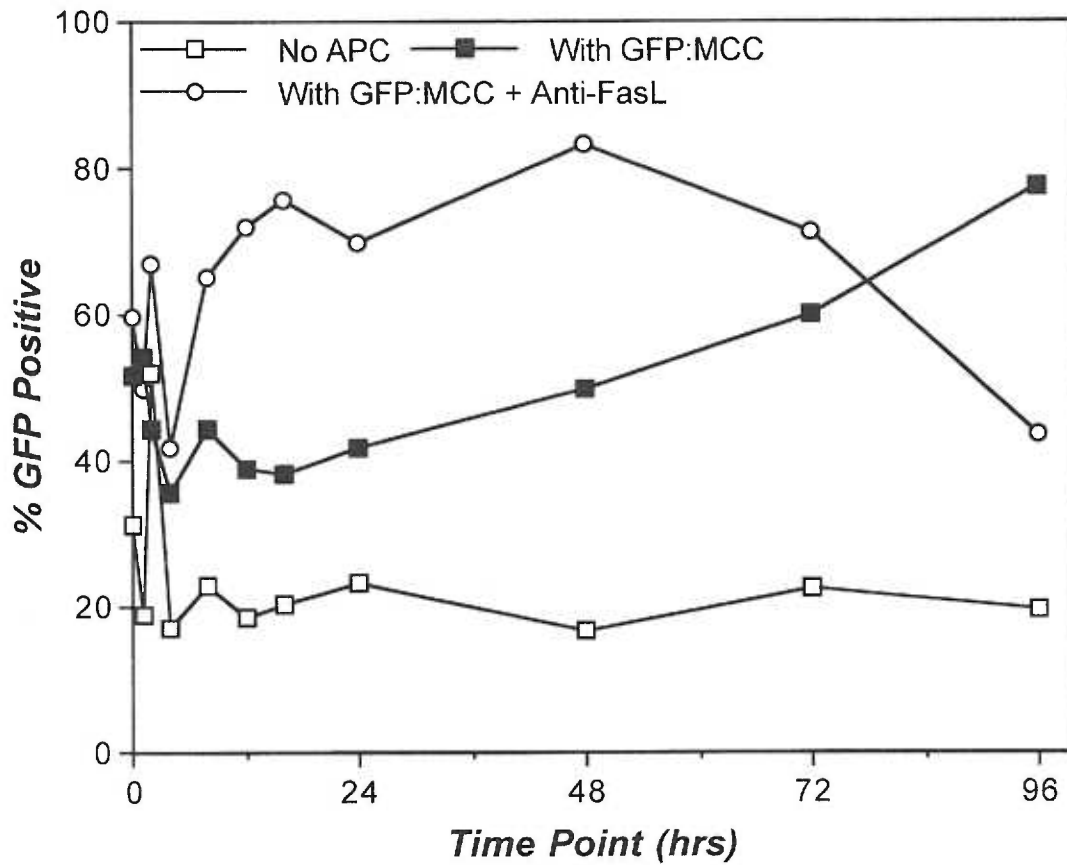


Figure 15. T cells incubated for 18 hours with MCC:GFP cells remain GFP⁺ for 96 hours.

T cells were incubated with MCC:GFP as described in Figure 13 and analyzed for GFP expression. Note the increase in GFP⁺ cells preincubated with GFP:MCC.

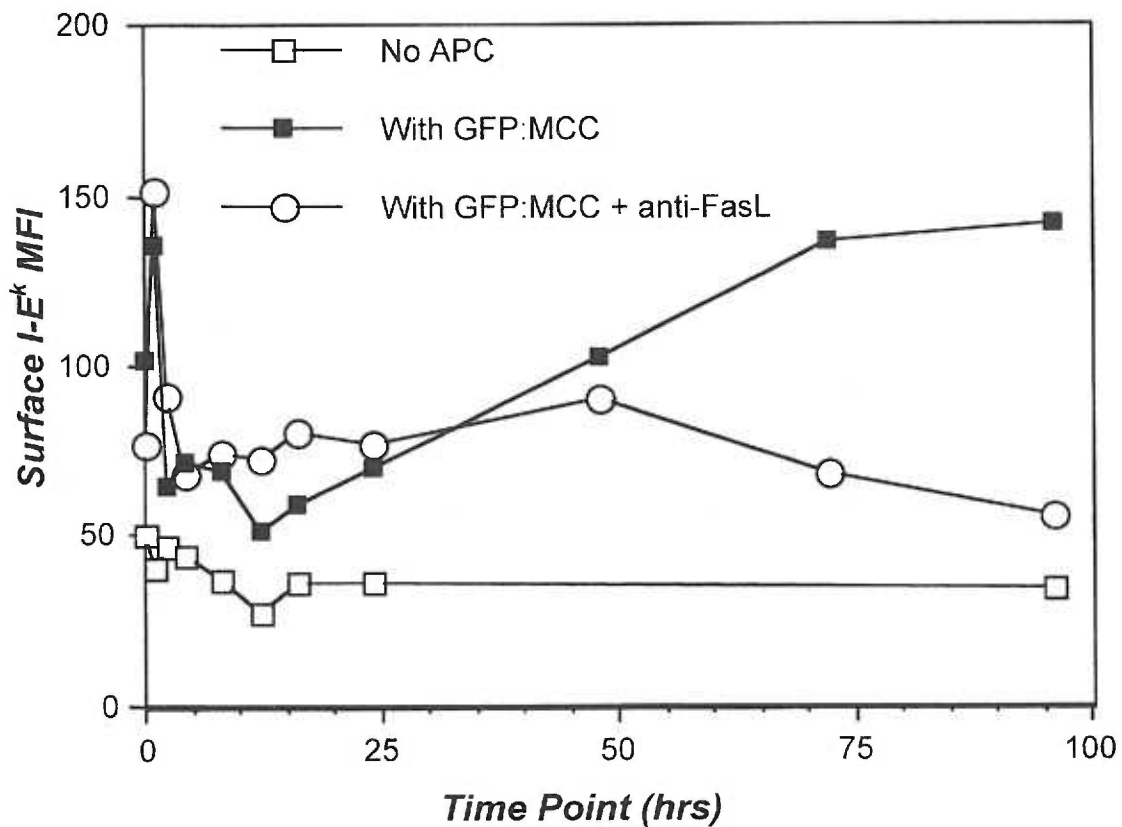


Figure 16. Apparent increase in I-E^k on T cells is due to Fas-mediated loss of I-E^{lo} cells.

The surface expression of I-E^k on the T cells after transfer drops significantly between 1 and 2 hours and then remains relatively stable for 96 hours. The apparent increase in I-E^k mean fluorescence intensity (MFI) is due to a selective loss of I-E^{lo} cells (Figure 13). Anti-FasL antibody prevents the loss of the I-E^{lo} cells, indicating that it is a Fas-mediated process.

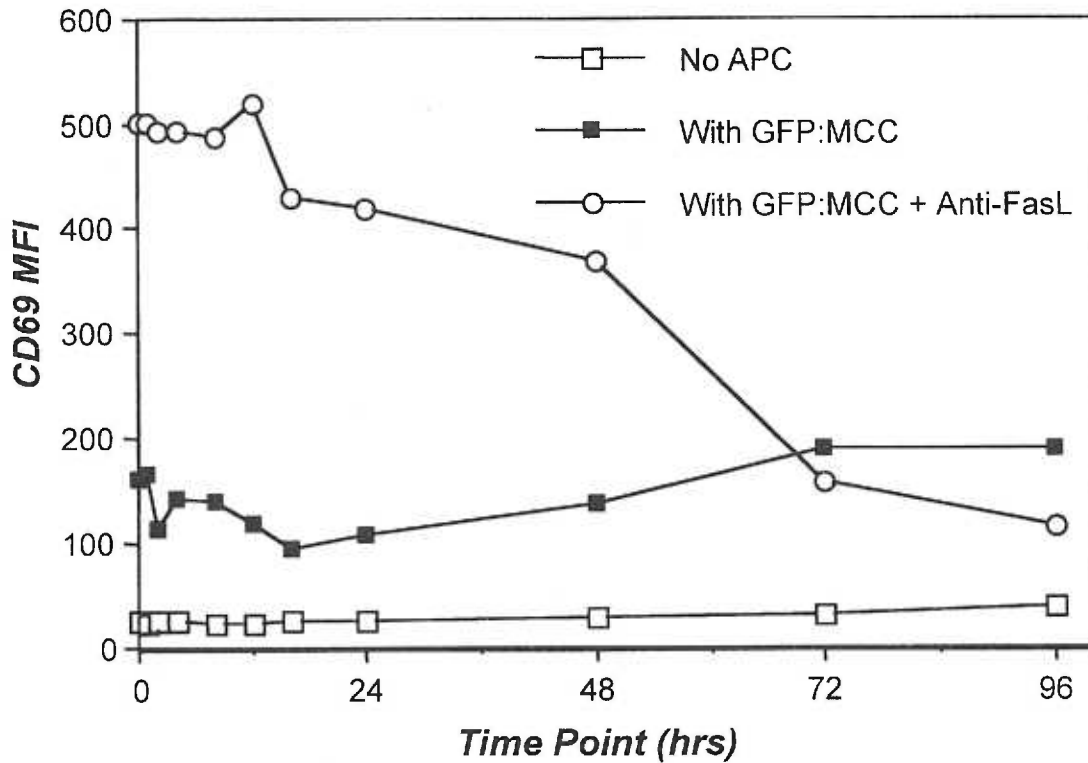


Figure 17. T cells capturing MHC:peptide complexes are CD69⁺

T cells were incubated with or without MCC:GFP cells for 18 hours before isolation and culturing, as described in Figures 13 and 14. In addition to I-E^k staining, cells were also stained for the activation marker CD69. The T cells exposed to MCC:GFP cells expressed higher levels of CD69 than T cells not incubated with APC. When anti-FasL was included in the cultures, CD69 expression was significantly higher up to 48 hours, presumably due to prevention of Fas-mediated activation induced cell death.

Stoichiometry of T:APC Interactions

In examining the immunological synapse, previous reports have relied extensively on transformed B cell lines to act as antigen presenting cells (50, 74, 94, 110, 111, 114, 115, 131). In those reports, individual APCs usually interact with only a single T cell (94). When we examined the interactions of the T cells with the APC in our system, the stoichiometry often varied from a 1:1 interaction. It was frequently observed that multiple AD10 T cells would interact with a single MCC:GFP cell and that mature immunological synapses would form at each interface with a T cell (Figure 18). This result was not as unexpected as the finding that a single T cell could simultaneously interact with multiple APC and induce the redistribution of MHC on each of those APC. Predictions from earlier experiments (94, 111, 144) would suggest that the polarization of the T cell cytoskeleton towards the interface of the T cell and APC would prevent multiple, simultaneous interactions. Figure 19A shows a series of images from live cell imaging where a single T cell interacts with two adjacent MCC:GFP cells and induces the redistribution of MHC on both APC. As the time progresses, the T cell appears to focus its “attention” on just one of the APC, subsequently forming a mature synapse, while the cluster with the other APC remains small. In over thirty of these interactions, when the 3D interfaces were reconstructed, one of the interfaces is clearly larger and is spatially organized to more closely resemble a mature synapse than the other (Figure 19D). That difference in size and organization between the two interfaces is a common feature.

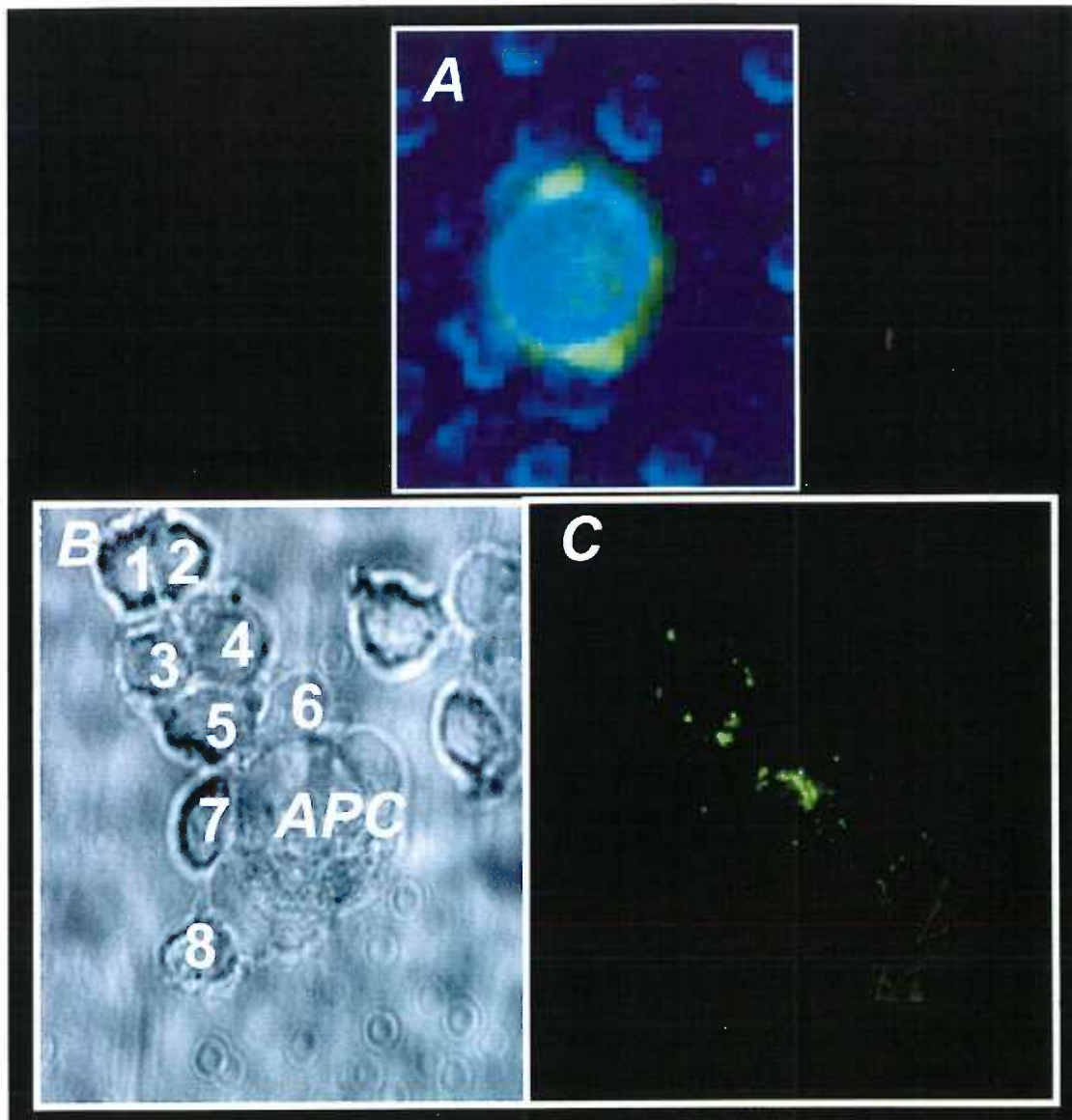


Figure 18. Multiple T cells can interact simultaneously with a single MCC:GFP cell and form immunological synapses.

(A) Live cell image showing 2 T cells interacting with a single APC, each making a mature immunological synapse. (B) DIC image of 8 individual AD10 T cells interacting with a single APC. A membrane projection from the APC bisects cell pairs 3/5 and 5/6 before terminating at 1/2. (C) Fluorescent image of the “stalk” of T cells showing the redistribution of MHC molecules to the interfaces of the T cells including formation of 2 mature immunological synapses.

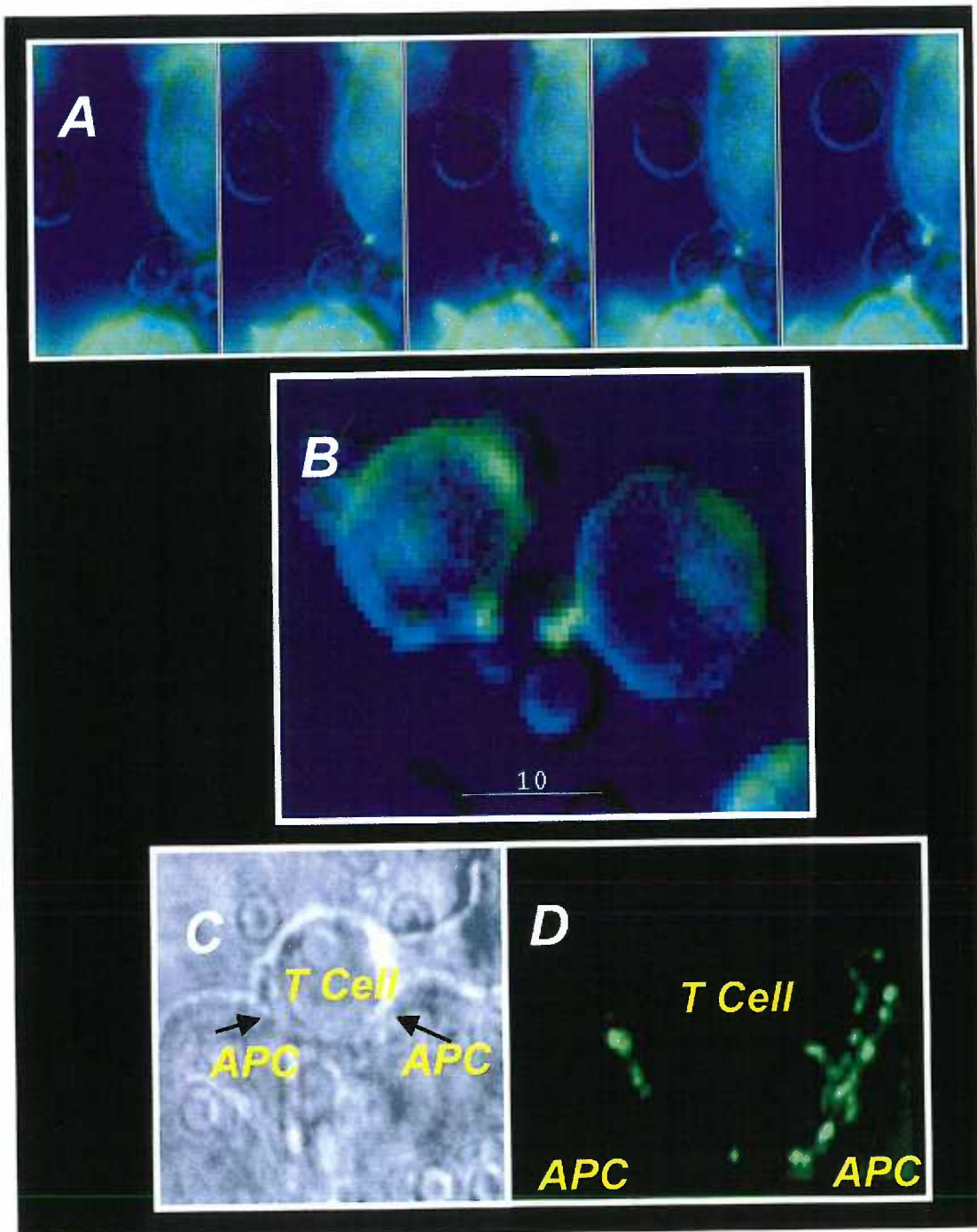


Figure 19. A single T cell can induce redistribution of MHC:peptide complexes on 2 adjacent APC, but forms a synapse with only 1 of them.

(A) Time series showing a single T cell inducing MHC redistribution on 2 adjacent APC. (B) A second live cell interaction showing a single T cell and 2 interfaces with redistributed MHC. (C) Fixed conjugate DIC image of a single T cell interacting with a pair of APC. (D) Fluorescent image of (C) showing MHC distribution and the unequal sizes of the accumulated MHC clusters. Mature immunological synapse is found only at the right interface.

Signaling and the Synapse

It has been proposed that the function of the immunological synapse is to facilitate the long-term downstream signaling within the T cell, which is necessary for full T cell activation. TCR-mediated tyrosine phosphorylation events can be detected within seconds after T-APC interactions, while it takes 30 seconds to 1 minute to observe the initial MHC redistributions, clearly demonstrating that the immunological synapse is not required for the initiation of intracellular signaling. This data also suggests that the formation of the immunological synapse is dependent upon signaling events within the T cell. It remains unknown which of the TCR-triggered intracellular signaling pathways are involved in the formation and maintenance of the immunological synapse. To address this, I examined the effects of specific pharmacological inhibitors of Ca^{++} increases, Src family tyrosine kinases (Lck and Fyn), and MEK (which blocks the MAPK pathway) on synapse formation and maintenance.

I began by examining the relationship between increases in intracellular Ca^{++} concentrations and the appearance of the immunological synapse. *In vitro* primed AD10 T cells were loaded with the ratiometric Ca^{++} indicator Fura-2 and added to plates containing MCC:GFP cells. I then followed the interactions of the T cells and APCs by digital microscopy to correlate initial T – APC interactions with the onset of intracellular signaling (as shown by Ca^{++} flux) and the formation of the immunological synapse. The image series in Figure 20 is representative of images collected in 9 separate experiments (over 100 T-APC interactions). In this series, three individual T cells interact with a single APC.

The initial contact between the T cell and APC is followed by a rapid

increase in intracellular Ca^{++} concentration within approximately 10 – 30 seconds (further time resolution is limited by image capture rate). The T cells rapidly flatten against the APC and within 30 seconds of the Ca^{++} flux (approximately 0.5 to 1 minute after initial contact) the initial MHC redistribution is visible. Finally, a full synapse forms 3 - 20 minutes after the initial contact of the T cell and the APC (average time is 5.5 minutes).

The temporal relationship between the Ca^{++} flux, T cell morphology alterations, and the mature immunological synapse is most clearly seen with the first T cell making contact with the APC. (Figure 20). Within 18 seconds of contact, there is a large increase in the intracellular concentration of Ca^{++} . By 1:59 the T cell morphology has undergone a dramatic change. The T cell is flattened against the APC increasing the contact area between the cells and a large cluster of redistributed MHC is visible at the T-APC interface. A mature synapse is formed by 7:40 and is maintained for the duration of imaging (approximately 19 minutes).

The relationship between the intracellular Ca^{++} increase and formation of the immunological synapse is best exemplified by the second T cell interacting with the APC in Figure 20. This T cell makes contact with the APC at 7:40 and 10 seconds later there is a large increase in intracellular Ca^{++} concentration. In the GFP+DIC image at this time point, a small MHC cluster is visible at the point of contact between the cells. Over the next 1:50, several smaller spots have merged and this cluster has intensified significantly; however, it is still relatively small compared to the mature synapse on the adjacent T cell. By 13:03, 5:23 after initial contact, a mature synapse has formed at the interface of this T cell and the APC. The Fura-2 ratios for each of these T cells along with the mean are plotted in

Figure 21. The open arrows indicate the time at which the first distinguishable MHC clusters formed and the closed arrows indicate the formation of the mature immunological synapse. This data shows that the initial visible MHC redistribution occurs simultaneous with, or shortly after intracellular Ca^{++} concentration increases. Mature synapse formation follows minutes later.

To determine the necessity of these increases in intracellular Ca^{++} in T – APC interactions and synapse formation, T cells were loaded with the Ca^{++} chelator BAPTA. After 50 μ M BAPTA loading, the T cells were motile and clearly viable, but very few interacted with APC (data not shown). When a few T cells did interact with the APC, the interactions were brief and there were no T cell morphological changes that would indicate that antigen recognition was occurring. This suggests that the Ca^{++} flux is required for the morphological changes that occur upon antigen recognition, in agreement with previous reports (106). Without the Ca^{++} increase, there was no observable MHC redistribution, no synapses formed and the T – APC interactions were nearly indistinguishable from the interactions between non-specific 3.L2 T cells with the APC. Thus, the increase in intracellular Ca^{++} occurs before, or simultaneous with, the initial redistribution of MHC and the Ca^{++} flux and the Ca^{++} - dependent morphological changes in the T cell upon antigen recognition are required for the formation of the immunological synapse.

To address the potential role of the MAP kinase pathway in the interactions of the T cells and APCs and their subsequent synapse formation, I loaded T cells with the MEK inhibitor PD98059 (2-(2'-amino-3'methoxyphenyl)-oxanaphtalen-4-one) (140) at 5 μ M, to block MEK activity. Under these conditions, the T cells interacted with the APC and underwent morphological changes that

are characteristic of normal antigen recognition. When compared to the DMSO only controls, the Ca^{++} flux in these cells was of normal magnitude and occurred with normal kinetics. MHC redistribution was clearly observable at the T – APC interface in more than 50% of the conjugates, but mature immunological synapses formed in less than 10% of the interactions. In contrast to the control conjugates, the PD98059 loaded T cells, which initially flattened against the APC and induced some MHC redistribution, rounded up and prematurely detached from the APC (Figure 22A). Thus, it looks as though MEK activity is not required for the initial interactions of the T cell, the Ca^{++} flux, or the initial MHC redistributions, but it is required to maintain the tight interaction of the T cell and the APC and appears to be crucial for the formation of the synapse. It is not clear whether MEK functions directly on the nascent synapse to mediate cluster aggregation or whether its effects are exerted through the ability to maintain a tight association between the T cells and the APC to allow synapse formation.

Finally, to assess the role of Src family kinases (p56^{Lck} , p59^{Fyn}) in T – APC interactions and the formation of the immunological synapse, T cells were loaded with the Src inhibitor PP2 (141). While Src activation is completely blocked at 100 μM PP2 (141), I used 50 μM to limit potential toxicity to the T cells. Under these conditions, ~66% of the T cells interacting with an APC underwent a morphological change which indicated that they were recognizing antigen. Interestingly, these cells did not take on the normal flattened appearance that is typically observed. Rather, they remained essentially round with just the leading edge slightly deforming against the APC surface (Figure 22B). In approximately 50% of the interactions, the T cells showed an increase in intracellular calcium,

but the magnitude of the flux was significantly reduced from the control or PD98059 treated T cells (data not shown).

The redistribution of MHC in these interactions was also clearly affected by blocking Src kinase activity. In approximately 77% of the interactions, there was some clustering of MHC, but in only ~10 % of cases did this lead to the formation of a mature immunological synapse. In the remaining cells, the clusters never coalesced into a mature synapse or they never showed any MHC clustering (~23%) at all. It is an important caveat to note that at this drug concentration I may not be completely inhibiting Src activity, but under these conditions it appears that the activity of Src family kinases (p56^{Lck}, p59^{Fyn}) is necessary for the normal morphological changes that occur during antigen recognition. Their activity is also required for the formation of a full synapse, but doesn't appear to be necessary for the formation of the small MHC clusters.

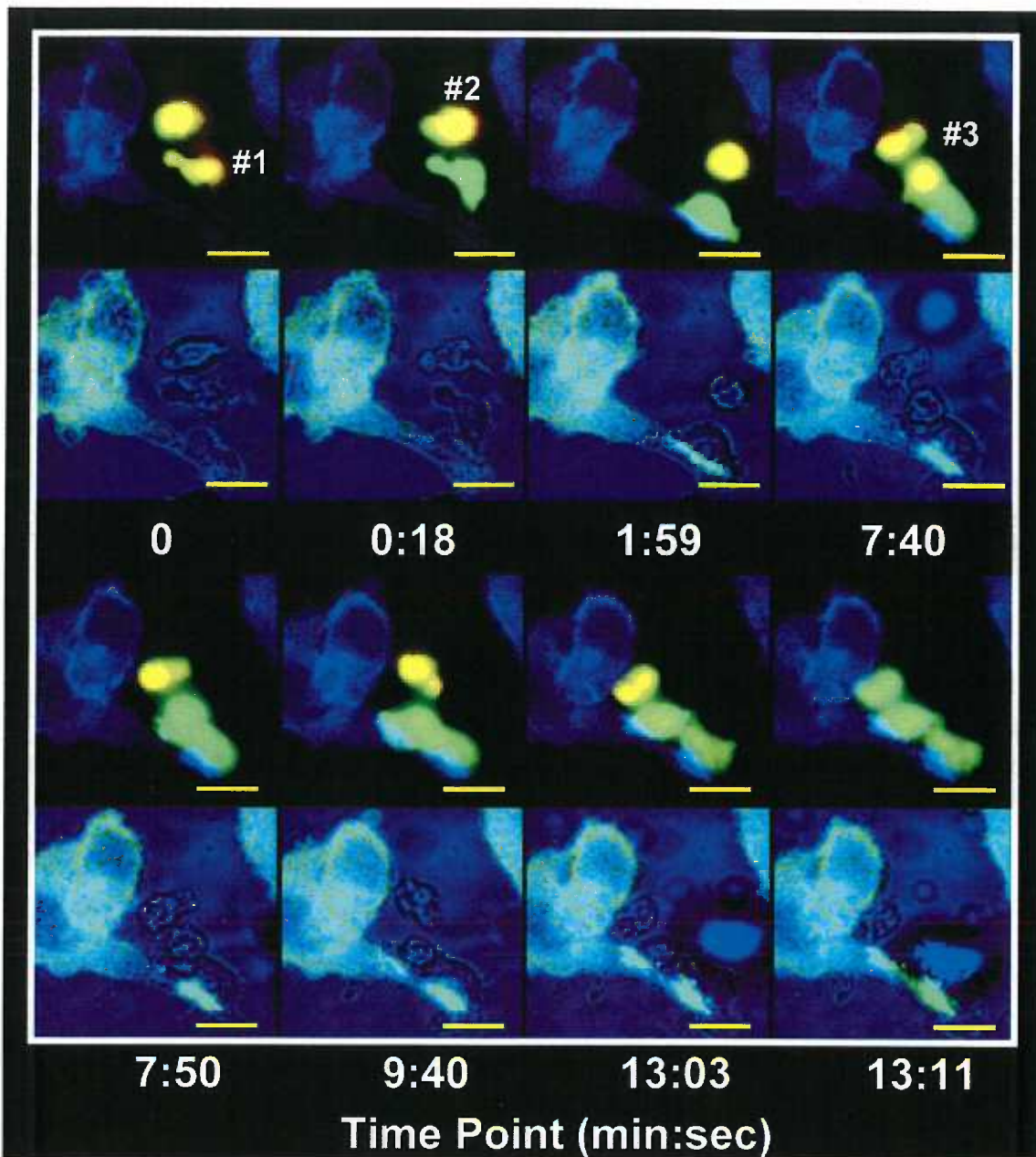
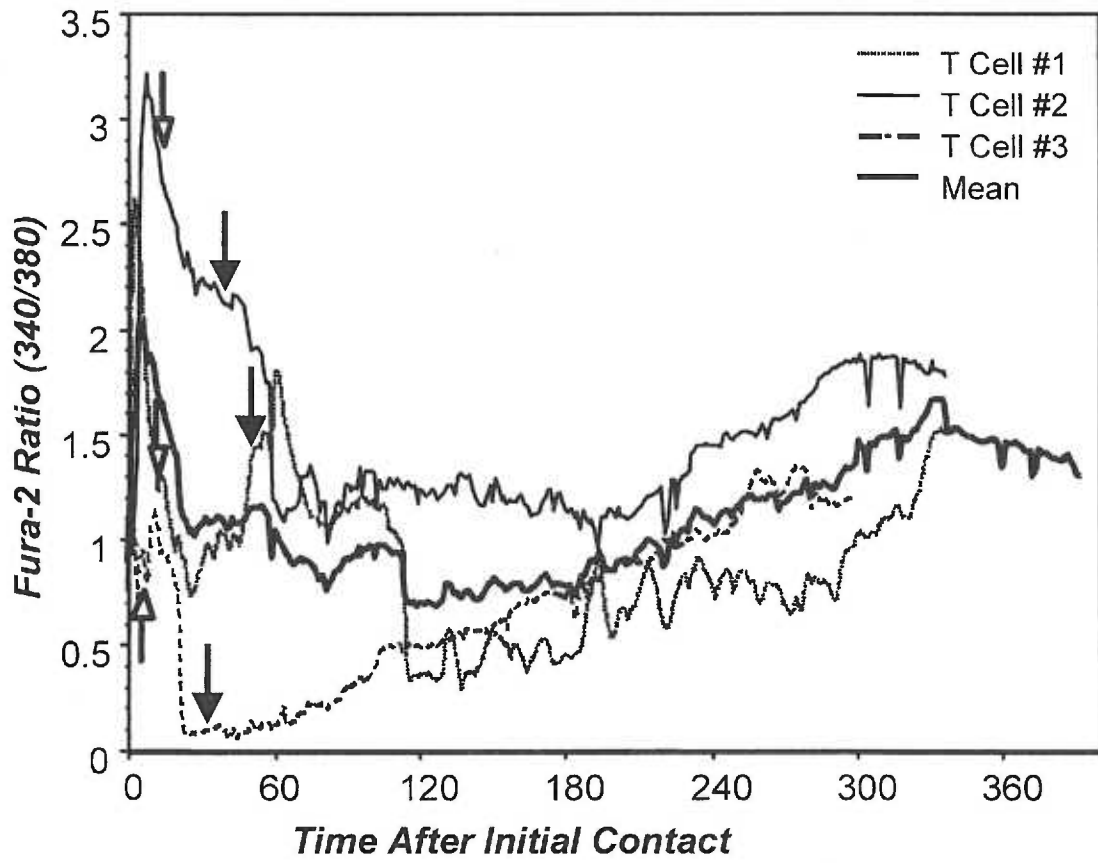


Figure 20. Ca^{++} flux within the T cell precedes synapse formation.

Three Fura-2 loaded AD10 T cells make contact with the APC and flux Ca^{++} within 30 seconds of contact. Ca^{++} flux occurs immediately before, or concurrent with, the first visible MHC clusters and several minutes before mature immunological synapse formation. In the top set of images, Fura-2 is imaged in green (340 nm) and red (380 nm), which are overlaid to form a yellow color in the non-activated T cells. When intracellular Ca^{++} concentrations increase, the 340 nm signal increases and the 380 nm signal decreases resulting in a color shift from yellow to green. The GFP on the APC is pseudocolored blue and synapses are visible as bright blue regions at the T - APC interface. To better visualize synapse formation, in the bottom images fluorescent (green) and DIC images (blue) are overlaid. Images obtained at 600X, Bar = 10 μm .



R2

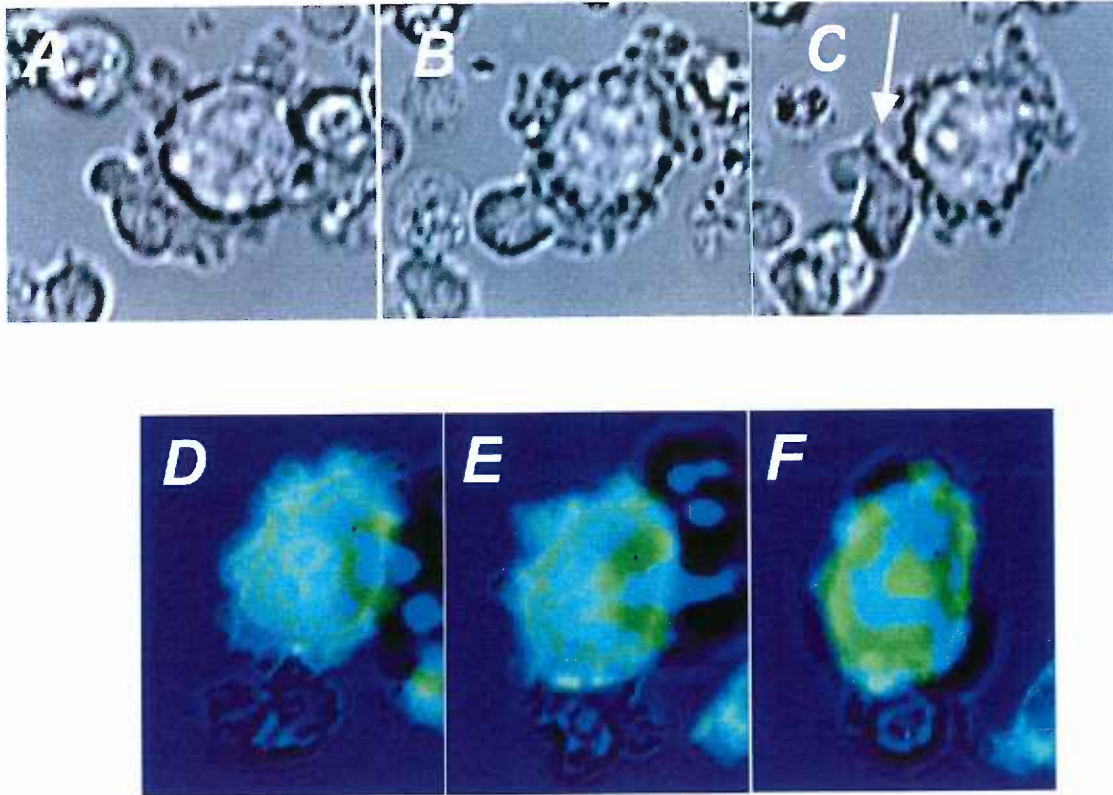


Figure 22. Blocking Src kinases and MAPK pathway in T cells results in unstable T-APC conjugates.

A-C) T cells were pre-treated with MEK inhibitor PD98059 and still formed normal conjugates. Conjugates were unstable because after 9 minutes, T cell started to round up and a new leading edge formed (arrow) before the T cell crawled away from the APC. (DIC images are presented to accentuate morphological changes.) (D-F) Src inhibitor PP2 pretreatment of T cells results in fewer productive T-APC engagements. In conjugates that form, T cells do not take on characteristic morphology and nor do they form mature immunological synapses.

Peptide Specificity

One of the most important questions surrounding T cell activation is the mechanism that underlies the TCR's ability to detect a specific MHC:peptide ligand, resulting in T cell activation. Central to that question is the identity of the MHC:peptide complexes accumulated in the immunological synapse. Knowledge of the identity of the accumulated peptide has broad implications for the mechanism of T cell activation. Inclusion of null self-peptide:MHC complexes in the immunological synapse would suggest that antigen recognition of foreign peptide:MHC complexes occurs in the context of self ligands and that these self ligands might set a signaling threshold that must be exceeded before activation of the T cell occurs. Circumstantial data from Mark Davis using varying ratios of agonist and null peptides to pulse APC suggest that the MHC accumulated at the interface of the T cell and APC contains both the cognate peptide as well as a host of irrelevant peptides at low agonist concentrations (132). This is in contrast to the work of Monks *et al*, who mentioned, in data not shown, that I-E^k but not the irrelevant I-A^k accumulated at the T-APC interface (50).

The presence of wild-type I-E^k on the surface of the GFP:MCC cells which can be loaded with exogenous Hb peptide and used to activate T cells from the Hb-specific 3.L2 TCR transgenic mouse, allowed me to investigate the peptide specificity of the MHC molecules accumulated within the immunological synapse. Under these conditions, the GFP-tagged MCC:I-E^k are irrelevant or null complexes because they aren't recognized by the 3.L2 T cells. If the MHC accumulated at the synapse contains only specific peptide, then there should be no alteration in the distribution of the irrelevant MCC:I-E^k:GFP complexes at the

T-APC interface. If, on the other hand, the synapse is composed of both specific and non-specific MHC:peptide complexes, then the irrelevant MCC:I-E^k:GFP molecules will accumulate at the interface.

When the *in vitro* activated 3.L2 T cells are incubated with the GFP:MCC cells in the absence of Hb peptide, T cell migration very briefly slows upon contact with the APC, and the T cell samples the APC surface as evidenced by the scrubbing morphology exhibited (Figure 23A – C). However, migration does not stop, and the T cell dissociates from the APC and moves away. This interaction is very short lived (usually less than 2 minutes) and never induces T cell morphological changes that are characteristic of antigen recognition. No visible MHC clusters form (Figure 23A-C), and in Fura-2 loaded T cells, intracellular Ca⁺⁺ does not increase (data not shown). This confirms that the synapses seen with the AD10 T cells are antigen-specific and not an antigen-independent event as has been observed with T cells and dendritic cells (123). This also shows that the interactions of the 3.L2 T cells with the GFP:MCC cells do not lead to the non-specific accumulation of MHC:peptide complexes nor do they lead to activation of the T cell.

When the APC were acid stripped and loaded with 20 μM Hb peptide overnight, the 3.L2 cells interacted with the MCC:GFP cells and formed stable conjugates. Antigen recognition by the 3.L2 T cells resulted in Ca⁺⁺ fluxes within the T cells similar in magnitude and kinetics to AD10 – GFP:MCC interactions (data not shown) and to a flattening of the T cell against the APC (Figure 23 D,E). From a morphological point of view, the 3.L2 – APC conjugates were indistinguishable from the AD10 – APC interactions. A 3D reconstruction of the T-APC interface in Figure 23D shows that there are no areas of increased GFP

density visible within the region of contact between the APC and the 3.L2 T cell (Figure 23F). When analyzed, the density and spatial organization of the MCC:I-E^k:GFP complexes at the interface of the cells does not differ from any other location on the surface of the MCC:GFP cells. In fact, in the interface in Figure 23F, it appears as though there is a displacement of the MCC:I-E^k:GFP complexes out of the interface region.

One potential criticism of this approach is that the I-E^k:Hb complexes can not be specifically visualized during this interaction. However unlikely, I cannot discount the possibility that the I-E^k:Hb complexes do not accumulate and form an immunological synapse and this could explain why the MCC:I-E^k:GFP molecules also weren't accumulated. In an attempt to address this criticism, I fixed T – APC conjugates and then stained with antibodies against protein kinase C - θ (PKC θ). PKC θ is known to co-localize with accumulated TCR-MHC:peptide complexes within the c-SMAC region of the immunological synapse (50). Therefore, its accumulation at the 3.L2 – GFP:MCC interface confirms that an immunological synapse formed. The results in the top row of Figure 24 show that at the interface between 3.L2 T cells and Hb-pulsed GFP:MCC cells, there is a clear accumulation of PKC θ (Figure 24C), proving that an immunological synapse was formed during the interaction of these two cells. When the distribution of GFP-tagged MCC:I-E^k complexes is examined, it does not significantly differ from the distribution seen on the opposite side of the APC from where the T cell is bound (Figure 24 D-F). However, on the opposite side, PKC θ is not accumulated (Figure 24 E,F). In the bottom row (24 G-I), the

accumulation and co-localization of the MCC:I-E^k:GFP and PKC θ that occurs within the synapses of AD10 T cells is shown for comparison.

These results clearly show that the 3.L2 T cells are interacting with the Hb-pulsed GFP:MCC cells and that this interaction results in the formation of an immunological synapse (as judged by PKC θ staining). However, there is no redistribution of the irrelevant MCC:I-E^k:GFP complexes to the interface of the 3.L2 T cells and the APC. This strongly suggests that the only MHC:peptide complexes accumulated in the immunological synapse contain the specific cognate peptide ligands.

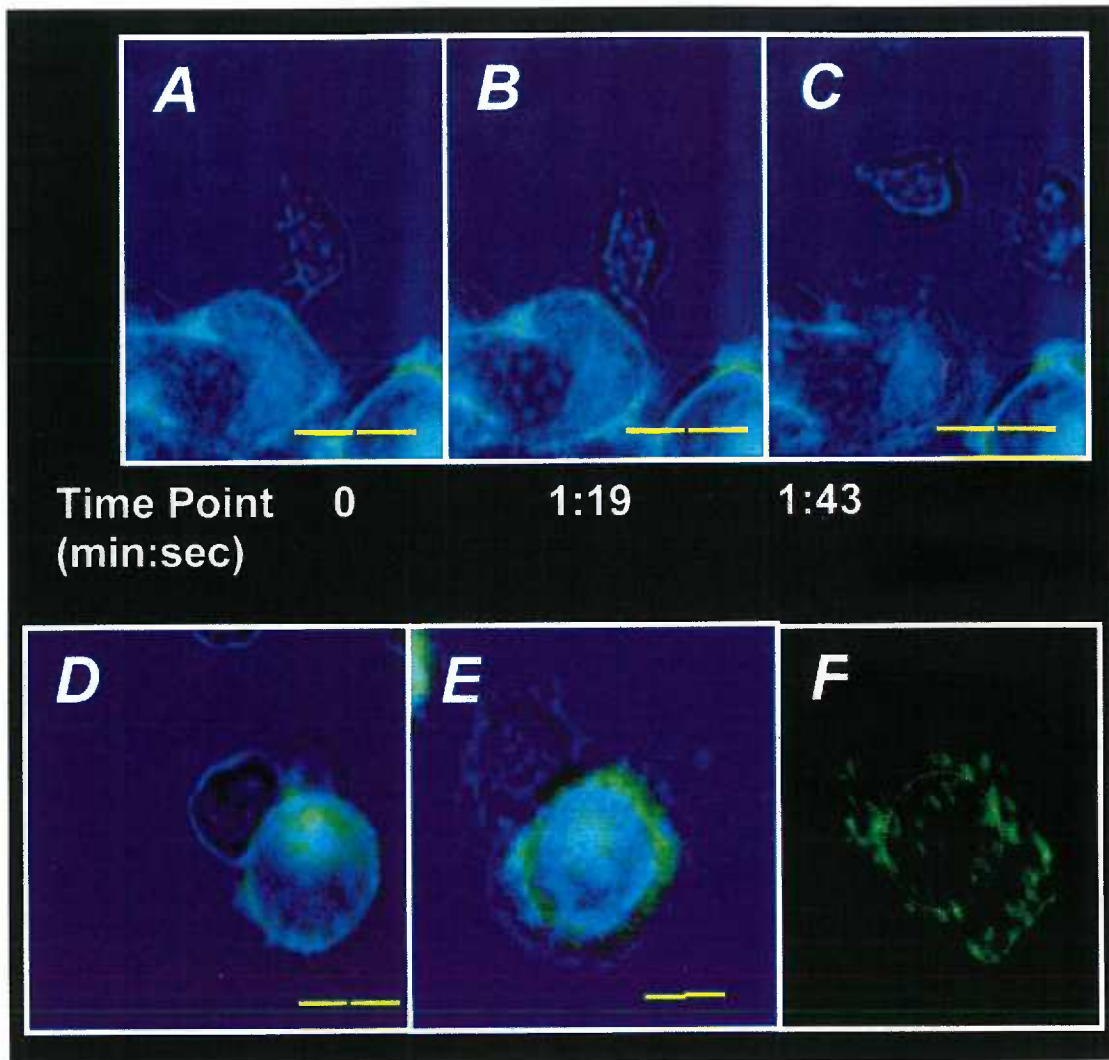


Figure 23. Hemoglobin-specific T cells do not cause accumulation of MCC:I-E^k:GFP molecules.

(A-C). Hemoglobin-specific 3.L2 T cells interacting with MCC:GFP cells without exogenous Hb peptide. The T cell contacts the MCC:GFP cell, migration slows and the T cell scrubs the APC surface. Ultimately, the T cell moves on without forming a stable conjugate. (D-E) When MCC:GFP cells are pulsed with Hb peptide, the 3.L2 T cells recognize antigen and form stable conjugates morphologically identical to AD10 -MCC:GFP conjugates, but no redistribution of MCC:I-E^k:GFP is observed. (F) Deconvolved, rotated 3D reconstruction of interface from E showing lack of MCC:I-E^k:GFP redistribution to the T - APC interface. The dotted circle approximates the edge of the T cell on the APC membrane. The live cell images (A-E) were obtained at 400X, Bar = 10 μm. Conjugate (F) image obtained at 1000X.

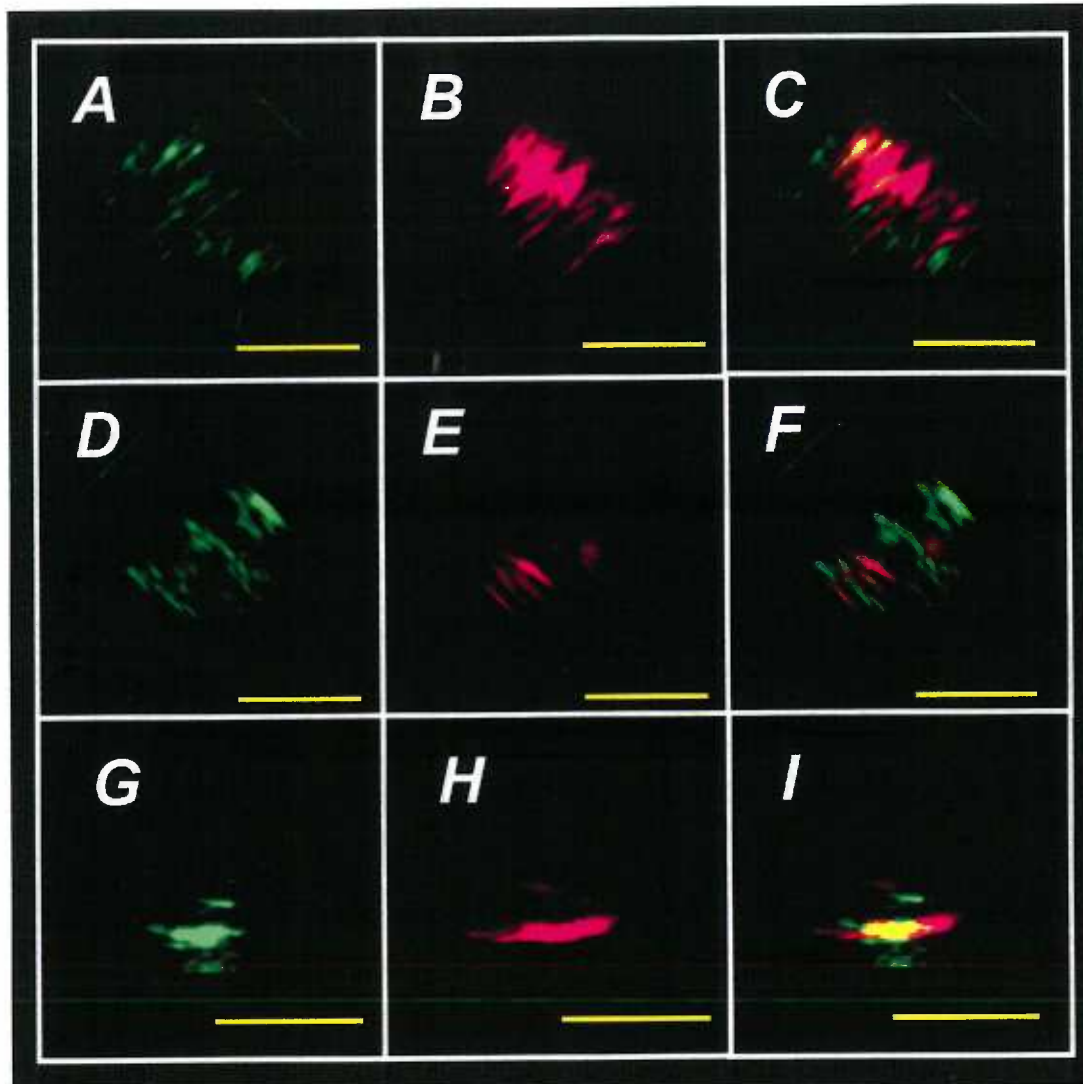


Figure 24. Hb-specific 3.L2 T cells induce localization of PKC θ in the absence of MCC:I-E^k:GFP redistribution, confirming that MHC:peptide complexes accumulated in immunological synapses are peptide specific.

GFP distribution patterns (A, D, G) and PKC θ staining (B, E, H) in fixed 3.L2-APC conjugates (A-C), AD10-APC conjugates (G-I) or the side of the APC opposing the 3.L2 – APC interface(D-F). The right column (C, F, I) shows the overlay of the GFP and PKC-q images. The images were obtained at 1000X, Bar = 5 μ m.

Effect Of Costimulation Blockade on Synapse Formation

The activation of naive T cells involves not only a signal generated by the engagement of the TCR with the cognate MHC:peptide ligand, but also requires the secondary molecular interactions between accessory molecules on the T cell and the APC collectively called costimulation. Wülfing et al have shown that providing costimulation through CD28 or LFA-1 in addition to a signal through the TCR induces the bulk flow of membrane proteins on the T cell towards the T-APC interface (74, 94). Blocking the B7-CD28 interactions prevents a CD3 ζ central cap from forming at the T-APC interface (69). CD28 engagement has also been linked to the accumulation of lipid rafts (130). To date, a thorough examination of the effects of costimulation on synapse formation including quantitative analysis has not been carried out.

To assess the role of B7-1 and ICAM-1 in immunological synapse formation, soluble blocking reagents were used. To block interactions between B7-1 and CD28, APC were pretreated for 1 hour with 25 μ g/ml CTLA-4Ig before imaging was initiated. Similarly, 25 μ g/ml of anti-ICAM-1 was used to block productive engagement of LFA-1 and ICAM-1. As a positive control, another set of cells were pre-incubated with 25 μ g/ml of anti-I-E^k to block antigen recognition.

When CTLA-4Ig is used to block B7-1:CD28 interactions, the mean time between initial T – APC contact and mature synapse formation increases modestly but significantly ($p=0.04$) from 5:30 ($\pm 0:16$) to 7:11 ($\pm 0:41$), an increase of 24%. Costimulation blockade also results in a reduction in the size and

intensity of the synapses in the live cell images (data not shown) but does not prevent characteristic morphologic changes (DIC images in Figure 25). However, because kinetic imaging is carried out only in one focal plane, movement of T cells in and out of that plane can alter the apparent size of a synapse, making quantitation difficult.

To more accurately measure the area and intensity of the synapse with the different treatments, T cells were incubated with the pretreated MCC:GFP cells for 30 minutes and were then fixed with 4% paraformaldehyde and 0.5 % glutaraldehyde. Conjugates were chosen based upon their characteristic flattened morphology in DIC. For imaging, 45 to 60 – 1000X images were taken 0.2 μ m apart in the z axis. These image stacks were deconvolved to clarify the images by reducing out of focus haze, thus improving spatial resolution and the overall fidelity of the image. These stacks of deconvolved images were then reconstructed into a 3D representation of the interface. A representative set of interface images for each treatment is shown in Figure 25 (Movies 25D, H, L, P).

Based upon analysis of more than 150 conjugates, several general observations can be made. The morphology and brightness of the synapse is clearly altered when the APCs are pre-incubated with the blocking reagents. The synapses of cells treated with control IgG (Figure 25D) generally have one or a few large, intense clusters surrounded by several smaller regions of increased density. This pattern is reminiscent of the MHC distribution in fixed AD10 T cell – B cell conjugates published by Monks *et al.* (50). By contrast when B7-1 or ICAM-1 are blocked, the synapses are more diffuse and irregular in shape and lack a dense central cluster. They are also smaller and less intense than the control IgG synapses. When APC are pretreated with anti-I-E^k to block TCR

engagement, the patterns were similar to those observed with costimulation blockade. The small synapses seen with anti-I-E^k may reflect incomplete blockade of the MCC:I-E^k:GFP complexes owing to high expression levels.

To assess the effect of these blocking reagents on full T cell activation, a 72 hour ³[H] thymidine incorporation experiment was performed. The APC (MCC:GFP cells or B10.BR spleen cells pulsed with 50 nM MCC peptide) were pre-incubated for 1 hour with the indicated blocking reagent prior to addition of T cells. Freshly isolated primary or *in vitro* primed AD10 T cells were used as responders. Cultures were pulsed with ³[H] thymidine for the final 12 hours of a 72 hour assay. As seen in Figure 26A, blockade of B7-1:CD28 engagement with CTLA-4Ig significantly reduced the proliferation of AD10 T cells under all conditions tested. Similar results were obtained by blocking with anti-B7-1 antibody (data not shown). The inhibition ranged from 58% with *in vitro* primed AD10 + MCC:GFP to 93% with primed AD10 plus peptide pulsed B10.BR splenocytes. Blockade of ICAM-1 / LFA-1 interactions also significantly reduced proliferation, although not quite as effective as CTLA-4Ig. The effects of anti-I-E^k were similar to CTLA-4Ig in each condition tested. Therefore, costimulation blockade conditions identical to those used in microscopy experiments resulted in significant reductions in T cell proliferation.

To determine whether the significant reduction in T cell proliferation reflects an alteration in immunological synapse formation, the area and intensity of the clustered MHC molecules in the synapse with fluorescence intensity at least 2 fold above background were quantified. The data in Figures 26B and 26C are representative of 6 separate experiments with similar results. Data from the

different experiments are not combined due to experiment-to-experiment variations in size and intensity.

The total area of MHC clusters in the synapse is significantly reduced by costimulation blockade. Treatment with the control IgG results in a synapse with a mean area of $2.8 \mu\text{m}^2$ (Figure 26C). CTLA-4Ig or anti-ICAM-1 treatment significantly reduces the size of the clustered MHC to a similar extent. No additive or synergistic effects of CTLA-4Ig and anti-ICAM-1 were observed, perhaps due to the relatively low ICAM-1 expression and/or the saturating concentration of the antibody reagents. For comparison, pretreatment of the APC with anti-I-E^k to block TCR engagement reduces synapse area to a similar degree. The reductions in MHC cluster area are similar in magnitude to the reductions seen in T cell proliferation using primed AD10 and MCC:GFP.

The intensity of the GFP signal is also significantly reduced by costimulation blockade (Figure 26B). Because the integrated intensity is proportional to the amount of MHC in the synapse, pretreatment of the APC with reagents to block B7-1 or ICAM-1 significantly reduces the overall area as well as the total amount of MHC within the synapse. Interestingly, while the blockade of B7-1 or ICAM-1 significantly reduced T cell proliferation as well as the size and intensity of the synapse, it had no effect on CD25 expression and TCR down-modulation (Figure 27B and 28A) and CTLA-4Ig only slightly reduced CD69 expression (Figure 27A and 28B).

When conjugates are examined at 15 minutes, the overall size and intensities are reduced, but the same effects of costimulation blockade are seen, suggesting that the effects are exerted early in the formation of the immunological synapse (data not shown). The magnitude of the reduction in

MHC cluster area and amount of the MHC clustered within the synapse
correlates with the reduction in T cell proliferation.

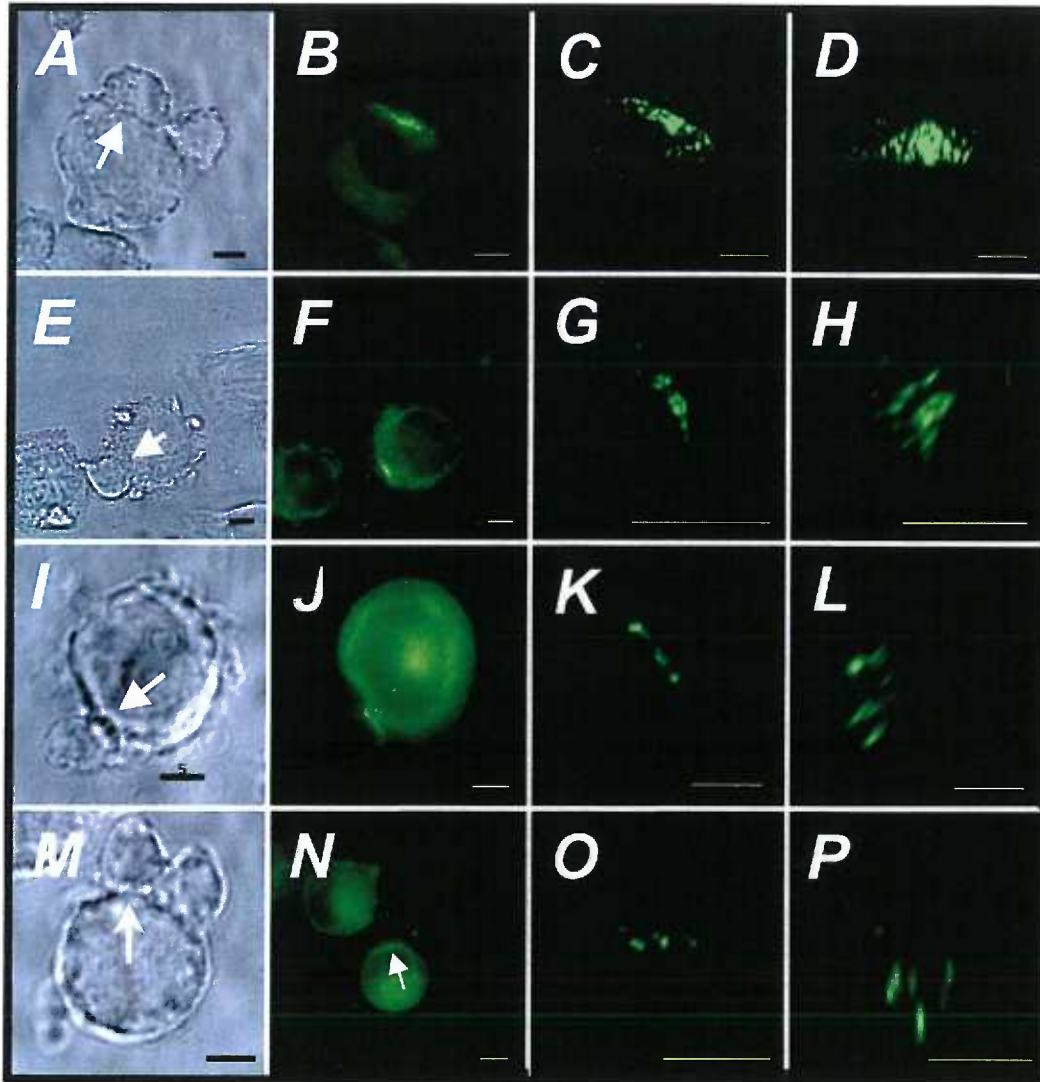
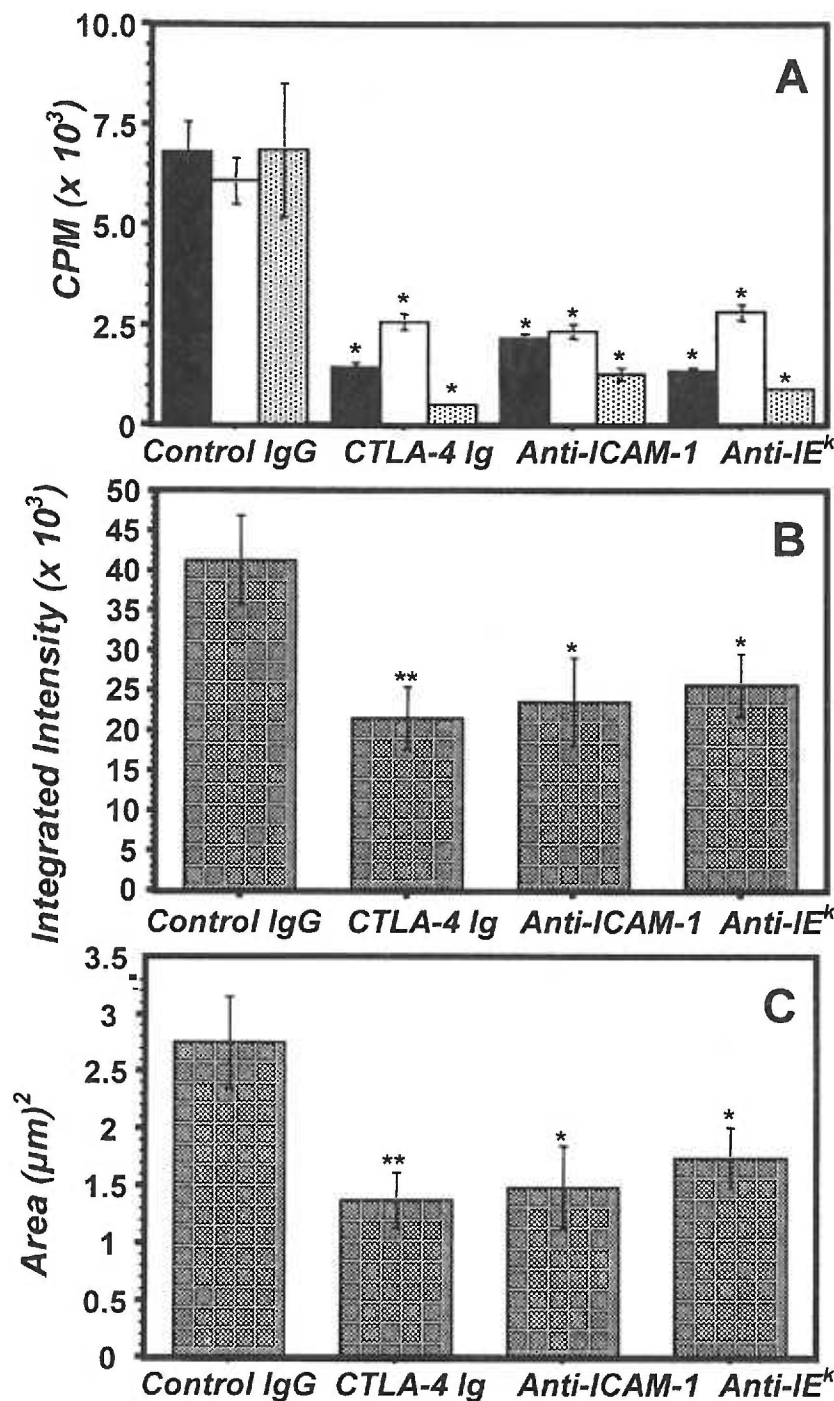


Figure 25. Effects of costimulation blockade on the mature immunological synapse.

Representative pictures of MHC clustering within the immunological synapse after MCC:GFP cells were preincubated with 25 $\mu\text{g/ml}$ human IgG (A-D), CTLA-4Ig (E-H), Anti-ICAM-1 (I-L), or Anti-I-E^k (M-P) for 1 hour prior to addition of AD10 T cells. The left column (A, E, I, M) contains DIC images with conjugates analyzed identified by the arrow. The second column (B, F, J, N) is GFP images of the same conjugates demonstrating the accumulation of MCC:I-E^k:GFP at the T-APC interface. The third and fourth columns show 3D reconstructions of the interface after image deconvolution. The third column (C, G, K, O) has the synapse oriented as in the second column for reference. The fourth column (D, H, L, P) shows the interface rotated 90° generating a view of the interface from the T cell perspective. Contrast and brightness settings are identical in the right two columns. Images were collected at 1000X, but image processing has resulted in non-uniform magnifications of reconstructed interfaces. Bar = 5 μm

Figure 26. Costimulation blockade significantly reduces size and intensity of the synapse.



(A) Costimulation blockade significantly reduces T cell proliferation. MCC:GFP cells were preincubated with 25 μg/ml of indicated blocking reagents for 1 hour before addition of primary (black) or *in vitro* primed AD10 T cells (white). Alternatively, 10⁵ fresh B10.BR spleen cells were pulsed for 1 hour with 50 nM MCC peptide and costimulation blocking reagents for 1 hour before addition of *in vitro* primed AD10 T cells (gray). (B and C) Quantitation of the MHC clusters with GFP intensity ≥ 2X background in 90° rotated images. (B) Integrated intensity of the MHC, which reflects the total amount of MHC accumulated. (C) The area of all MHC clusters was summed for each cell. Mean values ± SEM are shown. Values significantly

reduced relative to IgG control are indicated (* $p < 0.05$, ** $p < 0.01$). Data are representative of 6 separate experiments.

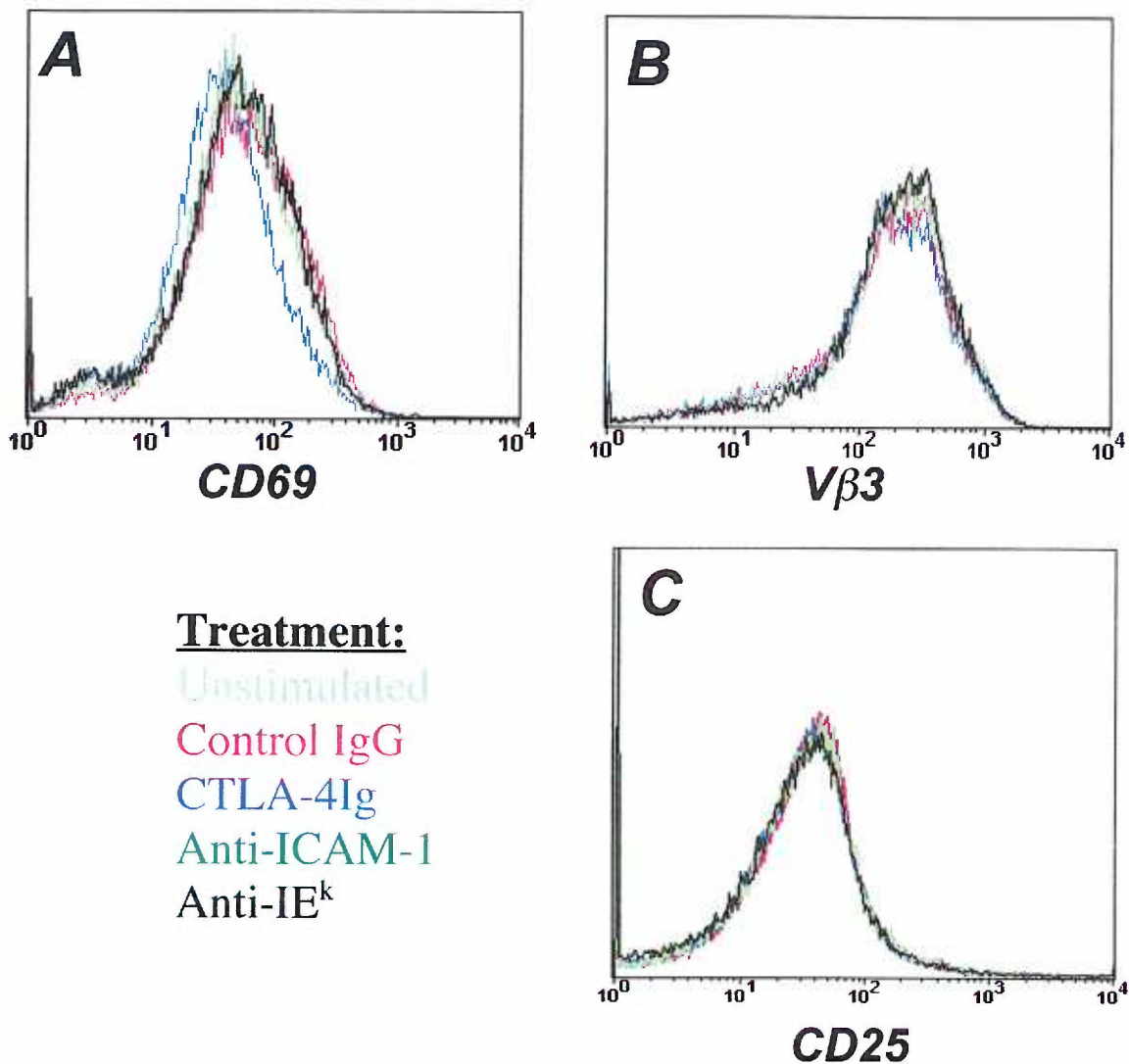


Figure 27. Costimulation blockade does not significantly alter CD69, CD25, or TCR (V β 3) expression on AD10 T cells.

MCC:GFP cells were preincubated with 25 μ g/ml of blocking reagents, as described in Figure 25 legend. *In vitro* primed AD10 T cells were incubated with treated MCC:GFP cells for 16 hours before isolation of T cells and staining with antibodies against (A) CD69, (B) V β 3, or (C) CD25.

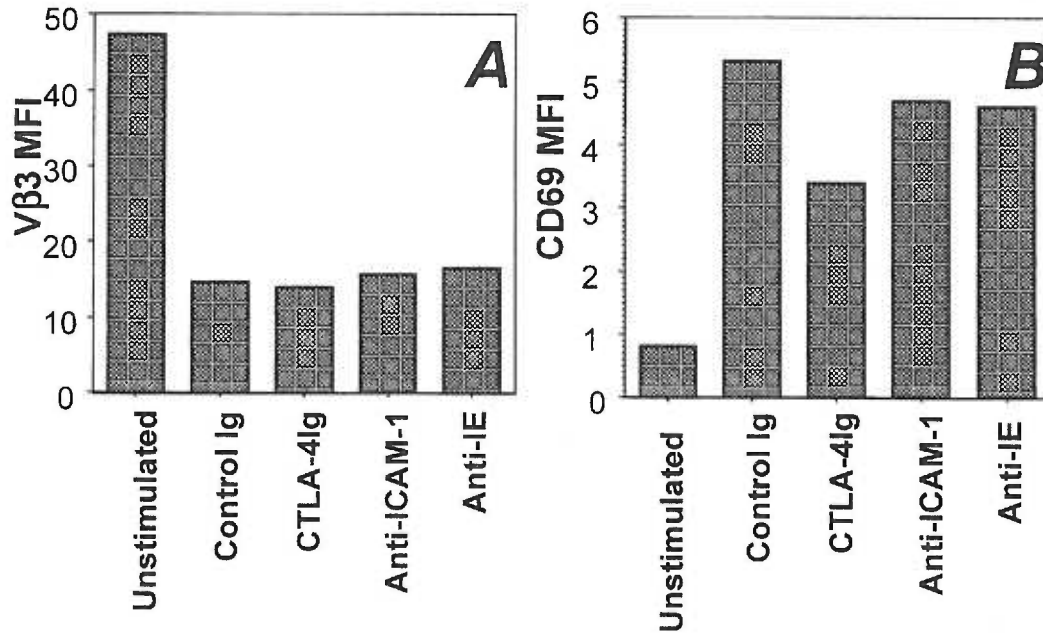


Figure 28. Quantification of figure 27 showing costimulation blockade does not significantly alter CD69, or TCR (Vβ3) expression on AD10 T cells.

Mean fluorescence intensity (MFI) values of (A) Vβ3 and (B) CD69 on T cells as a function of reagent used to block costimulation blockade

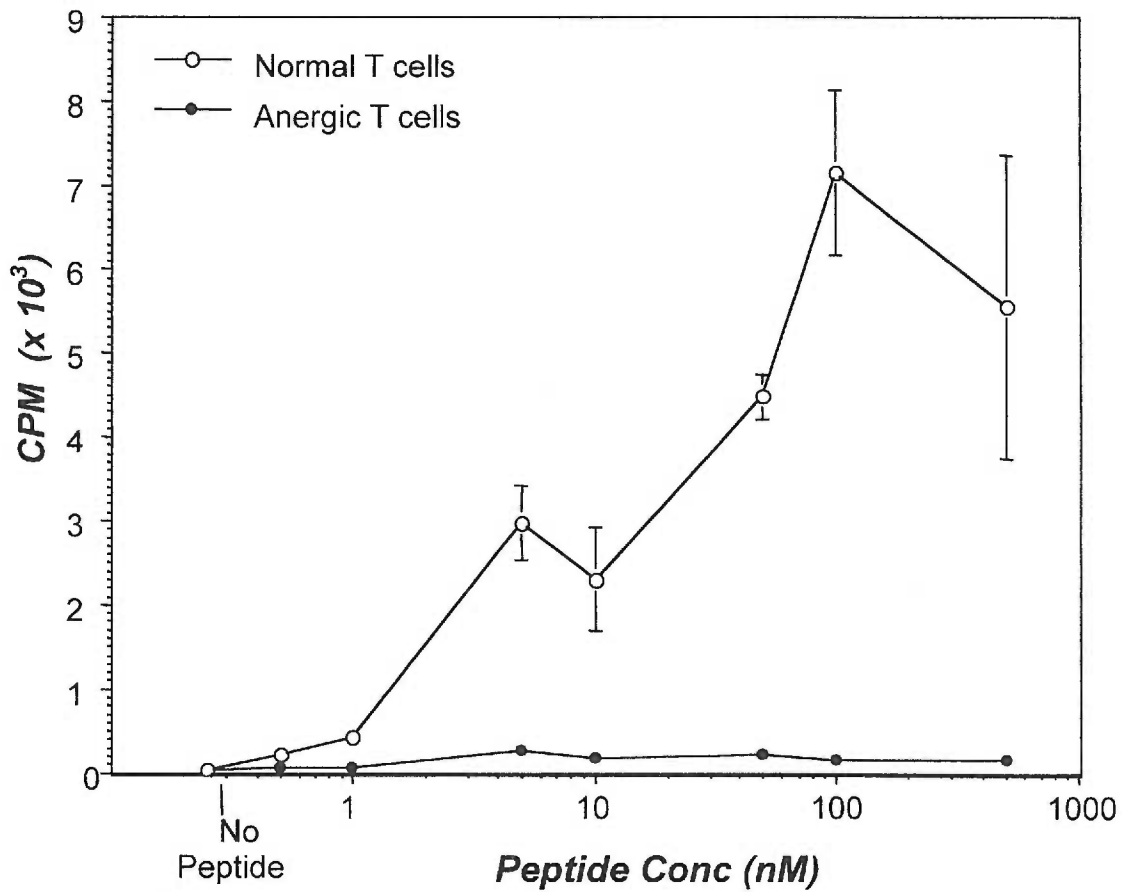


Figure 29. T Cells cultured overnight with anti-TCR antibodies become hyporesponsive (anergic).

In vitro activated AD10 T cells were isolated and cultured overnight in dishes coated with anti-TCR antibody. Cells were removed from the antibody and cultured an additional 48 hours before testing their response to peptide pulsed B10.BR splenocytes in a 72 hour ³H-thymidine incorporation assay.

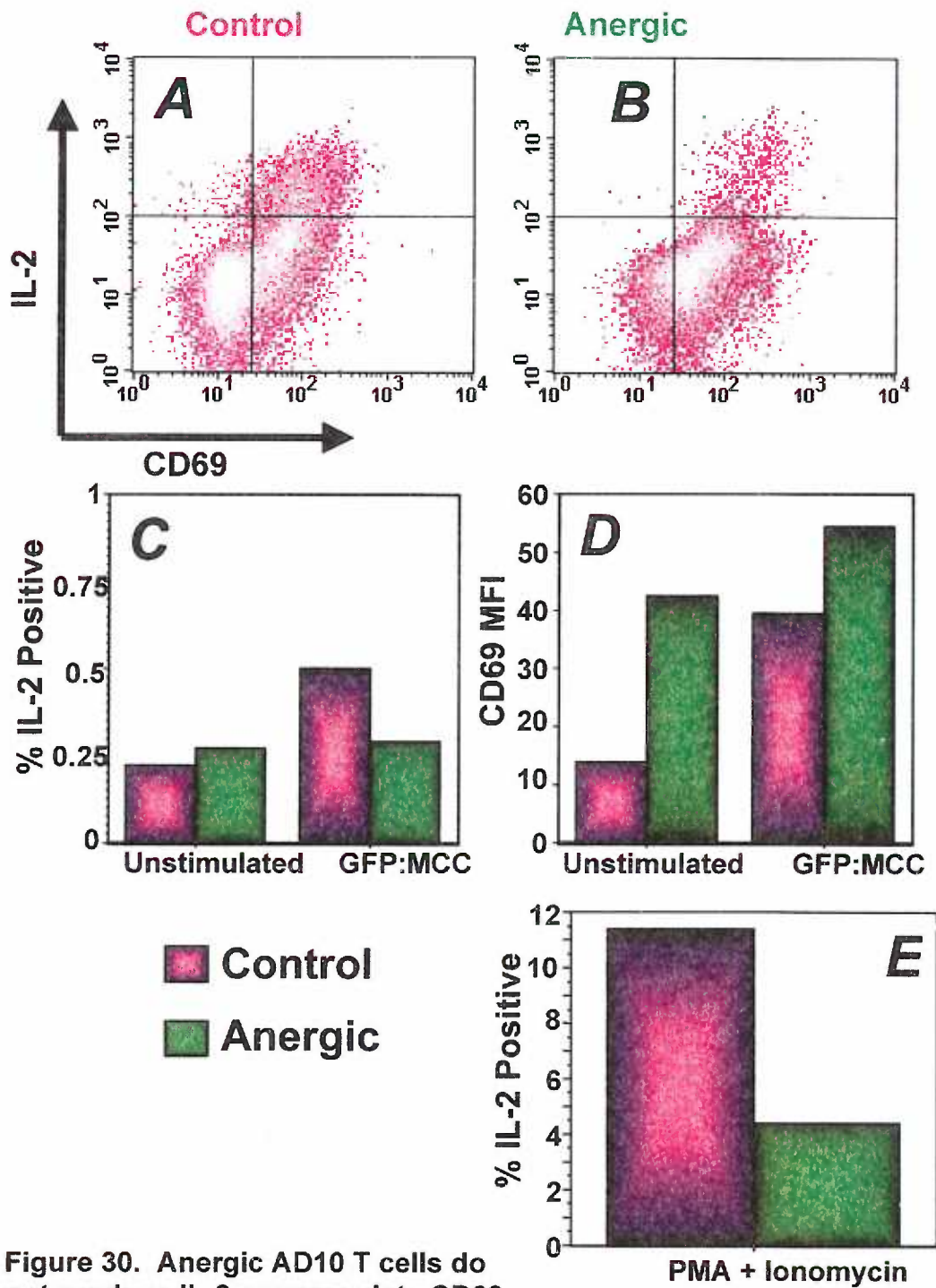


Figure 30. Anergic AD10 T cells do not produce IL-2 or upregulate CD69.

AD10 T cells energized as described for Figure 29 were stimulated for 18 hours with MCC:GFP cells or for 5 hours with PMA + Ionomycin. Fewer of the PMA+Ionomycin treated anergic T cells produced IL-2 (A, B, E). When stimulated with MCC:GFP cells, the anergic cells were similarly incapable of producing IL-2 (C). (D) CD69 was upregulated on control cells, but not on the anergic cells.

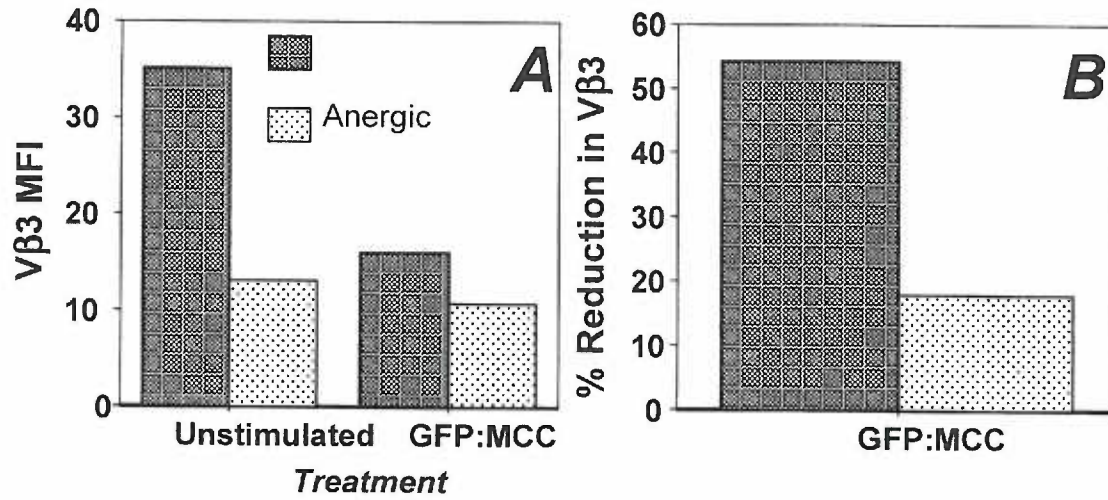


Figure 31. TCR down-modulation is defective on Anergic AD10 T cells.

AD10 T cells anergized as described for Figure 29 were stimulated for 18 hours with MCC:GFP cells before staining with anti-Vβ3. The initial TCR level was lower on anergic cells, presumably due to anergy induction protocol. Compared to control T cells, TCR down-modulation by the anergic T cells was minimal.

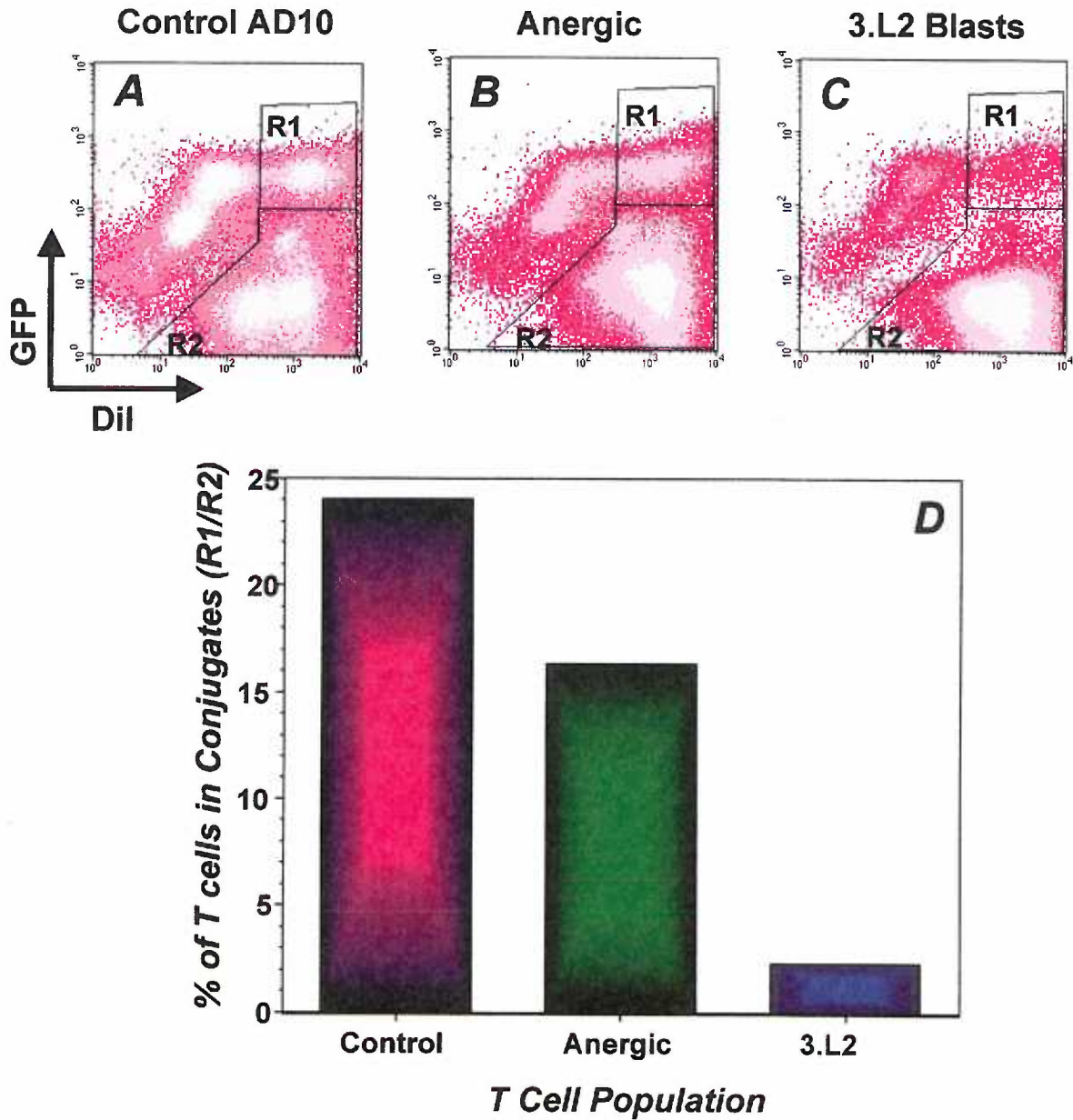


Figure 32 Anergic AD10 T cells form stable conjugates with MCC:GFP cells, albeit at slightly reduced frequencies.

(A) Control or (B) anergic AD10 T cells were labeled with the red membrane dye Dil and incubated with MCC:GFP cells for 30 minutes at 37°. Cultures were analyzed by flow cytometry, while being maintained at 37°. (D) Conjugate formation percentage was defined as the number of T cells conjugated to the MCC:GFP cells (R1) divided by the total number of T cells analyzed (R2). (C) Hb-specific 3.L2 T cells are an antigen specific control showing the background of activated T cell - MCC:GFP adherence.

Anergic Cell Synapses

In the absence of sufficient costimulation, T cell recognition of antigen leads to a state of hyporesponsiveness termed anergy (152). These anergic T cells respond weakly, if at all, to subsequent antigen challenge even in the presence of optimal costimulation. It has been suggested that this is a mechanism by which potentially self-reactive peripheral T cells are prevented from causing autoimmune disease. Many downstream defects in anergic T cells have been cataloged including altered signaling and the subsequent inability to produce IL-2 and progress through cell cycle (46, 153). To date, however, no studies have looked at the ability of anergic T cells to make immunological synapses, nor characterized the molecules that accumulate at the interface of anergic T cells and antigen presenting cells.

Having shown that costimulation is a critical component in the formation of a normal mature immunological synapse, I went on to examine whether anergic T cells would form immunological synapses and, if so, to characterize some of the accumulated molecules. After *in vitro* priming for four to six days, AD10 T cell blasts were rendered anergic by overnight (18 – 24 hours) incubation on plates coated with 10 µg/ml of the anti-TCRβ antibody, H57 (See Materials and Methods section for details). To confirm that these T cells were indeed rendered hyporesponsive by this treatment, their ability to proliferate in response to fresh splenic APC with PCC peptide was determined by a standard 72 hour ³[H] – thymidine incorporation assay. The results, shown in Figure 29, clearly show that these T cells are hyporesponsive compared to control T cells. In the classical definition of anergy, the T cells are hyporesponsive, in part, due to

an inability to secrete sufficient IL-2 to promote cell cycle progression (44, 154). Under this classical definition, T cell responsiveness can be restored by the addition of exogenous IL-2 to the cultures. Indeed, the proliferative capacity of these T cells was restored by the inclusion of low levels (50 U/ml) rIL-2 during the assay, confirming that these cells were anergic.

The anergic state of the T cells was further characterized by examination of phenotype by flow cytometry in response to the MCC:GFP (Figure 30). After a 16 hour incubation with GFP:MCC cells or B10.BR splenocytes pulsed with 2.5 μ M PCC, the expression of CD69, down modulation of the TCR, and intracellular IL-2 levels were examined. On the anergic cells, baseline CD69 levels were higher and TCR levels were lower, indicative of the interaction of the T cells with the anti-TCR β antibody used to induce anergy (IL-2 levels were unaffected).

When incubated for 16 hours with the GFP:MCC cells, the expression of the activation marker CD69 increased by 184% on the control cells, while the increase on the anergic cells was just 28% (Figure 30D). With peptide-pulsed B10.BR splenocytes as the APC, the results were similar, 185% vs. 58%, (data not shown). TCR down modulation was similarly affected on the anergic cells. Interaction with the GFP:MCC cells resulted in a 54% reduction in the V β 3 expression on the controls, while it decreased only 18% on the anergic cells (Figure 31). The V β 3 levels were not determined using the B10.BR splenocytes because of the presence of irrelevant V β 3 positive cells in the splenic cell preparations. Finally, when the levels of intracellular IL-2 were compared, the percentage of control cells that were IL-2 positive doubled, while for the anergic cells, there was only a 7% increase (Figure 30C). When these cells were

stimulated with PMA and Ionomycin for 5 hours to bypass TCR engagement, the percentage of IL-2 positive control cells increased from 0.22% to 11.42%, while with the anergic cells the increase was from 0.27 % to 4.4% (Figure 30E). The intensity of IL-2 staining was also reduced in the few IL-2 positive cells (Figure 30 A and B). Thus, the T cells treated for 18 to 24 hours with the anti-TCR β antibody are truly anergic.

Before beginning the microscopy experiments with the anergic cells, I examined the ability of the anergic T cells form stable conjugates with the MCC:GFP cells by flow cytometry. The plasma membranes of the T cells, both control and anergic, were labeled with the lipophilic dye DiI, which fluoresces in the red region of the spectrum (565 nm emission – compatible with FL2 on the FACSCalibur). These red-labeled T cells were mixed with the MCC:GFP cells at a ratio of 1:1 in suspension and were incubated at 37°C for 30 minutes. While being maintained at 37°C, this mixture was analyzed by flow cytometry for the formation of stable T – APC conjugates. In this experiment, conjugates were defined as a single event of the appropriate size having both red and green fluorescence. The data in Figure 32 shows that the anergic T cells do form stable conjugates with the MCC:GFP cells, albeit at a reduced rate, 24% for controls versus 16% for anergic T cells.

Having shown that the anergic T cells are interacting with the MCC:GFP cells and forming stable conjugates, but still responding very weakly as judged by proliferation or characteristic activation markers, the ability of these anergic T cells to form immunological synapses was then examined by live cell and fixed conjugate microscopy. In the live cell imaging, the morphological characteristics of the anergic cells are indistinguishable from the control T cells (Figure 33); the

anergic cells are polarized, motile, and highly active. When they encounter APC, they undergo the typical flattening against the APC triggered by antigen recognition and subsequent Ca^{++} fluxes.

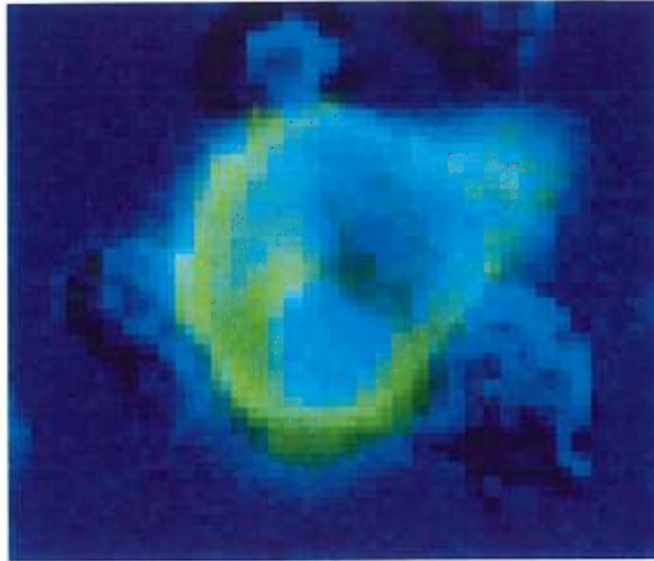


Figure 33. Anergic AD10 T cells display characteristic morphological changes upon recognizing antigen on MCC:GFP cells.

When the calcium responses in the anergic and control cells are compared at the single cell level, as shown in Figure 34, the kinetics are similar. The magnitude of the initial Ca^{++} peak is also similar in the two populations, with the anergic cells fluxing slightly more calcium. They differ, however, in the maintenance of the calcium response. In the control cells, the Fura-2 ratio plateaus at approximately 4 times the baseline value and is maintained at that level for the duration of imaging (>40 minutes). In the anergic cells, the Fura-2 ratio returns to the baseline values within 9 minutes and remains at that level for the duration of imaging.

I went on to quantify the MHC accumulation at the interface of the anergic T cells and the APC, as well as to characterize the molecules that are recruited in the different cells. Because of the dynamics of the interactions and our inability to capture 4D data at a rate that allows for accurate 3D reconstructions of the interface over time, live cell imaging was not technically possible. The T cells were allowed to interact with the MCC:GFP cells for 30 minutes at 37°C before fixation with 4% paraformaldehyde and 0.5 % glutaraldehyde. Conjugates were stained for several cell surface molecules including ICAM-1, as well as lipid rafts, using CTxB. For characterization of molecules accumulated within the T cell at the interface, the cells were permeabilized with 0.1% Triton X-100 before blocking and staining. Conjugates to be examined were chosen based solely upon their morphology in the DIC images.

A comparison of the clustered MCC:I-E^k:GFP molecules at the T-APC interface reveals no obvious morphological differences between the anergic cells and the controls (Figure 35A vs. 35B). As described above, at the interface there are one or two large regions of dense GFP accumulation surrounded by several smaller regions. Using the auto-polygon feature of the SoftWoRx software package to define areas with GFP intensity 2 fold or higher above the background, area and intensity of the GFP signal, which correlates with density of accumulated material, were quantified. In this experiment, 67 anergic conjugates and 80 control conjugates were analyzed. There were no obvious differences in the morphology of the accumulated GFP-tagged MHC:peptide complexes between the two groups. When comparing the total size of the accumulated GFP clusters, the clusters with the anergic cells were 15.4% smaller

than the control cells (Figure 35D). This difference was not statistically significant ($p=0.49$), nor was the 15.3% reduction in the integrated intensity of the clusters ($p=0.53$) (Figure 35C).

This data suggests that, when looking at only the accumulated MHC:peptide complexes, there is little or no difference between the anergic T cells and the controls. However, the MHC:peptide complexes are only one of many molecules that accumulate in the SMACs at the T-APC interface. Knowledge of the potential localization and spatial distribution of other molecules will allow a better analysis of the anergic synapses and may explain, in part, the defect in downstream signaling that occurs in the anergic cells. To assess the accumulation of molecules of potential importance in the formation and functions of the immunological synapse, fixed T – APC conjugates were stained with antibodies specific for several surface proteins.

Conjugates were stained with antibodies specific for the integrin ICAM-1, which I have already shown to be necessary for normal mature immunological synapse formation (see Figure 25). In the mature immunological synapse, ICAM-1 is located in the p-SMAC (49, 50). With the anergic cells, a similar pattern of ICAM-1 staining is observed (Figure 36A and B). There is a region staining positive for ICAM-1 (red) surrounding the accumulated MCC:I-E^k:GFP. There is essentially no overlap between these two regions and the distribution is nearly identical with the previously published reports (49, 50). The differential spatial organization of the ICAM-1 and MHC:peptide complexes at the T-APC interface confirms that the anergic T cells are making mature immunological synapses.

The T-APC conjugates were stained with Cholera Toxin B subunit (CTxB), which binds to asialo-GM1, a lipid enriched in so-called lipid rafts (124). Viola

and colleagues showed that CD28 engagement drove the accumulation of lipid rafts on the surface of T cells (130). While the existence of lipid rafts on the surface of living cells is still somewhat controversial (155), they are thought to be regions of the membrane where molecules important in generating intracellular signals are segregated, allowing them to efficiently interact and become activated (127). As such, knowledge as to whether these rafts aggregate at the T-APC surface in the anergic cells might give an insight in to the potential defects in those cells. As seen in Figure 36G and H, the CTxB stained lipid structures do tend to accumulate at the T-APC interface in the both the control and anergic T cells. Thus, lipid rafts appear to aggregate normally at the interface of anergic T cells and antigen presenting cells.

I next looked at intracellular proteins, which may be important in the initiation and transduction of downstream signals from the TCR. To facilitate intracellular staining, the fixed conjugates were permeabilized with 0.1% triton X-100 for 5 minutes before blocking and staining.

One of the hallmarks of mature immunological synapse formation is the accumulation of T cell-specific PKC θ within the c-SMAC. The fixed control and anergic T cell – APC conjugates were stained and examined for the specific accumulation of PKC θ . The results shown in figure 36C and D show that within the anergic T cells, the PKC θ accumulates at the interface and co-localizes with the GFP-tagged MHC:peptide complexes. This accumulation has been observed in a minority of synapses, but this is most likely due to a technical artifact, and not to a lack of PKC θ accumulation.

Another important set of molecules in the control of TCR signals are members of the Cbl oncogene family. One member of the Cbl family, Cbl-b, has been localized to the synapses formed by T cells from old, immunocompromised mice (156). Cbl-b is thought to act as a negative regulator of TCR signaling (75). Because Cbl-b^{-/-} T cells do not require costimulation for optimal activation, it is thought that Cbl-b may act as a negative regulator of TCR signaling. I examined the localization of Cbl-family members by staining the permeabilized conjugates with antibodies to c-Cbl. This molecule was not found within the normal T cell –APC conjugates, but c-Cbl was found to accumulate in anergic synapses (Figure 36 E and F). The images in figure 36 E and F are representative of 12 control and 12 anergic synapses imaged to date. Its distribution was somewhat surprising because a portion appears to co-localize with the MHC:peptide , but a large area does not and apparently extends into the p-SMAC region. It is unclear why this protein's distribution pattern differs from most of the proteins accumulated at the T-APC interface. Like Cbl-b, c-Cbl has also been implicated in the control of TCR signaling (226). Preliminary data also suggests that F-actin accumulation in the anergic synapses is also defective (data not shown), most likely due to the accumulation of c-Cbl, which is implicated in controlling F-actin dynamics (226). The final molecule that I have stained for is the small G-coupled protein Rap1. Rap1 is an antagonist of the Ras-mediated MAPK pathway initiated upon TCR signaling (157, 158) and it has been implicated in the induction of T cell anergy. These reports found that Rap1 was active in the absence of costimulation, but when costimulation is available, Rap1 is inactive and the Ras – mediated ERK kinase cascade is turned on (48, 157). Because of this potentially critical role in the induction of anergy, we hypothesized that it might be recruited to, or

constitutively expressed at, the immunological synapse in anergic T cells. However, when the distribution of Rap1 staining was analyzed, there appeared to be no preferential accumulation to the synapse, anergic or control (data not shown). Rather, Rap1 appears to be distributed throughout the cytoplasm of both T cells and APCs. This was somewhat surprising, but a recent report has indicated that in neuronal cells, Ras is found at the plasma membrane while active Rap1 is actually perinuclear (159).

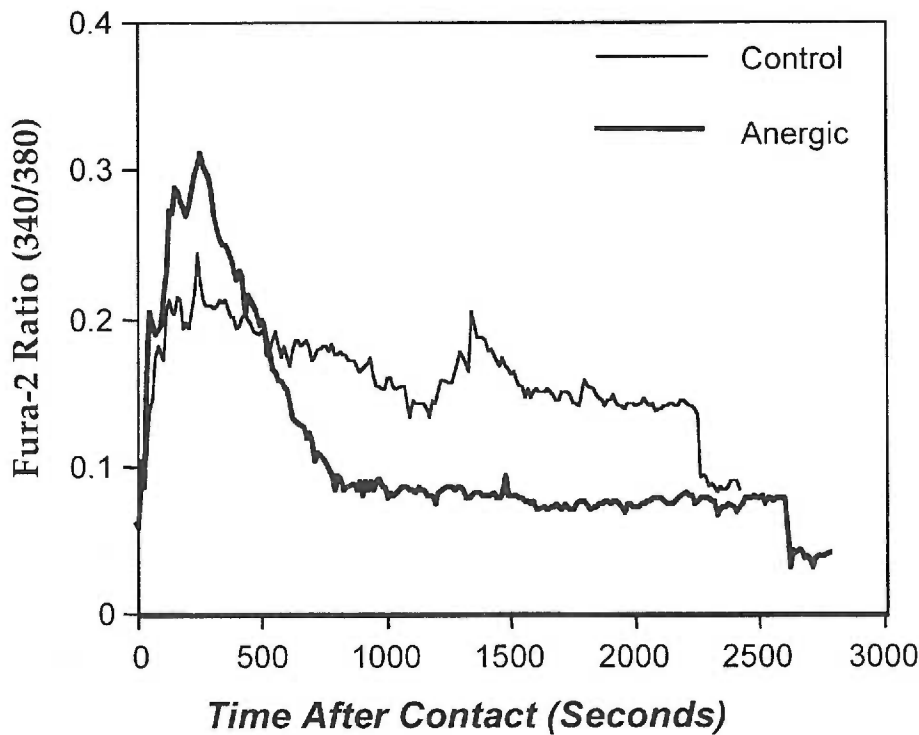


Figure 34. Ca^{++} flux in anergic AD10 T cells is relatively normal.

T cells were loaded with Ca^{++} ratiometric indicator Fura-2 before addition to dishes containing MCC:GFP cells. Fura-2 ratio values were calculated for individual T cells after imaging. Shown are mean Fura-2 ratio as a function of time after initial T-APC contact. Mean values are derived from at least 12 individual cells for each group. Data is representative of 3 separate experiments.

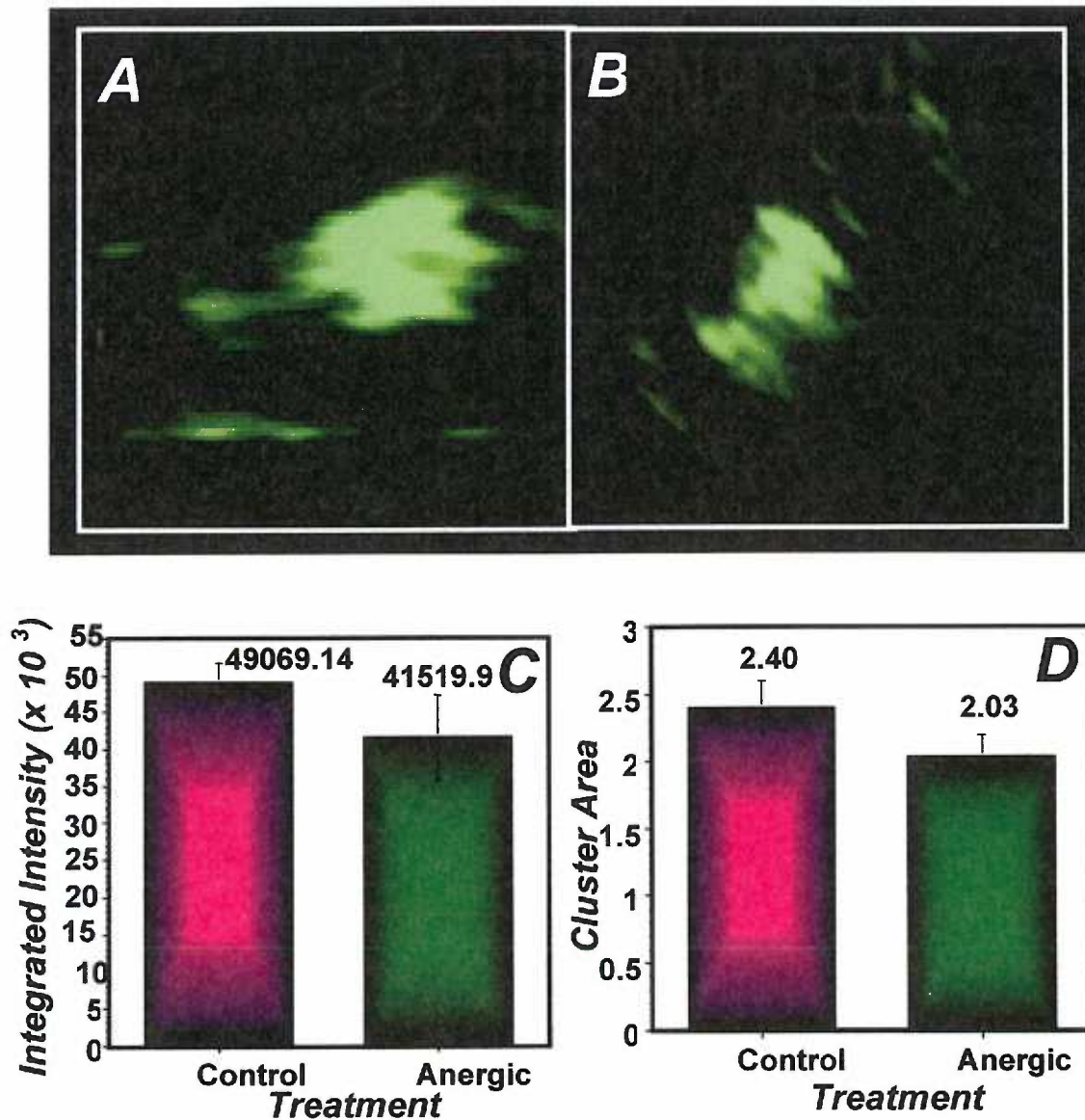


Figure 35. Anergic T cells make immunological synapses that are morphologically similar to controls and the density and area of clustered MHC are not significantly different.

(A and B) Representative images of synapses formed by (A) control and (B) anergic AD10 T cells displaying comparable morphology. (C and D) Quantitation of the (C) integrated intensity and (D) total area of MHC clusters accumulated within the immunological synapse with GFP intensity values $\geq 2X$ background. The mean values are shown on the graphs. The small differences between anergic and control T cells is not statistically significant. Data are representative of 3 separate experiments.

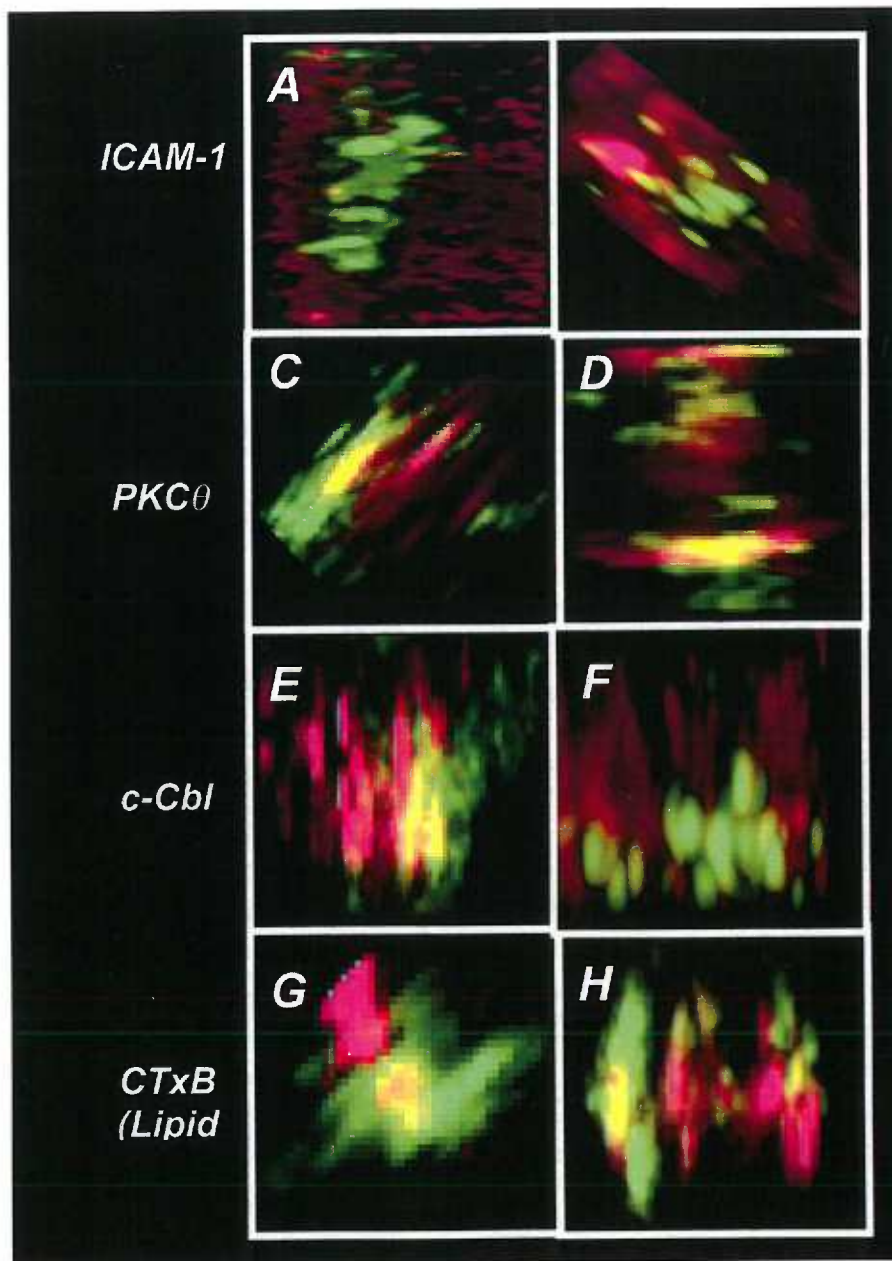


Figure 36. Further characterization of anergic immunological synapses shows that they are similar to control synapses except for increased accumulation of c-Cbl, a negative regulator of TCR signaling.

(A-B) Anergic T cell - APC interface displays prototypical ICAM-1 (red) and MHC:peptide (green) distribution. (C-H) Accumulation and distribution of several molecules accumulated in anergic synapses (left column-C, E, G) are similar to control synapses (right column - D, F, H) including (C - D) PKC θ and (G - H) CTxB stained lipid rafts. (E - F) In contrast, c-Cbl is preferentially recruited to anergic synapses, where it appears to localize in the c-SMAC with MHC:peptide.

Chapter 4

Discussion

T cell activation is a key event in the generation of an immune response. The ligation of the clonal T cell antigen receptor (TCR) with its cognate MHC:peptide ligand induces intracellular signaling. Secondary signals from the antigen presenting cell, collectively called costimulation, are required in addition to TCR ligation to fully activate the T cell. Because the TCR and associated CD3 molecules lack any intrinsic enzymatic activity, a complex scheme involving numerous proteins whose concerted activity is essential to full T cell activation has evolved to transmit signals from the TCR to the nucleus. Pioneering work from the 1980's and early 1990's, carried out primarily by Abraham Kupfer and colleagues, showed that many of these key molecules in T cell activation (TCR, CD4, MHC, talin, LFA-1/ICAM-1, PKC θ) were accumulated at the interface of the T cell and APC (109-111, 114, 115, 144). These results fit into a generalized model that predicted that molecules involved in facilitating intracellular adhesion (any receptor/ligand pair) would be enriched in the cell-cell contact area. This enrichment is characterized by an increase in the local density of the involved molecules in the contact space (115, 160). However, in 1998, Monks *et al.* showed that these molecules were not simply randomly distributed at the interface of the T cell and APC (50). These molecules were spatially segregated into specific regions and they coined the term supramolecular activation complex (SMAC) to describe them. TCR-ligated to MHC:peptide (113), CD28/B7-1, and

PKC θ are located in the central portion of the interface, the central SMAC (c-SMAC) (50). Surrounding that central region, is the peripheral SMAC (p-SMAC), containing ICAM-1/LFA-1 and talin (50). A recent addition to this model is a ring surrounding the p-SMAC called the distal SMAC (d-SMAC) that contains the phosphatase CD45 (113). This molecular assembly along with the observation that cytokines are directionally secreted (114) lead to widespread adoption of the term “immunological synapse” (49, 117, 118) to describe this interface.

While it now appears that all 3 lymphocyte subsets (T, B, NK) make immunological synapses (49, 161, 162), the best characterized is the synapse that forms between T cells and APC. Still, relatively little is known about the formation of this immunological synapse. There are models that help to explain the process such as van der Merwe’s kinetic segregation model (26, 112), and the lipid raft accumulation model (22, 129), but none satisfactorily explains all of the experimental evidence. While both models can account for the accumulation of similar sized molecules at the T-APC interface, neither satisfactorily explains the precise spatial organization of molecules at the synapse, the accumulation of cytoplasmic proteins, or the mechanism used to generate this arrangement.

This failure of these models is due, in part, to the lack of information on the interaction between live T cells and live APC. This can be traced to the limitations of the systems used to examine synapse formation. Early work has utilized fixed conjugates with transformed B cells or artificial membranes with embedded proteins as “APC” (50, 110, 111, 114, 144). The approach used by Dustin and colleagues employs glass-supported artificial lipid bilayers embedded with defined proteins (49, 103, 104). This system allows for exquisite pictures of the early events of T cell antigen recognition and the formation of the

immunological synapse (49). However this approach also has some drawbacks. The first is that these lipid bilayers contain only a subset of proteins that are involved in the interaction between T cells and antigen presenting cells. This allows for the detailed analysis of the role of a single protein in the immunological synapse, but in the absence of the full complement of interacting proteins, it can be difficult to get an accurate understanding of the importance of a particular protein. Additionally, the artificial bilayer is completely passive in this interaction. It cannot respond to signals from the T cell as living APC might by potentially changing its complement or concentration of surface proteins. With these limitations noted, this system has given us our only high resolution imaging of synapse formation using living T cells (49).

T-B conjugates have been fixed and examined at various time points to generate a “snapshot” of events as they occur over time (113). The data generated with this method are very compelling about the spatial organization of the molecules accumulated at the synapse, but they lack any information on dynamic interactions between T cells and APC and, as such, make conclusions about events during synapse formation more difficult. Davis and colleagues have addresses this problem and were the first group to visualize TCR and MHC interactions by live cell video microscopy (69, 74, 94, 131). However their system uses APC transfected with GFP-tagged wild type MHC which is exogenously loaded with peptide. With this approach they can not discriminate between complexes loaded with cognate peptide and those loaded with non-cognate peptide.

In this thesis, I have described the generation of a system with which I have been able to examine the dynamics of immunological synapse formation

during the interactions between live T cells and antigen presenting cells. One of the key features of this system is that the specific MHC:peptide complexes are tagged with GFP on the cytoplasmic tail. As such, I have been able to assess the redistribution of specific MHC:peptide complexes at all stages of T – APC interactions. This is a major advantage over B lymphoma cells transfected with GFP-tagged wild type MHC exogenously loaded with antigenic peptide because only a fraction of those GFP-tagged molecules will be loaded with cognate peptide and it is impossible to know whether any particular molecule contains cognate peptide. It also has advantages over the systems which have relied on fluorescent proteins embedded in an artificial, glass-supported lipid bilayers in that the APC are capable of responding to the T cells. As adherent cells, my transfected fibroblasts make imaging technically easier because they remain in the focal plane during imaging. Of course, it must be noted that this system has drawbacks as well. These are not physiological APC and may not respond as a dendritic cell or B cell might. These cells also express relatively high levels of the cognate MHC:peptide complex. However, the advantages of this system far outweigh these potential limitations.

Using this system, I have been able to show that costimulation is critical to the formation of the immunological synapse and that T cells rendered anergic by stimulation in the absence of costimulation form relatively normal synapses when encountering antigen in the context of optimal costimulation. I have also been able to assess the role of different intracellular signaling events in the formation of the synapse. The importance of the MAP kinase pathway in sustaining the immunological synapse, a novel finding, is made possible, in part,

by this system in which specific MHC:peptide complexes can be visualized (Figure 22).

As stated above, one of the keys to the success of this project was the generation of an antigen presenting cell line with optimal characteristics for imaging. The MCC:GFP cells were chosen because they displayed sufficient costimulatory capacity to allow for full activation of the antigen specific AD10 T cells and they expressed a level of the GFP-tagged I-E^k:MCC protein optimal for imaging. The MCC:I-E^k:GFP fusion protein is uniformly distributed on the surface of the cells with just a small amount detectable in the cytoplasm, presumably in the Golgi and trans-Golgi network in transit to the plasma membrane. Higher expression levels increased the background and the resulting poor signal to noise ratio prevented observation of any MHC redistributions (data not shown). Similarly, cells with lower MCC:I-E^k:GFP complexes were also sub-optimal due to the low level of expression which made imaging technically difficult because exposure times, on the order of 7 – 10 seconds, were prohibitively long to capture the dynamic live cell images. The increased exposure time also leads to photobleaching of the already dim GFP as well as to detectable phototoxicity of the cells. The synapses formed with these APC were faint and indistinct due to the low GFP signal.

Fibroblasts were chosen as the parent for the transfections because as adherent cells, imaging of live cell interactions is more readily facilitated by the fact that these cells will remain within the plane of focus for the duration of the imaging. Suspension cells like B cell lymphomas may not stay within the focal plane unless tethered to the coverslip by artificial means like poly-L-lysine, which might alter cellular interactions. Additionally, the fibroblasts lack

invariant chain, so greater than 90% of the covalent MHC:peptide molecules actually reach the cell surface with the peptide in the peptide binding groove of the MHC (163).

Another key feature of these APC is the fact that they express fairly high levels of wild type I-E^k that can be exogenously loaded with peptides. This better mimics physiologic APC where the specific MHC:peptide complexes are found in a sea of non-specific ligands and presumably imposes some sorting, since not every TCR – MHC:peptide interaction will be a productive engagement. Preloading the MCC:GFP cells with Hb peptide also allowed them to act as efficient APC for Hb-specific 3.L2 T cells. This feature allowed me to show that the MHC:peptide complexes specifically accumulated in the immunological synapse contain just cognate peptide for the TCR, as discussed below.

Synapse Formation is a Dynamic Process

I began my imaging studies by examining the interactions between the APC and the T cell, which are very dynamic and complex. Previous reports published over the past 10 years have described a series of discrete events that occur when T cells recognize antigen on the surface of an antigen presenting cell or planar lipid bilayer. Importantly, my results correlate very well with those previous reports and they extend our knowledge of these events by examining them in a single system which utilizes living T cells and APCs and has the ability to monitor the movement of specific MHC:peptide complexes. Initially, a polarized T cell makes contact with the APC via a slender membrane projection from the leading edge and stops migrating. TCR recognition of antigen induces a

rapid morphological change within the T cell resulting in a flattening against the APC and a resulting dramatic increase in contact area (Figures 11A, 20). This typical flattened appearance served as the basis for selecting fixed T-APC conjugates for further examination of potential immunological synapses.

In my system, I observed that this flattening was preceded by a rapid increase in the concentration of intracellular Ca^{++} (Figure 20). This Ca^{++} flux, which requires specific antigen recognition (103, 107, 108), occurred almost simultaneously with the initial contact of the APC. The role of the Ca^{++} flux in the morphological changes associated with antigen recognition is unclear. Increasing intracellular Ca^{++} concentration with the pharmacological agent thapsigargin results in cessation of T cell migration and loss of polarity (102), but does not induce tight T-APC couples or ICAM-1 rearrangements (94). Anti-CD3 treatment induces a Ca^{++} flux, but does not induce a morphological change (107). When combined with results showing that chelation of intracellular Ca^{++} with BAPTA blocks morphological changes, Donnadieu et al. concluded that a Ca^{++} flux was required, but did not drive the morphological changes induced by antigen recognition (107). However, other reports have suggested that Ca^{++} chelation with BAPTA has no effect (94, 103) on initial morphological changes, but that Ca^{++} is instead required for sustained stable T-APC conjugates (69, 108). My results support the necessity of a Ca^{++} flux in the cessation of T cell migration and morphological changes induced by antigen recognition, as BAPTA loaded cells did not slow or undergo any morphological changes typically associated with antigen recognition. Without the formation of the stable contacts, I could not assess the necessity of Ca^{++} in the continued stability of the T-APC conjugates.

When I made 3D reconstructions of the interface of the T cell and the APC, I often observe that after initial T-ACP contact, but before an immunological synapse forms, a peripheral ring on the T cell appeared to be pushing against the APC membrane resulting in a bulging out or “blistered” appearance of the APC membrane within this ring (Figure 8). This observation is consistent with a model of immunological synapse formation predicted by Dustin and colleagues (49, 118, 119) which suggested that a “protrusive force” mediated by the T cell cytoskeleton pushed the two membranes into close apposition and allowed for sampling of the MHC:peptide complexes on the APC. These images also corroborate the observed formation of a polymerizing actin ring at the periphery of a T cell interacting with anti-CD3 antibodies on a glass coverslip (85).

Within approximately 0.5 – 1 minute of the first contact, and concomitant with the morphological changes of the T cell, small spots with increased GFP fluorescence become visible at several locations along the T-APC interface (Figure 9A). The appearance of these MHC clusters is antigen specific because no similar structures are observed when the Hb-specific 3.L2 T cells encounter these same APC (Figure 23). The existence of these spots, and the timing of their appearance, correlates well with the early clustering of CD3 ζ observed by Krummel *et al.* (69). As with those CD3 ζ clusters (69), the early MCC:I-E^k:GFP clusters are very dynamic (Figure 9). They form and break apart rapidly during the first 2 – 3 minutes. Ultimately, these spots coalesce into a large cluster at the T-APC interface. When the accumulated GFP reaches maximal intensity, it is defined as a mature immunological synapse. This definition was confirmed in fixed conjugate imaging based upon characteristic p-SMAC ICAM-1 and c-

SMAC PKC θ distribution. The process of synapse formation takes 3 – 20 minutes, with a mean time of 5.5 minutes.

The formation of these small MHC:peptide clusters is independent of the T cell cytoskeleton, but the movement and increase in size leading ultimately to the coalescing into a mature synapse, is dependent upon the actin cytoskeleton of the T cell (Figure 11). This is due, in part, to the very high level of expression of the cognate MHC:peptide complexes on the surface of the APC. Cytoskeleton-independent clustering was predicted by Dustin and Cooper under conditions of high cognate MHC:peptide concentration on an APC (119). While the T cell's actin cytoskeleton is required for synapse formation, intact microtubules appear to be dispensable in this process (74, 94).

Once the T cell and APC made tight conjugates with the attendant morphological changes of the T cell, the T cells continued to actively project and then retract lamellipodia from the edge contacting the APC. Based upon the literature (102), I had expected that the T cell would maintain some activity while in contact with the APC, but the extent and duration of these interactions was somewhat surprising. This "scrubbing" morphology was accompanied by formation of MHC clusters within the highly active interface that ultimately lead to the formation of an immunological synapse. Negulescu *et al.* saw similar membrane activity and described it as "palpating" the APC (102). This activity was evident even in non-productive T-APC engagements where the T cell dissociated from the APC before any detectable MHC:peptide redistribution. The formation of MHC:peptide clusters within these highly active regions suggests that this is a mechanism to facilitate more efficient sampling of the APC surface for cognate MHC:peptide complexes.

T Cell Movement Across APC and MHC Transfer

T cells have been shown to migrate across the surface of macrophages during antigen recognition and even jump from one macrophage (M ϕ) to an adjacent one (145) after a period of stasis upon initial T-M ϕ interaction. Similarly, in a 3D collagen matrix T cells move from one antigen-pulsed dendritic cell to another, “summing” up signals generated during each interaction until the cells are fully activated (146, 164). However neither of these reports examined the formation and stability of the immunological synapse during these encounters. On the artificial lipid bilayers and transformed B cells, no such movement has been detected after synapse formation, leading to the argument that this movement from cell to cell is the result of a “defective” immunological synapse. In my experiments, I frequently observed that after the formation of a mature immunological synapse, T cells would reinitiate locomotion across the surface of the MCC:GFP cells. During that movement, the immunological synapse is dragged along and is relatively unchanged during that process, as judged by MHC density and morphology. Thus it appears that the movement is not initiated by faulty synapses. However, since I examined only the MHC molecules during this movement, it is conceivably possible that the morphology or components of the synapse are altered when the T cells are moving across the APC surface. To rule that possibility out, plans are underway to utilize YFP-tagged ICAM-1 molecules in addition to CFP-tagged MHC:peptide on the APC. This will allow me to assess both the spatial distribution of the MHC as well as that of ICAM-1. If the mature synapse is being “dragged along”, the relative

spatial positioning of ICAM-1 in the p-SMAC and MHC:peptide in the c-SMAC should be maintained.

One of the more interesting observations made during the live cell imaging is that in approximately 10% of interactions resulting in a mature synapse, the T cells dissociate from the APC. Very often when this occurs, there is transfer of GFP-tagged MHC:peptide complexes to the T cell directly from the immunological synapse. While the transfer of MHC and other membrane proteins from the APC to the T cell during antigen recognition has been previously described (63, 116, 147-151, 165-169), this is the first description of the transfer coming directly from the immunological synapse between CD4⁺ T cells and APC. The capture of membrane bound antigen has recently been described after the formation of a synapse between an antigen-specific B cell and an antigen displaying cell (ADC) (162). Transfer of MHC Class I molecules to NK cells mediated by allele-specific interactions with human KIR (170) or murine Ly49 (171, 172) molecules after the formation of an NK immunological synapse has also recently been documented.

Since I see the transfer of MHC as a single large piece from the synapse, my results are at odds with Hudrisier *et al.* who suggested that there was continual transfer of small amounts of MHC rather than transfer of a large single piece (167). However, their study did not include any imaging, instead relying on biochemical detection of the transferred MHC. Additionally, I consistently observed the transfer of small MHC clusters to the T cell during the early phases of T-APC interactions. These spots generally migrated back to the T-APC interface and became part of the immunological synapse (Figure 8). Thus, at the early times, small amounts of MHC are associated with the T cell but these

interactions are transient. The material transferred to the T cell upon dissociation appears to be captured in one large bolus from the immunological synapse, not from these early, transient events.

The transfer of MHC from APC to T cells was first recognized in the early 1980's by several groups (147, 165, 166). Studies done since that time to characterize protein transfer have focused almost exclusively on CTL and the transfer of MHC class I molecules. These previous reports have found that transfer requires antigen recognition (148, 149, 151, 167) and is dependent upon the dose of antigenic peptide present on the APC (148, 167). Transfer is mediated by signals from the TCR (149-151, 167) and requires CD28 but not LFA-1 (150, 151). Similar to the results of Nepom *et al.* (166), I showed, using the Hb-specific 3.L2 T cells, that non-specific bystander T cells do not pick up MHC molecules from APC (data not shown). The transfer of the MHC and other transferred proteins from the APC to the T cell, such as ICAM-1 and B7-1 / -2, requires direct T cell – APC contact (150, 167, 168) and is not simply a case of passive acquisition from apoptotic debris (150, 167, 168) or released molecules from intact APC (162). This transfer is not an *in vitro* artifact as it can be detected *in vivo* using rat T cells transferred into SCID mice (150). In addition, thymocytes from parent (P1) to F1 (P1 x P2) bone marrow chimeras have on their surface MHC from the other parental strain (P2) (165) showing that they are capturing MHC from thymic stroma.

In my experiments, after of rapid loss from the peak at 1 hour the transferred MHC:peptide complexes remain on the surface of the T cells for up to 96 hours (Figure 13 - 16). This is seemingly at odds with the majority of previous reports. When examining the transfer of MHC class I to the surface of CD8⁺ CTL,

Sprent and colleagues have found that the captured MHC is rapidly internalized (148) with a $t_{1/2}$ of approximately 4 hours and only a slight increase above background detectable at 16 hours (148). The time course of MHC class I transfer to CTL is much more rapid in that transfer can be detected within 5 minutes after T-APC contact and reaches its peak at 30 minutes (148, 167). However the consensus that MHC is rapidly internalized upon transfer to the T cell does not necessarily hold true for MHC class II molecules. Isolated murine thymocytes express detectable levels of class II even after 48 hours of suspension culture *in vitro* (169). When examining the transfer of B7-1 to T cells using PCC:I-E^k-specific 5C.C7 TCR transgenic T cells, Sabzevari *et al.* observed that the T cells expressing the captured B7-1 molecules could present antigen to fresh T cells several days later without the addition of exogenous antigen (151). While they did not specifically examine the fate of transferred I-E^k:PCC complexes, the antigen presentation results suggest that the T cells also captured the MHC:peptide complexes and retained them on their surface for several days. Similarly, Patel *et al.* were able to use T cells that had acquired antigen from APC *in vitro* to induce *in vivo* tolerance to myelin basic protein in an EAE model (149).

Several previous studies have clearly demonstrated that the transfer of MHC to activated T cells is more efficient than is the transfer to naive cells (149, 151, 168). In T cells recovered from rheumatoid synovial with transferred B7-1, CD69 and CD25 levels were elevated indicating that these T cells were activated (63). This is similar to my results, which showed that the T cells expressing the transferred I-E^k:MCC complexes were CD69⁺, while the I-E^{kLo} cells were CD69⁻ (Figure 17). Since CD69 expression is induced by antigen recognition, it is

presumed that the CD69 on the T cells serves as a marker of those that have responded to the MCC:GFP cells, rather than directly mediating MHC capture.

The T cells that have captured MHC are preferentially surviving in my experiments, in an apparent discrepancy with previous reports (148, 151). In the studies with Class I transfer to CTL, the T cells expressing the transferred proteins became targets of fresh CTL added to the cultures (116, 150, 168) and were killed. In the class II system, the T cells which had absorbed B7-1 (and presumably MHC:peptide) from the APC were more susceptible to activation induced cell death than those that did not capture B7-1 (151) when fresh T cells were added. However, in my results, the I-E^{k+} T cells actually survived while the I-E^{k-} cells slowly disappeared after 24 hours. This reduction in the I-E^{k-} cells was responsible for the apparent increase in the mean fluorescence intensity (MFI) of GFP and surface I-E^k expression during the course of the experiment, as the levels present on the positive cells did not significantly change (Figures 13, 14). The loss of the I-E^{k-} cells was Fas -dependent because inclusion of blocking anti-FasL antibodies to the cultures delayed their disappearance and also blocked the apparent increase in I-E^k and GFP MFI. It is unclear why the I-E^k positive T cells preferentially survived in my experiments in contrast to the previous reports. It must be noted that the same bimodal profiles were seen in three separate experiments, but results involving anti-FasL are from a single preliminary experiment. One possibility is that the T cells that have captured MHC:peptide are incapable of presenting antigen to other T cells. While there are numerous reports of T cells acting as APC (116, 149, 173-176), the T cells may lack sufficient costimulatory molecules or the transferred MHC:peptide molecules are still attached via the TCR and are not accessible to other T cells. These MHC:peptide

complexes may be continuing to signal the T cell, providing a tonic stimulus that results in the survival of the cells. Another possibility could be that since only about 50% of the T cells picked up the MCC:I-E^k:GFP molecules during the overnight incubation, the I-E^k cells are not antigen reactive and so don't respond to the MHC:peptide complexes present on the remaining T cells. Without the addition of fresh, antigen-reactive cells, there would be no responders to mediate cell death. While appealing at first, this ignores the fact that the antigen was present on T cells, who themselves might be antigen responsive. Nepom et al. showed that T cells which captured I-A molecules from APC were still antigen reactive after 3 days in culture (166). It is unclear why these I-E^k T cells are preferentially surviving, but future experiments will address whether the T cells are continuing to be signaled by the captured MHC, as well as examining the ability of these T cells to present antigen.

The mechanism by which this transfer from the APC to the T cell occurred is unclear, but recently published studies have begun to elucidate the details. One mechanism proposed was that only proteins were being selectively plucked from the APC upon binding to proteins on the surface of the T cell. This is apparently not the case. Using APC with membranes labeled with the lipophilic dye PKH26, two independent groups have demonstrated that there is transfer of both membrane and the membrane associated proteins from the APC to the membrane (149, 167). Stinchcombe *et al.* recently showed by transmission electron microscopy that CTL and target cell membranes actually fuse in small regions they termed membrane bridges, and that these bridges likely served as the mechanism for MHC class I transfer to the T cell from the target (116). While the results suggest that the membrane is incorporated into the T cell membrane

in the correct orientation, it is also possible that it is held as a vesicle tethered to the T cell via the embedded proteins. Knowledge of the location of the transferred proteins (extracellular or integrated into the plasma membrane) will tell us much about the function of the transfer.

Stoichiometry of T – APC Interactions

Previous reports examining the immunological synapse have relied extensively on transformed B cell lines to act as antigen presenting cells (50, 74, 94, 109-111, 114, 115, 131, 132, 144, 177). In those T cell – B cell conjugates, the B cells are capable of interacting with multiple T cells, while the T cells are monogamous, interacting with only 1 APC (102). Wülfing stated unequivocally that after examining several hundred conjugates, he failed to find a “single instance where one T cell and multiple B cells interacted” (94). My results show clearly that a single T cell could interact with multiple APC and induce the redistribution of the GFP-tagged MHC:peptide complexes. However, as far back as 1978, several studies have clearly shown that a single T cell could interact with more than one APC simultaneously (107, 114, 115, 178, 179). These reports were published many years before the discovery of the immunological synapse, and so the state of the synapse was unknown under these conditions. In my studies, when the sizes of the redistributed GFP regions are compared, in every case (>30) one of the interfaces was larger, contained more MHC and was a mature synapse, while the other interface was small and poorly organized (Figure 19) . This result is reminiscent of the findings of Kupfer who found that when a single T cell engaged 2 adjacent APC, talin accumulated at both interfaces, but the

MTOC reoriented under only one of the interfaces (114). In these conjugates, mitotic B cells were only found where the T cell MTOC reoriented, correlating with the directed secretion of cytokines towards that B cell (114, 115). Thus, a single T cell can interact with two adjacent APC and induce the redistribution of MHC molecules, but it appears that a mature immunological synapse is formed with only one of these APC. This implies that synapse formation requires T cell polarization, as has been previously proposed (111).

Intracellular Signaling and Synapse Formation

In continuing to characterize the formation of the immunological synapse, I next turned to examine the relationship between intracellular signaling and the synapse. It has been proposed that the function of the immunological synapse is assembly of a stable supramolecular signaling complex (49, 118, 180) that allows for the sustained signaling needed for full T cell activation (86, 93, 181).

However, to date no systematic examination of the signaling required to form or to maintain the immunological synapse has been undertaken. Freiberg showed that Lck is phosphorylated rapidly after antigen recognition (113). Based upon my observations, in agreement with others (49), that the synapse takes approximately 5 minutes to form after T-APC interaction and the fact that intracellular signaling cascades are triggered within seconds of TCR ligation with cognate MHC:peptide complexes (182), I expected that signaling was triggered prior to mature synapse formation. However, it is unclear whether the initiation of intracellular signaling occurs before the initial redistribution of MHC:peptide in the early clusters, or whether the formation of the clusters triggers signaling.

This question relates directly to the mechanism of TCR triggering; aggregation vs. serial triggering vs. conformational change of the TCR.

If the TCR signals as a result of oligomerization, it would be expected that the MHC:peptide ligand would cluster immediately prior to the initiation of intracellular signaling. This initial clustering would occur independently of the T cell cytoskeleton since TCR-mediated signaling is required for cytoskeletal alterations (85, 112, 182, 183) and might be directly observable with the system I have developed. To examine this question, I chose to monitor changes in intracellular Ca^{++} concentration using the ratiometric Ca^{++} indicator, Fura-2. Because Fura-2 is optimally excited by two different wavelengths dependent upon Ca^{++} binding, it is possible to determine a ratio of the emission of Ca^{++} bound and Ca^{++} free states. Using this method, the absolute ratio values are not affected by differences in dye loading between cells, making direct comparison between cells and treatment conditions possible.

The data in Figure 20, representative of 7 experiments and >100 T-APC interactions, shows that the Ca^{++} response is triggered almost immediately upon contact with the antigen-bearing APC. The lag time between contact and the first detectable Ca^{++} response is as fast as 12 seconds in our system. This is very fast and may appear to be at odds with previous reports that have shown that the Ca^{++} increase follows T-APC contact by 20 – 62 seconds (101, 102, 108, 184). One possible explanation involves the density of the cognate MHC:peptide ligand on the surface of the MCC:GFP cells. With the high density of specific MHC:peptide ligands, the initial interactions of the T cell with the APC will result in productive TCR-MHC:peptide engagements resulting in a very short lag time between contact and Ca^{++} flux.

Since we can specifically visualize MHC:peptide complexes, we are in a unique position to analyze the relationship between the onset of intracellular signaling and the redistribution of specific MHC:peptide complexes. In the images I collected, the first visible redistribution of the MHC:peptide complexes occurs either simultaneously with, or shortly after, the initial increase in intracellular Ca^{++} concentration. Since Ca^{++} release is downstream of the initial phosphorylation events that occur upon TCR ligation of cognate MHC:peptide complexes (185, 186), this data clearly suggests that even the earliest visible redistributions of MHC:peptide complexes driven by T cell antigen recognition follow the initiation of intracellular signaling, and do not drive the initial signaling events. Further experiments utilizing a recent upgrade to the imaging system allowing for faster image capture rates are planned to address this question with even better temporal resolution.

I then went on to determine whether the mitogen activated protein kinase (MAPK) pathway and Src-family kinases (p56^{Lck} and P59^{Fyn}) play a role in the formation and/or maintenance of the immunological synapse. When T cells were pretreated with the MEK-specific inhibitor PD98059 (140), the initial morphological interactions appeared quite normal, in agreement with a previous study that demonstrated that the ERK pathway does not contribute to the actin cytoskeletal rearrangements in Jurkat cells stimulated with anti-CD3 antibody (85). The formation of the immunological synapse also appeared normal. According to Ron Germain's "spreading raindrop" model of TCR antagonism, this result was not expected (187). According to this model, a population of MEK is associated with the plasma membrane and when TCR – triggering results in the phosphorylation of ITAM motifs on the CD3 complex, MEK binds and

protects the phosphorylated tyrosine residues from the action of phosphatases like SHP-1. One prediction from this model is that use of the MEK inhibitor would blunt TCR – mediated signaling and result in an altered activation phenotype similar to T cell responses to TCR antagonist peptides. TCR antagonists induce molecular accumulation at the T-APC interface, but do not induce the formation of mature immunological synapses (50, 113), so it would be expected that use of PD98059 would prevent mature synapse formation. However, my results clearly show that it does not. What does occur is that several minutes after the formation of tight T-APC conjugates and the formation of a mature immunological synapse, the T cells repolarize and move away or simply fall off of the APC (Figure 22). This was somewhat surprising, but it correlates well with a recent report from Weber *et al.* who demonstrated that Jurkat cells would adhere to a surface coated with ICAM-1 protein, but between 5 and 30 minutes, the Jurkat cells treated with PD98059 would lose adherence, presumably due to an undefined effect on the activity of H-Ras (188). Thus, the MAPK pathway is not involved in the initial interactions of the T cell and APC or in the formation of a mature immunological synapse, but it is required for the sustained interactions between these cells and the long-term maintenance of the immunological synapse.

The results were very different when the activity of the Src-family tyrosine kinases (Lck and Fyn) were inhibited by Src-specific inhibitor PP2 (141). In those interactions the T cells interacted with the APC and small MHC clusters formed. However, the morphological changes associated with antigen recognition did not occur and in only approximately 10% of the interactions did a mature immunological synapse form. This is consistent with a requirement of actin

polymerization in synapse formation as well as recent reports that show that Src kinases are required for actin-driven events in cell spreading and actin “collar” formation (85).

Peptide Specificity Of the Immunological Synapse

It is unknown whether the MHC:peptide complexes accumulated contain a mixture of cognate and irrelevant peptides, or whether the cognate peptides are specifically accumulated. This is one of the major unresolved questions about immunological synapse formation and has broad implications for our understanding of T cell activation. We now have a fairly detailed understanding of the intracellular signaling events initiated by TCR engagement of MHC:peptide complexes, although much remains to be elucidated. Based on X-ray crystallography, the structural aspects of MHC:peptide – TCR interactions is also reasonably well understood (17). However, the events linking the physical interaction of the TCR with MHC:peptide complexes to the initiation of the intracellular signaling are unknown and still the focus of vigorous debate.

Several different models have been proposed to explain what van der Merwe calls the “TCR triggering puzzle” (26). Various models invoke TCR conformational changes (189), monovalent serial engagement of a few MHC:peptide ligands with numerous TCR (18, 19, 21, 190), aggregation or multimerization of the TCR (28, 191, 192), or topological restraints between the membranes of the T cell and antigen presenting cell (25-27).

In the kinetic proofreading model, proposed by our collaborator Tim McKeithan (28) and later refined by Rabinowitz et al. (29), TCR engagement

initiates a multi-step program which leads to T cell activation. One potential step in the kinetic proofreading model is oligomerization of the TCR (28). The role for TCR oligomerization in T cell activation is supported by biochemical data (191-194) and has received considerable attention since the description of the immunological synapse (49, 50). One of the predictions made by the initial kinetic proofreading model is that TCR antagonism could result from inclusion of lower-affinity MHC:peptide ligands in aggregated TCR/MHC:peptide clusters. This could tie up TCRs in non-productive engagements, preventing aggregation or reducing the avidity between the clustered receptors and clustered MHC molecules (28). This obviously requires the inclusion of MHC molecules loaded with closely related peptides that interact with the TCR, but does not address the question of peptide specificity in general.

Non-cognate MHC:self peptide molecules may be important in controlling T cell activation. Tonic signaling from these molecules has been linked to T cell survival in the periphery (195-198), although in some systems, this is not required (199, 200). Activation of the T cell would require that signaling would have to exceed a critical threshold set by the tonic signaling through these MHC:self peptide complexes. Their inclusion in the synapse could be a mechanism by which this requirement to exceed this threshold is enforced, by potentially tying up TCR or by generating a unique signal. Exclusion of the irrelevant ligands from the synapse might lower this threshold or facilitate the assembly of more stable signaling structures, allowing for signaling of longer duration required for T cell activation (120, 154).

The presence of wild type I-E^k on the surface of the MCC:GFP cells allowed me to address the question of peptide specificity. The cells were

exogenously loaded with Hb peptide and used as APC for Hb-specific T cells from the 3.L2 TCR transgenic mouse. Under these conditions, the GFP-tagged MCC:I-E^k molecules are considered null complexes. The basic experiment and interpretation are found in Figure 37 below.

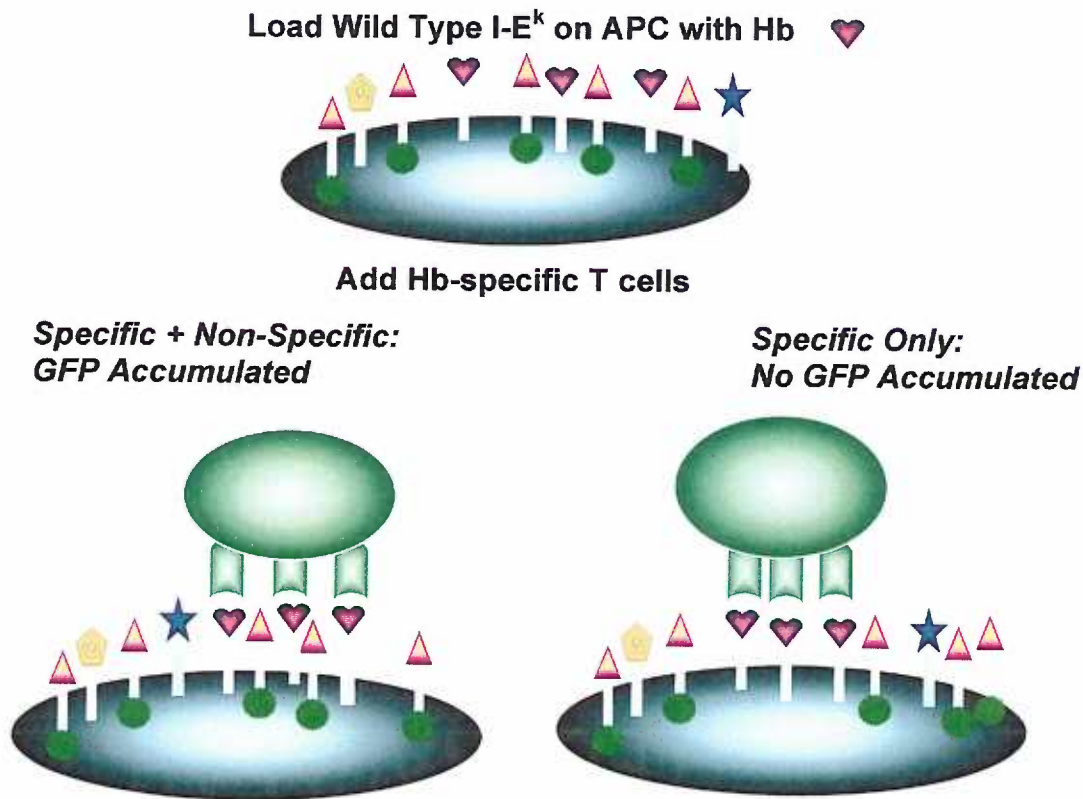


Figure 37. Schematic of MHC:peptide specificity experimental design.

The results in figure 23 show that when the 3.L2 T cells encounter I-E^k:Hb complexes on the surface of the MCC:GFP cells, they form tight conjugates which are stable for at least 1 hour and that there is no specific accumulation of GFP-tagged MCC:I-E^k complexes. This shows that MHC:peptide complexes accumulated in the immunological synapse are peptide specific. PKC θ staining of the 3.L2 – MCC:GFP conjugates was very similar to AD10 – MCC:GFP

conjugates, indicating that the 3.L2 T cells were forming immunological synapses upon antigen recognition (Figure 24).

My observation that the immunological synapse specifically accumulates cognate MHC:peptide complexes clearly indicates that there is some peptide-specific sorting mechanism operating during synapse formation. It is unclear whether this sorting mechanism is functioning early in the process, during the formation of the early MHC clusters, or whether this is occurring during the coalescing of these clusters to form the synapse. If the initial clusters contain only specific complexes, it would imply that a sorting mechanism is functioning very rapidly, and also suggests that receptor aggregates, containing only cognate complexes are required for the generation of intracellular signaling. This hypothesis cannot be directly examined in the current system, nor can the timing of the MHC:peptide sorting, because the I-E^k:Hb complexes cannot be directly visualized on living cells. To address this question, a new set of transfectants with cyan fluorescence protein (CFP)-tagged I-E^k:MCC and yellow fluorescence protein (YFP)-tagged I-E^k:Hb molecules has been made. This will allow for direct visualization of both complexes during antigen recognition on live cells. If the molecules are aggregated at the submicroscopic level (<100 nm), they might undergo fluorescence resonance energy transfer (FRET) (201, 202). To date these experiments have not been performed due to difficulties in CFP-tagged protein expression patterns.

With the basic system in place, we will proceed to experiments examining the potential inclusion of weak agonist or antagonist peptides in immunological synapses. Based upon the predictions from the kinetic proofreading model, antagonist ligand should be accumulated, but the structure and molecular

components of the synapse would be significantly different. With the FRET approach, we can assess the degree of interaction between agonist and antagonist or weak agonist complexes at the T-APC interface.

The Role of Costimulation in Synapse Formation

One major focus of these imaging studies has been to examine the role of costimulation in the formation of the immunological synapse. While B7-1 (CD80)/CD28 are localized in the central portion of the immunological synapse (c-SMAC) and LFA-1/ICAM-1 are located in the p-SMAC, the role of these molecules in the formation of the immunological synapse is not clear. It has been suggested that ICAM-1 may be involved in driving synapse formation (203), but there is no direct evidence for the requirement of ICAM-1 in synapse formation. CD28 does not appear to be directing the early steps in synapse formation because it does not move into the c-SMAC of the nascent synapse until approximately 3 minutes after T-APC contact (113). In support of a central role of costimulation in synapse formation, Wülfing and Davis have shown that the polarized bulk flow of T cell surface molecules towards the engaged APC could be inhibited by antibody blocking of B7:CD28 or LFA-1:ICAM-1 interactions (74, 94). In data not shown, they reported that anti-B7-1/-2 antibodies also blocked accumulation of GFP-tagged MHC molecules to the synapse (131). Using T cells from mice lacking a key downstream mediator of CD28 signals, *Vav1*, Wülfing *et al.* also showed that MHC accumulation at the T-APC interface was “defective” (131). Similarly, Krummel *et al.* (69) showed that a “central capping” phenotype of CD3 ζ could be diminished by blocking B7:CD28 interactions. The importance

of costimulation in synapse formation in the Davis system is confirmed in a recently published paper (132). This is in contrast to results from Dustin and colleagues showing that incorporation of B7-1 in their planar lipid bilayers has no effect on the frequency of synapse formation or the density of MHC:peptide complexes accumulated (49, 121). *In vitro*, PKC θ and LAT are accumulated at the T-APC interface in CD28^{-/-} T cells, although they are uniformly distributed rather than accumulating in the c-SMAC (113). In addition, CD28^{-/-} T cells show redistribution of the TCR toward the APC *in vivo* (133)

Using my system, with which I can follow the movement of specific MHC:peptide ligands, I have confirmed that B7-1:CD28 and ICAM-1:LFA-1 are indeed important mediators of mature synapse formation. To accurately quantify the synapses, I adapted the fixed conjugate methodology of Kupfer and colleagues (50, 109, 111, 113, 115, 144). A reconstructed 3D interface was generated from which I can measure the intensity and area of clustered MHC. The resulting areas are small (Figure 26) because MHC clusters were defined as areas with MHC twice background values and not the entire contact region between the APC and T cell. Monks *et al.* have estimated that only about 6% of the contact zone contains accumulated TCR (50).

Upon quantitation of the area and amount of MHC accumulated in the synapses, I determined that CTLA-4Ig or anti-ICAM-1 treatments (Figure 26) significantly reduce both the size (Figure 26C) and intensity (Figure 26B) of accumulated MHC. The morphology of the clustered MHC is also altered in the treated synapses (Figure 25). The synapses with control IgG (Figure 25D) generally have one or a few large, intense clusters surrounded by several smaller regions with increased density. This pattern is reminiscent of the MHC

distribution in fixed AD10 T cell – B cell conjugates published by Monks *et al.* (50). With costimulation blockade no central dense cluster is observed and the MHC clusters formed are irregularly spaced. However, costimulation blockade does not completely block MHC redistribution indicating that even in the absence of costimulation an immunological synapse, albeit altered, can form. This is consistent with data in Bromley *et al.* (121).

After observing the significant affects of costimulation blockade on the size, density, and morphology of the immunological synapse, I wanted to see if these differences correlated with differences in T cell functional outcomes. In examining the proliferative capacity of T cells to respond to MCC:GFP cells, I found that the magnitude of the reduction of synapse size and intensity are very similar to reductions in T cell proliferation measured after 3 days of co-culture (Figure 26A). This indicates that the size and/or intensity and/or morphology of the immunological synapse present at 30 minutes may be predictive of full T cell activation. These results are in agreement with the models that propose that synapse formation may serve as a “checkpoint” for full T cell activation (78, 112, 118, 121).

By contrast, with the exception of a slight reduction in CD69 expression when the APC were preincubated with CTLA-4Ig, blockade of B7-1, ICAM-1 or I-E^k has virtually no affect on CD69 or CD25 expression or TCR down-modulation, all phenotypic markers of T cell activation (Figure 27). These findings are not unprecedented. CTLA-4Ig does not block CD69 expression *in vivo*, even though it reduces diabetes in NOD mice (62). Others have also found that CD28 also has no apparent effect on TCR downmodulation (121). Our results with anti-ICAM-1 blockade are consistent with previous studies that suggested that ICAM-1 is

critical in TCR down-modulation at low ligand density (98, 204), but at higher antigen doses the importance of ICAM-1 in TCR down-modulation is reduced. While widely accepted as an accurate predictor of T cell activation, previous studies have shown that TCR downmodulation does not always correlate with T cell activation (98, 205-207). The lack of a correlation between TCR down-modulation and the properties of the immunological synapse suggests that these two phenomena of T cell activation are independent. Based upon these findings, I propose that the properties of the synapse are a better predictor of full T cell activation than TCR down-modulation.

It is not clear how costimulation through CD28 and LFA-1 are controlling the formation of the immunological synapse. My experiments did not directly address this question, but the mechanisms involved are likely linked to the mechanisms of costimulation in general. It has been suggested that costimulation has two major functions in T cell activation:

1. initiate unique signals which overlap and synergize with TCR-mediated signals to induce full T cell activation; and
2. control cytoskeletal rearrangements that are crucial for T cell activation (182).

While unique intracellular signaling pathways initiated by these costimulatory interactions are important, it is more likely that the control of the actin cytoskeleton by costimulation is more significant in the context of immunological synapse formation, in light of the evidence implicating the actin cytoskeleton in synapse formation (94, 108).

There is much evidence linking costimulation, particularly through CD28, to the actin cytoskeleton (see Figure 37). Actin filament regulation involves

members of the Rho GTPase family (Rac1, RhoA, Cdc42). Rho family members work through downstream mediators, such as the Wiskott-Aldrich syndrome protein (WASP) and the Arp2/3 complex, to control the initiation of actin polymerization (75, 80, 81, 182, 208-210). Vav1 is a guanine exchange factor that activates members of the Rho family (76, 79). In the presence of a TCR signal, ligation of CD28 induces the hyperphosphorylation and activation of Vav1 (75, 83, 182), but CD28 ligation alone can also result in Vav activation (182). Vav1^{-/-} T cells have normal TCR proximal signaling (e.g. phosphorylation of ZAP-70, LAT, SLP-76, etc.), but have defects in Ca⁺⁺ responses (78, 82, 84) and NFκB activation (82). These T cells also have significantly reduced proliferation and IL-2 secretion (82, 83) in response to anti-CD3, and addition of a signal through CD28 does not restore full activation (83). Interestingly, the Vav^{-/-} T cells do not down regulate p27^{Kip1} upon activation (83), reminiscent of T cells rendered anergic by the absence of costimulation (47, 48). Phenotypically, these T cells have been compared to normal T cells responding to antigen on costimulation deficient APC (131). Most relevant to this study, Vav1^{-/-} T cells do not display TCR clustering in response to CD3 crosslinking (83), and they form defective immunological synapses, in that MHC molecules do not accumulate within the c-SMAC (131).

A tempting model for CD28 direction of synapse formation can be drawn from our knowledge of CD28's control of actin rearrangements. Signals through the TCR, which precede CD28 ligation, induce some phosphorylation of Vav1 as well as generating unknown signals which favor B7-1/CD28 interactions (121). Among the effects of CD28 ligation is the hyperphosphorylation and activation of Vav1. Vav1 activation serves to activate several downstream events including

sustained Ca^{++} increases (131), PKC θ activation (211), and Rho family GTPase activation. Rho activation, in turn, controls the polymerization of the actin cytoskeleton, which has been shown to be a central mediator of immunological synapse formation (74, 94, 108, 131). Consistent with this model, cytochalasin D poisoning of the cytoskeleton prevents stable synapse formation (69) and Figure 11).

An alternative model for the mechanism by which CD28 costimulation might control immunological synapse formation involves the redistribution of lipid microdomains called lipid rafts on the surface of the T cells (124, 125, 212). These microdomains are enriched in signaling-associated molecules such as LAT, Lck, ZAP-70, PIP₂, and Ras (22-24). The aggregation of these microdomains by crosslinking associated proteins or by use of Cholera toxin B results in protein phosphorylation and cellular activation (88, 213, 214). Raft accumulation and subsequent kinase activation has also been linked to the reorientation of F-actin (22, 213), and thus might be involved in the initiation of the actin-based model described above. Viola showed that crosslinking CD28 results in the accumulation of lipid rafts (130). It has been proposed that costimulation actually results from the aggregation of these lipid rafts and this might explain the ability of raft-associated proteins like ICAM-1, CD48 and CD59 to provide costimulation (127, 215). Based upon these results and the findings of Viola *et al.* (130), a model has been proposed in which lipid raft accumulation is a central event in immunological synapse formation (215, 216). There are a couple of caveats to this model. First, a formal demonstration of lipid rafts in the immunological synapse has not been made (129). Second, CD28 is not a raft-associated protein and the kinetics of CD28-mediated raft accumulation, on the order of 15 minutes (130), is

difficult to reconcile with the timing of synapse formation (~5 minutes) (130, 180) and the appearance of CD28 within the c-SMAC (3 minutes) (113).

Anergic T Cell Synapses

T cells that encounter antigen in the absence of appropriate costimulation enter a state of hyporesponsiveness termed anergy (35, 39, 217, 218). These cells do not proliferate or secrete cytokines upon reencountering antigen, even in the presence of antigen presenting cells displaying optimal costimulation (152). This has led to the proposal that anergy induction is critical in maintenance of peripheral T cell tolerance *in vivo* (48) since normal somatic tissues would not be expected to express costimulation constitutively. Many of the molecular details which result in anergy induction have been elucidated, but the underlying mechanism which results in anergy induction remains to be determined.

In classical anergy, there are many signaling alterations within the anergic T cell that result in the inability to synthesize IL-2 (46, 219). These defects include decreases in the transcription factor AP-1 (43, 220), altered Ca^{++} responses (40), alterations in NF- κ B and NFAT/AP-1 transcription factor activity (43), impaired expression of c-fos, c-jun, and JunB (44), differential recruitment of p56^{Lck} and p59^{lyn} (42), and altered CD3 ζ phosphorylation patterns (41). Anergic T cells do not proliferate and are arrested early in the G₁ phase of the cell cycle (47). This growth arrest has been linked to upregulation of a pair of cyclin-dependent kinase inhibitors, p21^{Cip1} and p27^{Kip1} (47, 48, 83, 221). Administration of exogenous IL-2, which rescues the cells from anergy (38), induces the down regulation of p27^{Kip1}, allowing the cells to transit through the cell cycle (47, 48). It

is this transit through the cell cycle induced by the signals through CD28, and not merely physical engagement of CD28 alone, which is responsible for the prevention of anergy when costimulation is present (38).

CD28 signaling is also linked to anergy prevention by controlling activation of Rap1. Activation of the small G protein Rap1 occurs when T cells recognize antigen in the absence of costimulation (157). Rap1 is an inhibitor of the Ras-mediated MAPK signaling pathway, and signals through CD28 inhibit Rap1 activation (158). It is unknown how CD28 signals inhibit Rap1 activation and facilitate Ras activation or why TCR signals alone induce Rap1 activation, though differential activation of p59^{Fyn} has been implicated (48).

With the discovery of the immunological synapse, and the suggestion that the synapse serves to facilitate signaling by serving as a platform for signaling molecules to accumulate, it is possible that synapses formed by anergic cells will be quantitatively or qualitatively different from normal synapses. To date, however, no studies have addressed the ability of anergic T cells to make immunological synapses or characterized the molecules that accumulate at the T-APC interface of anergic cells.

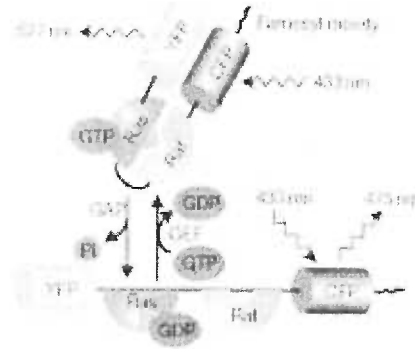
To test the hypothesis that anergic T cells form altered synapses, *in vitro* primed AD10 T cells were anergized by incubating them overnight on plates coated with anti-TCR antibody. These anergized T cells were hyporesponsive (Figures 29 – 31) but are still capable of forming conjugates with APC (Figure 32). Surprisingly, the anergic T cells are able to form immunological synapses (Figure 35). This contrasts with predictions Mark Davis made at the 11th International Congress of Immunology in 2001 that anergic T cells would not be capable of making immunological synapses. When the size and density of MHC:peptide

clusters are calculated, there is only a very small reduction that is not statistically significant (Figure 35). The morphology of the MHC:peptide clusters is also very similar in normal and anergic T cells (Figure 35). Based upon MHC:peptide accumulation patterns, there is very little difference between normal and anergic synapses.

However, the engaged TCR/MHC:peptide complexes are only one part of the immunological synapse. Because they make synapses, it is possible that differential recruitment of various signaling molecules to the anergic synapse could explain differences in downstream events associated with anergy. To examine this possibility, I stained for several different molecules (Figure 36). In somewhat unexpected results, there was no apparent difference in recruitment of PKC θ (Figure 36 C and D) or CTxB-stained lipid rafts (36 E and F) to anergic synapses. By contrast, c-Cbl was preferentially recruited to the anergic synapses (Figure 36G and H). The importance of this difference in c-Cbl recruitment to the anergic synapse is unclear. Members of the Cbl family are negative regulators of TCR signaling and have been implicated in controlling the Vav-WASP pathway leading to actin cytoskeletal rearrangements (75). Another Cbl family member, Cbl-b has been implicated in controlling synapse formation in T cells from aged mice which functionally resemble anergic T cells (222). Cbl-b^{-/-} T cells are costimulation independent, and when crossed to Vav^{-/-} T cells, the loss of Cbl-b restores normal synapse formation to the Vav^{-/-} T cells, suggesting that Cbl-b functions as a negative regulator of synapse formation (156). Thus, the differential recruitment of c-Cbl may be consistent with generation of altered signaling pathways within the anergic T cells. Experiments are planned to examine the recruitment of Cbl-b to the anergic synapse, as well.

The differential recruitment of c-Cbl to the synapse is an interesting finding, but there are many other molecules that need to be assessed before we reach a complete understanding of the

anergic synapse. Experiments are planned which will examine both the activation state and the cellular localization of Rap1 in the anergic T cells using a novel reagent used to image



Rap1 in neuronal cells (159). This reagent contains, in order, cyan fluorescent protein, Rap1, the Ras binding domain of Raf (Raf-RBD), and yellow fluorescent protein. When in the active GTP-bound form, the Rap1 will bind the Raf-RBD, bringing the CFP and YFP into close proximity allowing for fluorescence resonance transfer (FRET). In the inactive, GDP-bound form, the Rap1 will not bind the Raf-RBD, and the CFP and YFP will not be within the required 50 – 70 Å radius to allow for the generation of a FRET signal.

In addition to Rap1, there are several other molecules which potentially mediate, or may be altered in, the anergic state that I plan to examine. Among these are:

C3G/CrkL – alternate adapter to Grb2/Sos implicated in Rap1 activation

p59^{Fyn} – Src kinase implicated in signaling in anergy induction

P-Tyr - to show that tyrosine phosphorylation is occurring

Phalloidin – are actin rearrangements the same?

SHP-1 – Phosphatase implicated in controlling TCR signaling

CD45 – Phosphatase implicated in controlling TCR signaling

Gamma tubulin - allows for analysis of MTOC movement

Knowledge of the spatial and temporal localization of these molecules within the anergic immunological synapse might help us to better understand the molecular events leading to this hyporesponsive state and will give us a deeper appreciation for the mechanisms underlying tolerance induction and maintenance.

Chapter 5

Summary and Future Directions

In this thesis, I have described the development of a system to examine the dynamics of immunological synapse formation. This system utilizes fibroblast cells transfected with a green fluorescence protein (GFP)-tagged MHC class II molecule with covalent antigenic peptide. This approach allows me to follow the redistribution of specific MHC:peptide molecules during T cell antigen recognition.

Dynamics of Synapse Formation – Signaling To and From the Synapse

In corroboration with previous reports (49), I found that upon contact with antigen-bearing fibroblasts, T cells underwent a rapid, Ca^{++} -dependent morphological change resulting in a dramatic increase in contact area with the APC (Figures 7 and 10). The Ca^{++} flux is induced immediately upon APC contact and precedes the initial redistribution of MHC: (Figures 20 and 21). These small clusters of MHC:peptide coalesce to form a mature immunological synapse, characterized by recruitment of PKC θ and ICAM-1 (Figure 36). The morphological changes and subsequent synapse formation, depends upon the activity of Src-family kinases like p56^{Lck} but not the MAP kinase pathway. Continued MAPK activity, however, is necessary for long-term stability of the T-APC conjugates (Figure 22).

Costimulation is Crucial to Synapse Formation.

While B7-1 / CD28 is located in the c-SMAC and ICAM-1/LAFA-1 is found in the p-SMAC (118), the role of these costimulatory molecules in synapse formation of the synapse is controversial (49, 74, 94, 103, 121, 131, 132). In the first quantitative examination of the effects of costimulation, I found that costimulation is required for normal immunological synapse formation. The mechanism by which costimulation contributes to mature immunological synapse formation was not directly tested in this thesis, but control of cytoskeletal rearrangements necessary for synapse formation seem most likely.

Anergic T cells Make Immunological Synapses

When T cells encounter antigen in the absence of costimulation, they enter a hyporesponsive state termed anergy (152). The mechanism of anergy maintenance is unknown. I tested to determine whether anergy maintenance involves differences in the ability to form synapses or differential recruitment of proteins involved in signaling. I found that anergic T cells did make immunological synapses with no significant difference in morphology, area, or amount of accumulated MHC molecules (Figure 35) compared to non-anergic T cells. There were also no differences in the accumulation of ICAM-1, PKC θ , or lipid rafts to the anergic synapses (Figure 36). However, there was a clear difference in the distribution of c-Cbl. Another member of the Cbl family, Cbl-b, has been linked to inhibition of TCR (156) signaling and is accumulated in the synapses of T cells from aged mice, which are phenotypically similar to anergic T cells (222). C-Cbl has also been implicated in the negative regulation of TCR

signaling (226). These results are a starting point for further characterization of the anergic synapses. In future experiments, I plan to examine the distribution of Cbl-b and several other molecules that could be important in the maintenance of an anergic state, such as CrkL/C3G, P59Fyn, SHP-1 and Rap1.

Peptide Specificity of the Synapse

The final set of experiments presented in this thesis relate to the identity of the MHC:peptide complexes accumulated within the immunological synapse. In my system, wild-type I-E^k on the APC can be loaded with exogenous peptide and present it to antigen-specific T cells. Under these conditions, the GFP-tagged I-E^k:MCC molecules act as a non-cognate ligand and are not accumulated within the synapse, showing that the synapse accumulates specific MHC:peptide ligands but not a non-cognate MHC:peptide ligand.

Future Directions: Imaging TCR Peptide Specificity and TCR Antagonism

Knowledge of whether the immunological synapse contains only specific MHC:peptide complexes or rather contains a mixture of cognate and non-cognate complexes has several implications for the nature of T cell activation. Inclusion of self peptide-containing complexes might increase the threshold for TCR triggering due to the tonic signaling these ligands provide in the periphery involved in long-term survival of the T cells (196, 197, 223). One proposed model of the phenomenon of TCR antagonism envisions inclusion of the antagonist ligand in receptor aggregates potentially altering signaling. While not directly addressed in this thesis, I have transfected fibroblasts with cyan fluorescent protein (CFP)-tagged MHC:peptide complexes and yellow fluorescence protein

(YFP)-tagged wild type MHC. With these APC, I will be able to visualize both cognate and non-cognate ligands simultaneously. These APC will be loaded with a range of peptides including null, weak agonist/antagonists, and heteroclitic peptide to examine whether they are included in the synapse and/or how they affect synapse formation. This combination of CFP and YFP has the added advantage that if they are localized within ~60 nm, fluorescence resonance energy transfer (FRET) may occur. This will give us data on TCR aggregation at the submicroscopic level, which will help solve the TCR triggering “puzzle” detailed above.

Future Directions: MCC:I-E^k:GFP Transgenic Mice and Imaging of Physiologic T – APC Interactions

These imaging studies prove the power of the techniques employed, and set the stage for some very exciting and informative experiments. One of the most exciting prospects involves the generation of transgenic mice expressing the same MCC:I-E^k:GFP construct used to transfect the fibroblast APC in this thesis. These mice will allow me to examine synapse formation with real, physiologic APC such as B cells and dendritic cells. I will begin by imaging synapse formation between naive, effector, and anergic T cells and DC. Recent reports suggest that that DC have unique properties related to synapse formation which may explain their ability to activate naive T cells (123, 224, 225). I will characterize the synapses formed between these various T cells and DC. I will also compare the ability of naive DC to in vivo activated DC to see if DC maturation increases the ability of these cells to participate in immunological synapse formation.

Experiments are planned with B cells that will examine the functions of the immunological synapse between T cells and B cells. The first experiment is to determine whether normal B cells can induce synapse formation, as most previous work utilizing B cells as APC used transformed B cell lines. The most interesting experiment may be to examine the function of the synapse in cognate T-B interactions. T-B conjugates will be stained to determine whether molecules important in providing help to the B cells (e.g., CD40-CD40L) localize to the synapse. This would suggest that the synapse serves as a bi-directional signaling structure, activating both the T cell and the B cell simultaneously. This will provide insight not only into the signaling functions of the synapse for the T cell, but may also provide evidence that this structure is directly involved in T_H cell effector functions as well.

References

1. Kappler, J.W., B. Skidmore, J. White, and P. Marrack. 1981. Antigen-inducible, H-2 restricted, interleukin-2 producing T cell hybridomas. Lack of independent antigen and H-2 recognition. *J Exp Med* 153:1198.
2. Heber-Katz, E., D. Hansburg, and R.H. Schwartz. 1983. The Ia molecule of the antigen-presenting cell plays a critical role in immune response gene regulation of T cell activation. *J Mol Cell Immunol* 1:3.
3. Rock, K.L., and B. Benacerraf. 1983. Inhibition of antigen-specific T lymphocyte activation by structurally related Ir gene-controlled polymers. Evidence of specific competition for accessory cell antigen presentation. *J Exp Med* 157:1618.
4. Samelson, L.E., and R.D. Klausner. 1992. Tyrosine kinases and tyrosine-based activation motifs. Current research on activation via the T cell antigen receptor. *Journal of Biological Chemistry* 267:24913.
5. Straus, D.B., and A. Weiss. 1992. Genetic evidence for the involvement of the lck tyrosine kinase in signal transduction through the T cell antigen receptor. *Cell* 70:585.
6. Chan, A.C., M. Iwashima, C.W. Turck, and A. Weiss. 1992. ZAP-70: a 70 kd protein-tyrosine kinase that associates with the TCR zeta chain. *Cell* 71:649.
7. Wange, R.L., A.N. Kong, and L.E. Samelson. 1992. A tyrosine-phosphorylated 70-kDa protein binds a photoaffinity analogue of ATP and associates with both the zeta chain and CD3 components of the activated T cell antigen receptor. *Journal of Biological Chemistry* 267:11685.

8. van Oers, N.S., N. Killeen, and A. Weiss. 1996. Lck regulates the tyrosine phosphorylation of the T cell receptor subunits and ZAP-70 in murine thymocytes. *J Exp Med* 183:1053.
9. Kersh, E.N., A.S. Shaw, and P.M. Allen. 1998. Fidelity of T cell activation through multistep T cell receptor ζ phosphorylation. *Science* 281:572.
10. Clements, J.L., N.J. Boerth, J.R. Lee, and G.A. Koretzky. 1999. Integration of T cell receptor-dependent signaling pathways by adapter proteins. *Annu Rev Immunol* 17:89.
11. Chan, A.C., D.M. Desai, and A. Weiss. 1994. The role of protein tyrosine kinases and protein tyrosine phosphatases in T cell antigen receptor signal transduction. *Annu Rev Immunol* 12:555.
12. Isakov, N., R.L. Wange, and L.E. Samelson. 1994. The role of tyrosine kinases and phosphotyrosine-containing recognition motifs in regulation of the T cell-antigen receptor-mediated signal transduction pathway. *Journal of Leukocyte Biology* 55:265.
13. Germain, R.N., and I. Stefanova. 1999. The dynamics of T cell receptor signaling: complex orchestration and the key roles of tempo and cooperation. *Annu Rev Immunol* 17:467.
14. Janeway, C.A., Jr. 1995. Ligands for the T-cell receptor: hard times for avidity models. *Immunol Today* 16:223.
15. Alam, S.M., G.M. Davies, C.M. Lin, T. Zal, W. Nasholds, S.C. Jameson, K.A. Hogquist, N.R. Gascoigne, and P.J. Travers. 1999. Qualitative and quantitative differences in T cell receptor binding of agonist and antagonist ligands. *Immunity* 10:227.

16. Baker, B.M., and D.C. Wiley. 2001. $\alpha\beta$ T cell receptor ligand-specific oligomerization revisited. *Immunity* 14:681.
17. Hennecke, J., and D.C. Wiley. 2001. T cell receptor-MHC interactions up close. *Cell* 104:1.
18. Valitutti, S., S. Muller, M. Cella, E. Padovan, and A. Lanzavecchia. 1995. Serial triggering of many T-cell receptors by a few peptide-MHC complexes. *Nature* 375:148.
19. Viola, A., and A. Lanzavecchia. 1996. T cell activation determined by T cell receptor number and tunable thresholds. *Science* 273:104.
20. Lanzavecchia, A., G. Iezzi, and A. Viola. 1999. From TCR engagement to T cell activation: a kinetic view of T cell behavior. *Cell* 96:1.
21. Davis, M.M. 1995. T-cell receptors. Serial engagement proposed. *Nature* 375:104.
22. Janes, P.W., S.C. Ley, A.I. Magee, and P.S. Kabouridis. 2000. The role of lipid rafts in T cell antigen receptor (TCR) signalling. *Semin Immunol* 12:23.
23. Janes, P.W., S.C. Ley, and A.I. Magee. 1999. Aggregation of lipid rafts accompanies signaling via the T cell antigen receptor. *J Cell Biol* 147:447.
24. Xavier, R., T. Brennan, Q. Li, C. McCormack, and B. Seed. 1998. Membrane compartmentation is required for efficient T cell activation. *Immunity* 8:723.
25. Shaw, A.S., and M.L. Dustin. 1997. Making the T cell receptor go the distance: a topological view of T cell activation. *Immunity* 6:361.
26. van der Merwe, P.A. 2001. The TCR triggering puzzle. *Immunity* 14:655.

27. Wild, M.K., A. Cambiaggi, M.H. Brown, E.A. Davies, H. Ohno, T. Saito, and P.A. van der Merwe. 1999. Dependence of T cell antigen recognition on the dimensions of an accessory receptor-ligand complex. *J Exp Med* 190:31.
28. McKeithan, T.W. 1995. Kinetic proofreading in T-cell receptor signal transduction. *Proc Natl Acad Sci U S A* 92:5042.
29. Rabinowitz, J.D., C. Beeson, D.S. Lyons, M.M. Davis, and H.M. McConnell. 1996. Kinetic discrimination in T-cell activation. *Proceedings of the National Academy of Sciences of the United States of America* 93:1401.
30. Lyons, D.S., S.A. Lieberman, J. Hampl, J.J. Boniface, Y. Chien, L.J. Berg, and M.M. Davis. 1996. A TCR binds to antagonist ligands with lower affinities and faster dissociation rates than to agonists. *Immunity* 5:53.
31. Kersh, B.E., G.J. Kersh, and P.M. Allen. 1999. Partially phosphorylated T cell receptor zeta molecules can inhibit T cell activation. *J Exp Med* 190:1627.
32. Bretscher, P., and M. Cohn. 1970. A theory of self - nonself discrimination. *Science* 169:1042.
33. Lafferty, K.J., and A.J. Cunningham. 1975. A new analysis of allogeneic interactions. *Australian Journal of Biomedical Science* 53:27.
34. Cunningham, A.J., and K.J. Lafferty. 1977. A simple conservative explanation of the H-2 restriction of interactions between lymphocytes. *Scandinavian Journal of Immunology* 6:1.
35. Jenkins, M.K., and R.H. Schwartz. 1987. Antigen presentation by chemically modified splenocytes induces antigen-specific unresponsiveness *in vitro* and *in vivo*. *J Exp Med* 165:302.

36. Quill, H., and R.H. Schwartz. 1987. Stimulation of normal inducer T cell clones with antigen presented by purified Ia molecules in planar lipid membranes: specific induction of a long-lived state of proliferative nonresponsiveness. *J Immunol* 138:3704.
37. Jenkins, M.K., P.S. Taylor, S.D. Norton, and K.B. Urdahl. 1991. CD28 delivers a costimulatory signal involved in antigen-specific IL-2 production by human T cells. *J Immunol* 147:2461.
38. Wells, A.D., M.C. Walsh, J.A. Bluestone, and L.A. Turka. 2001. Signaling through CD28 and CTLA-4 controls two distinct forms of T cell anergy. *J Clin Invest* 108:895.
39. Schwartz, R.H., D.L. Mueller, M.K. Jenkins, and H. Quill. 1989. T-cell clonal anergy. *Cold Spring Harb Symp Quant Biol* 54:605.
40. Gajewski, T.F., D. Qian, P. Fields, and F.W. Fitch. 1994. Anergic T-lymphocyte clones have altered inositol phosphate, calcium, and tyrosine kinase signaling pathways. *Proc Natl Acad Sci U S A* 91:38.
41. Sloan-Lancaster, J., A.S. Shaw, J.B. Rothbard, and P.M. Allen. 1994. Partial T cell signaling: altered phospho-zeta and lack of Zap70 recruitment in APL-induced T cell anergy. *Cell* 79:913.
42. Quill, H., M.P. Riley, E.A. Cho, J.E. Casnellie, J.C. Reed, and T. Torigoe. 1992. Anergic Th1 cells express altered levels of the protein tyrosine kinases p56lck and p59fyn. *J Immunol* 149:2887.
43. Sundstedt, A., M. Sigvardsson, T. Leanderson, G. Hedlund, T. Kalland, and M. Dohlsten. 1996. In vivo anergized CD4⁺ T cells express perturbed AP-1 and NF- κ B transcription factors. *Proc Natl Acad Sci U S A* 93:979.

44. Mondino, A., C.D. Whaley, D.R. DeSilva, W. Li, M.K. Jenkins, and D.L. Mueller. 1996. Defective transcription of the IL-2 gene is associated with impaired expression of c-Fos, FosB, and JunB in anergic T helper 1 cells. *J Immunol* 157:2048.
45. Jenkins, M.K., D.M. Pardoll, J. Mizuguchi, T.M. Chused, and R.H. Schwartz. 1987. Molecular events in the induction of a nonresponsive state in interleukin 2-producing helper T-lymphocyte clones. *Proc Natl Acad Sci U S A* 84:5409.
46. Madrenas, J., R.H. Schwartz, and R.N. Germain. 1996. Interleukin 2 production, not the pattern of early T-cell antigen receptor-dependent tyrosine phosphorylation, controls anergy induction by both agonists and partial agonists. *Proc Natl Acad Sci U S A* 93:9736.
47. Boussiotis, V.A., G.J. Freeman, P.A. Taylor, A. Berezovskaya, I. Grass, B.R. Blazar, and L.M. Nadler. 2000. p27kip1 functions as an anergy factor inhibiting interleukin 2 transcription and clonal expansion of alloreactive human and mouse helper T lymphocytes. *Nat Med* 6:290.
48. Appleman, L.J., D. Tzachanis, T. Grader-Beck, A.A. van Puijenbroek, and V.A. Boussiotis. 2001. Helper T cell anergy: from biochemistry to cancer pathophysiology and therapeutics. *J Mol Med* 78:673.
49. Grakoui, A., S.K. Bromley, C. Sumen, M.M. Davis, A.S. Shaw, P.M. Allen, and M.L. Dustin. 1999. The immunological synapse: a molecular machine controlling T cell activation. *Science* 285:221.
50. Monks, C.R., B.A. Freiberg, H. Kupfer, N. Sciaky, and A. Kupfer. 1998. Three-dimensional segregation of supramolecular activation clusters in T cells. *Nature* 395:82.

51. Krummel, M.F., and J.P. Allison. 1995. CD28 and CTLA-4 have opposing effects on the response of T cells to stimulation [see comments]. *J Exp Med* 182:459.
52. Galvin, F., G.J. Freeman, Z. Razi-Wolf, W. Hall, B. Benacerraf, L. Nadler, and H. Reiser. 1992. Murine B7 antigen provides a sufficient costimulatory signal for antigen-specific and MHC-restricted T cell activation. *J Immunol* 149:3802.
53. Linsley, P.S., W. Brady, L. Groamair, A. Aruffo, N.K. Damle, and J.A. Ledbetter. 1991. Binding of the B cell activation antigen B7 to CD28 costimulates T cell proliferation and interleukin 2 mRNA accumulation. *J Exp Med* 173:721 .
54. Deeths, M.J., and M.F. Mescher. 1999. ICAM-1 and B7-1 provide similar but distinct costimulation for CD8⁺ T cells, while CD4⁺ T cells are poorly costimulated by ICAM-1. *Eur J Immunol*, 45.
55. Razi-Wolf, Z., G.J. Freeman, F. Galvin, B. Benacerraf, L. Nadler, and H. Reiser. 1992. Expression and function of the murine B7 antigen, the major costimulatory molecule expressed by peritoneal exudate cells. *Proc Natl Acad Sci U S A* 89:4210.
56. Lane, P., W. Gerhard, S. Hubele, A. Lanzavecchia, and F. McConnell. 1993. Expression and functional properties of mouse B7/BB1 using a fusion protein between mouse CTLA4 and human gamma 1. *Immunology* 80:56.
57. McKnight, A.J., V.L. Perez, C.M. Shea, G.S. Gray, and A.K. Abbas. 1994. Costimulator dependence of lymphokine secretion by naive and activated CD4⁺ T lymphocytes from TCR transgenic mice. *J Immunol* 152:5220.
58. Dubey, C., M. Croft, and S.L. Swain. 1995. Costimulatory requirements of naive CD4⁺ T cells. ICAM-1 or B7-1 can costimulate naive CD4 T cell activation but both are required for optimum response. *Journal of Immunology* 155:45.

59. Girvin, A.M., M.C. Dal Canto, L. Rhee, B. Salomon, A. Sharpe, J.A. Bluestone, and S.D. Miller. 2000. A critical role for B7/CD28 costimulation in experimental autoimmune encephalomyelitis: a comparative study using costimulatory molecule- deficient mice and monoclonal antibody blockade. *J Immunol* 164:136.
60. Karandikar, N.J., C.L. Vanderlugt, T. Eagar, L. Tan, J.A. Bluestone, and S.D. Miller. 1998. Tissue-specific up-regulation of B7-1 expression and function during the course of murine relapsing experimental autoimmune encephalomyelitis. *J Immunol* 161:192.
61. Shao, H., M.D. Woon, S. Nakamura, J.H. Sohn, P.A. Morton, N.S. Bora, and H.J. Kaplan. 2001. Requirement of B7-mediated costimulation in the induction of experimental autoimmune anterior uveitis. *Invest Ophthalmol Vis Sci* 42:2016.
62. Lenschow, D.J., S.C. Ho, H. Sattar, L. Rhee, G. Gray, N. Nabavi, K.C. Herold, and J.A. Bluestone. 1995. Differential effects of anti-B7-1 and anti-B7-2 monoclonal antibody treatment on the development of diabetes in the nonobese diabetic mouse. *J Exp Med* 181:1145.
63. Verwilghen, J., R. Lovis, M. De Boer, P.S. Linsley, G.K. Haines, A.E. Koch, and R.M. Pope. 1994. Expression of functional B7 and CTLA4 on rheumatoid synovial T cells. *J Immunol* 153:1378.
64. Tuosto, L., and O. Acuto. 1998. CD28 affects the earliest signaling events generated by TCR engagement. *Eur J Immunol* 28.
65. Kane, L.P., P.G. Andres, K.C. Howland, A.K. Abbas, and A. Weiss. 2001. Akt provides the CD28 costimulatory signal for the up-regulation of IL-2 and IFN- γ but not for T_H2 cytokines. *Nat Immunol* 2:37.

66. Tsuchida, M., E.R. Manthei, S.J. Knechtle, and M.M. hamawy. 1999. CD28 ligation induces rapid tyrosine phosphorylation of the linker molecule LAT in the absence of Syk and ZAP-70 tyrosine phosphorylation. *Eur J Immunol* 29:2354.
67. Gibson, S., K. Triuitt, Y. Lu, R. lapushin, H. Khan, J.B. Imboden, and G.B. Mills. 1998. Efficient CD28 signaling leads to increases in the kinase activities of the TEC family tyrosine kinase EMT/ITK/TSK and the Src family tyrosine kinase Lck. *Biochem J* 330:1123.
68. Okkenhaug, K., L. Wu, K.M. Garza, J. La Rose, W. Khoo, B. Odermatt, T.W. Mak, P.S. Ohashi, and R. Rottapel. 2001. A point mutation in CD28 distinguishes proliferative signals from survival signals. *Nat Immunol* 2:325.
69. Krummel, M.F., M.D. Sjaastad, C. Wulfig, and M.M. Davis. 2000. Differential clustering of CD4 and CD3 ζ during T cell recognition. *Science* 289:1349.
70. Verweij, C.L., M. Geerts, and L.A. Aarden. 1991. Activation of interleukin-2 gene transcription via the T-cell surface molecule CD28 is mediated through an NF- κ B-like response element. *J Biol Chem* 266:14179.
71. Lai, J.H., G. Horvath, Y. Li, and T.H. Tan. 1995. Mechanisms of enhanced nuclear translocation of the transcription factors c-Rel and NF-kappa B by CD28 costimulation in human T lymphocytes. *Ann N Y Acad Sci* 766:220.
72. Jung, S., A. Yaron, I. Alkalay, A. Hatzubai, A. Avraham, and Y. Ben-Neriah. 1995. Costimulation requirement for AP-1 and NF-kappa B transcription factor activation in T cells. *Ann N Y Acad Sci* 766:245.
73. Coudronniere, N., M. Villalba, N. Englund, and A. Altman. 2000. NF- κ B activation by T cell receptor/CD28 costimulation is mediated by protein kinase C - θ . *Proc Natl Acad Sci U S A* 97:3394.

74. Wülfing, C., and M.M. Davis. 1998. A receptor/cytoskeletal movement triggered by costimulation during T cell activation. *Science* 282:2266.
75. Krawczyk, C., and J.M. Penninger. 2001. Molecular controls of antigen receptor clustering and autoimmunity. *Trends Cell Biol* 11:212.
76. Han, J., B. Das, W. Wie, L. Van Aelst, R.D. Mosteller, R. Khosravi-Far, J.K. Westwick, C.J. Der, and D. Broek. 1997. Lck regulates Vav activation of members of the Rho family of GTPases. *Mol Cell Biol* 17:1346.
77. Krawczyk, C., and J.M. Penninger. 2001. Molecular motors involved in T cell receptor clusterings. *J Leukoc Biol* 69:317.
78. Penninger, J.M., and G.R. Crabtree. 1999. The actin cytoskeleton and lymphocyte activation. *Cell* 96:9.
79. Olson, M.F., N.G. Pasteris, J.L. Gorski, and A. Hall. 1996. Faciogenital dysplasia protein (FGD1) and Vav, two related proteins required for normal embryonic development, are upstream regulators of Rho GTPases. *Curr Biol* 6:1628.
80. Rohatgi, R., L. Ma, H. Miki, L. M., T. Kirchhausen, T. Takenawa, and M. Kirschner. 1999. The interaction between N-WASP and the Arp 2/3 complex links Cdc42-dependent signals to actin assembly. *Cell* 97:1.
81. Yarar, D., W. To, A. Abo, and M.D. Welch. 1999. The Wiskott-Aldrich syndrome protein directs actin-based motility by stimulating actin nucleation with the Arp 2/3 complex. *Curr Biol* 9:555.
82. Costello, P.S., A.E. Walters, P.J. Mee, M. Turner, L.F. Reynolds, A. Prisco, N. Sarner, R. Zamoyska, and V.L.J. Tybulewicz. 1999. The Rho-family GTPase

exchange factor Vav is a critical transducer of T cell receptor signals to the calcium, ERK, and NF- κ B pathways. *Proc Natl Acad Sci U S A* 96:3035.

83. Fischer, K.D., Y.Y. Kong, H. Nishina, K. Tedford, L.E. Marengere, I. Kozieradzki, T. Sasaki, M. Starr, G. Chan, S. Gardener, M.P. Nghiem, D. Bouchard, M. Barbacid, A. Bernstein, and J.M. Penninger. 1998. Vav is a regulator of cytoskeletal reorganization mediated by the T- cell receptor. *Curr Biol* 8:554.

84. Holsinger, L.J., I.A. Graef, W. Swat, T. Chi, D.M. Bautista, L. Davidson, R.S. Lewis, F.W. Alt, and G.R. Crabtree. 1998. Defects in actin-cap formation in Vav-deficient mice implicate an actin requirement for lymphocyte signal transduction. *Curr Biol* 8:563.

85. Bunnell, S.C., V. Kapoor, R.P. Tribble, W. Zhang, and L.E. Samelson. 2001. Dynamic actin polymerization drives T cell receptor-induced spreading: a role for the signal transduction adaptor LAT. *Immunity* 14:315.

86. Valitutti, S., M. Dessing, K. Aktories, H. Gallati, and A. Lanzavecchia. 1995. Sustained signaling leading to T cell activation results from prolonged T cell receptor occupancy. Role of T cell actin cytoskeleton. *Journal of Experimental Medicine* 181:577.

87. Woodside, D.G., D.K. Wooten, and B.W. McIntyre. 1998. Adenosine diphosphate (ADP)-ribosylation of the guanosine triphosphatase (GTPase) rho in resting peripheral blood human T lymphocytes results in pseudopodial extension and the inhibition of T cell activation. *J Exp Med* 188:1211.

88. Gaglia, J.L., E.A. Greenfield, A. Mattoo, A.H. Sharpe, G.J. Freeman, and V.K. Kuchroo. 2000. Intercellular adhesion molecule 1 is critical for activation of CD28- deficient T cells. *J Immunol* 165:6091.

89. van de Stolpe, A., and P.T. van der Saag. 1996. Intercellular adhesion molecule-1. *Journal of Molecular Medicine* 74:13.

90. Chen, T., J.S. Goldstein, K. O'Boyle, M.C. Whitman, M. Brunswick, and S. Kozlowski. 1999. ICAM-1 co-stimulation has differential effects on the activation of CD4⁺ and CD8⁺ T cells. *Eur J Immunol* 29:809.
91. Kuhlman, P., V.T. Moy, B.A. Lollo, and A.A. Brian. 1991. The accessory function of murine intercellular adhesion molecule-1 in T lymphocyte activation. Contributions of adhesion and co-activation. *J Immunol* 146:1773.
92. Van Seventer, G.A., Y. Shimizu, K.J. Horgan, and S. Shaw. 1990. The LFA-1 ligand ICAM-1 provides an important costimulatory signal for T cell receptor-mediated activation of resting T cells. *Journal of Immunology* 144:4579.
93. Van Seventer, G.A., E. Bonvini, H. Yamada, A. Conti, S. Stringfellow, C.H. June, and S. Shaw. 1992. Costimulation of T cell receptor/CD3-mediated activation of resting human CD4⁺ T cells by leukocyte function-associated antigen-1 ligand intercellular cell adhesion molecule-1 involves prolonged inositol phospholipid hydrolysis and sustained increase of intracellular Ca²⁺ levels. *Journal of Immunology* 149:3872.
94. Wülfing, C., M.D. Sjaastad, and M.M. Davis. 1998. Visualizing the dynamics of T cell activation: intracellular adhesion molecule 1 migrates rapidly to the T cell/B cell interface and acts to sustain calcium levels. *Proc Natl Acad Sci U S A* 95:6302.
95. Geginat, J., B. Clissi, M. Moro, P. Dellabona, J.R. Bender, and R. Pardi. 2000. CD28 and LFA-1 contribute to cyclosporin A-resistant T cell growth by stabilizing the IL-2 mRNA through distinct signaling pathways. *Eur J Immunol* 30:1136.
96. Dubey, C., M. Croft, and S.L. Swain. 1996. Naive and effector CD4 T cells differ in their requirements for T cell receptor versus costimulatory signals. *J Immunol* 157:3280.

97. Kearney, E.R., T.L. Walunas, R.W. Karr, P.A. Morton, D.Y. Loh, J.A. Bluestone, and M.K. Jenkins. 1995. Antigen-dependent clonal expansion of a trace population of antigen-specific CD4⁺ T cells in vivo is dependent on CD28 costimulation and inhibited by CTLA-4. *J Immunol* 155:1032.
98. Cai, Z., H. Kishimoto, A. Brunmark, M.R. Jackson, P.A. Peterson, and J. Sprent. 1997. Requirements for peptide-induced T cell receptor downregulation on naive CD8⁺ T cells. *Journal of Experimental Medicine* 185:641.
99. London, C.A., M.P. Lodge, and A.K. Abbas. 2000. Functional responses and costimulator dependence of memory CD4⁺ T cells. *J Immunol* 164:265.
100. Marelli-Berg, F.M., O. Barroso-Herrera, and R.I. Lechler. 1999. Recently activated T cells are costimulation-dependent in vitro. *Cell Immunol* 195:18.
101. Wei, X., B.J. Tromberg, and M.D. Cahalan. 1999. Mapping the sensitivity of T cells with an optical trap: polarity and minimal number of receptors for Ca(2+) signaling. *Proc Natl Acad Sci U S A* 96:8471.
102. Negulescu, P.A., T.B. Krasieva, A. Khan, H.H. Kerschbaum, and M.D. Cahalan. 1996. Polarity of T cell shape, motility, and sensitivity to antigen. *Immunity* 4:421.
103. Dustin, M.L., S.K. Bromley, Z. Kan, D.A. Peterson, and E.R. Unanue. 1997. Antigen receptor engagement delivers a stop signal to migrating T lymphocytes. *Proc Natl Acad Sci U S A* 94:3909.
104. Dustin, M.L., J.M. Miller, S. Ranganath, D.A. Vignali, N.J. Viner, C.A. Nelson, and E.R. Unanue. 1996. TCR-mediated adhesion of T cell hybridomas to planar bilayers containing purified MHC class II/peptide complexes and receptor shedding during detachment. *J Immunol* 157:2014.

105. Pardigon, N., C. Cambouris, N. Bercovici, F. Lemaitre, R. Liblau, and P. Kourilsky. 2000. Delayed and separate costimulation In vitro supports the evidence of a transient "Excited" state of CD8+ T cells during activation [In Process Citation]. *J Immunol* 164:4493.
106. Donnadieu, E., G. Bismuth, and A. Trautmann. 1994. Antigen recognition by helper T cells elicits a sequence of distinct changes of their shape and intracellular calcium. *Curr Biol* 4:584.
107. Donnadieu, E., D. Cefai, Y.P. Tan, G. Paresys, G. Bismuth, and A. Trautmann. 1992. Imaging early steps of human T cell activation by antigen-presenting cells. *J Immunol* 148:2643.
108. Delon, J., N. Bercovici, R. Liblau, and A. Trautmann. 1998. Imaging antigen recognition by naive CD4⁺ T cells: compulsory cytoskeletal alterations for the triggering of an intracellular calcium response. *Eur J Immunol* 28:716.
109. Kupfer, A., S.J. Singer, C.A. Janeway, and S.L. Swain. 1987. Coclustering of CD4 (L3T4) molecule with the T-cell receptor is induced by specific direct interaction of helper T cells and antigen-presenting cells. *Proc Natl Acad Sci U S A* 84:5888.
110. Monks, C.R.F., H. Kupfer, A. Tamir, A. Barlow, and A. Kupfer. 1997. Selective modulation of protein kinase C- θ during T cell activation. *Nature* 385:83.
111. Kupfer, A., S.L. Swain, and S.J. Singer. 1987. The specific direct interaction of helper T cells and antigen-presenting B cells. II. Reorientation of the microtubule organizing center and reorganization of the membrane-associated cytoskeleton inside the bound helper T cells. *J Exp Med* 165:1565.
112. van der Merwe, P.A., S.J. Davis, A.S. Shaw, and M.L. Dustin. 2000. Cytoskeletal polarization and redistribution of cell-surface molecules during T cell antigen recognition. *Semin Immunol* 12:5.

113. Freiberg, B. 2000. Spatial-temporal visualization of molecular events during T cell/antigen presenting cell interactions, University of Colorado Health Sciences Center.
114. Kupfer, H., C.R.F. Monks, and A. Kupfer. 1994. Small splenic B cells that bind to antigen-specific T helper (Th) cells and face the site of cytokine production in the Th cells selectively proliferate: immunofluorescence microscopic studies of Th-B antigen-presenting cell interactions. *J Exp Med* 179:1507.
115. Kupfer, A., and S.J. Singer. 1989. Cell biology of cytotoxic and helper T cell functions: immunofluorescence microscopic studies of single cells and cell couples. *Annu Rev Immunol* 7:309.
116. Stinchcombe, J.C., G. Bossi, S. Booth, and G.M. Griffiths. 2001. The Immunological Synapse of CTL Contains a Secretory Domain and Membrane Bridges. *Immunity* 15:751.
117. Paul, W.E., and R.A. Seder. 1994. Lymphocyte responses and cytokines. *Cell* 76:241.
118. Bromley, S.K., W.R. Burack, K.G. Johnson, K. Somersalo, T.N. Sims, C. Sumen, M.M. Davis, A.S. Shaw, P.M. Allen, and M.L. Dustin. 2001. The immunological synapse. *Annu Rev Immunol* 19:375.
119. Dustin, M.L., and J.A. Cooper. 2000. The immunological synapse and the actin cytoskeleton: molecular hardware for T cell signaling. *Nat Immunol* 1:23.
120. Iezzi, G., K. Karjalainen, and A. Lanzavecchia. 1998. The duration of antigenic stimulation determines the fate of naive and effector T cells. *Immunity* 8:89.

121. Bromley, S.K., A. Iaboni, S.J. Davis, A. Whitty, J.M. Green, A.S. Shaw, A. Weiss, and M.L. Dustin. 2001. The immunological synapse and CD28-CD80 interactions. *Nat Immunol* 2:1159.
122. Delon, J., K. Kaibuchi, and R.N. Germain. 2001. Exclusion of CD43 from the Immunological Synapse Is Mediated by Phosphorylation-Regulated Relocation of the Cytoskeletal Adaptor Moesin. *Immunity* 15:691.
123. Revy, P., M. Sospedra, B. Barbour, and A. Trautmann. 2001. Functional antigen-independent synapses formed between T cells and dendritic cells. *Nat Immunol* 2:925.
124. Harder, T., P. Scheiffele, P. Verkade, and K. Simons. 1998. Lipid domain structure of the plasma membrane revealed by patching of membrane components. *J Cell Biol* 141:929.
125. Viola, A. 2001. The amplification of TCR signaling by dynamic membrane microdomains. *Trends Immunol* 22:322.
126. Moran, M., and M.C. Miceli. 1998. Engagement of GPI-linked CD48 contributes to TCR signals and cytoskeletal reorganization: a role for lipid rafts in T cell activation. *Immunity* 9:787.
127. Bi, K., and A. Altman. 2001. Membrane lipid micodomains and the role of PKC θ in T cell activation. *Semininars in Immunology* 13.
128. Bi, K., Y. Tanaka, N. Coudronniere, K. Sugie, S. Hong, M.J. van Stipdonk, and A. Altman. 2001. Antigen-induced translocation of PKC-theta to membrane rafts is required for T cell activation. *Nat Immunol* 2:556.
129. Cherukuri, A., M. Dykstra, and S.K. Pierce. 2001. Floating the raft hypothesis: lipid rafts play a role in immune cell activation. *Immunity* 14:657.

130. Viola, A., S. Schroeder, Y. Sakakibara, and A. Lanzavecchia. 1999. T lymphocyte costimulation mediated by reorganization of membrane microdomains. *Science* 283:680.
131. Wülfing, C., A. Bauch, G.R. Crabtree, and M.M. Davis. 2000. The vav exchange factor is an essential regulator in actin-dependent receptor translocation to the lymphocyte-antigen-presenting cell interface. *Proc Natl Acad Sci U S A* 97:10150.
132. Wülfing, C., C. Sumen, M.D. Sjaastad, L.C. Wu, M.L. Dustin, and M.M. Davis. 2002. Costimulation and endogenous MHC ligands contribute to T cell recognition. *Nat Immunol* Published Online.
133. Reichert, P., R.L. Reinhardt, E. Ingulli, and M.K. Jenkins. 2001. Cutting Edge: In Vivo Identification of TCR Redistribution and Polarized IL-2 Production by Naive CD4 T Cells. *J Immunol* 166:4278.
134. Adler, B., S. Ashkar, H. Cantor, and G.F. Weber. 2001. Costimulation by extracellular matrix proteins determines the response to TCR ligation. *Cell Immunol* 210:30.
135. Kaye, J., N.J. Vasquez, and S.M. Hedrick. 1992. Involvement of the same region of the T cell antigen receptor in thymic selection and foreign peptide recognition. *Journal of Immunology* 148:3342.
136. Kersh, G.J., D.L. Donermeyer, K.E. Frederick, J.M. White, B.L. Hsu, and P.M. Allen. 1998. TCR transgenic mice in which usage of transgenic alpha- and beta-chains is highly dependent on the level of selecting ligand. *J Immunol* 161:585.
137. Liu, C.P., D. Parker, J. Kappler, and P. Marrack. 1997. Selection of antigen-specific T cells by a single IE^k peptide combination. *J Exp Med* 186:1441.

138. Gunning, P., J. Leavitt, G. Muscat, S.Y. Ng, and L. Kedes. 1987. A human beta-actin expression vector system directs high-level accumulation of antisense transcripts. *Proc Natl Acad Sci U S A* 84:4831.
139. Miller, J., and R.N. Germain. 1986. Efficient cell surface expression of class II MHC molecules in the absence of associated invariant chain. *J Exp Med* 164:1478.
140. Dudley, D.T., L. Pang, S.J. Decker, A.J. Bridges, and A.R. Saltiel. 1995. A synthetic inhibitor of the mitogen-activated protein kinase cascade. *Proc Natl Acad Sci U S A* 92:7686.
141. Hanke, J.H., J.P. Gardner, R.L. Dow, P.S. Changelian, W.H. Brissette, E.J. Weringer, B.A. Pollok, and P.A. Connelly. 1996. Discovery of a novel, potent, and Src family-selective tyrosine kinase inhibitor. Study of Lck- and Fyn T-dependent T cell activation. *J Biol Chem* 271:695.
142. Hiraoka, Y., J.W. Sedat, and D.A. Agard. 1990. Determination of three-dimensional imaging properties of a light microscope system. Partial confocal behavior in epifluorescence microscopy. *Biophys J* 57:325.
143. Wallace, W., L.H. Schaefer, and J.R. Swedlow. 2001. A workingperson's guide to deconvolution in light microscopy. *Biotechniques* 31:1076.
144. Kupfer, A., and S.J. Singer. 1988. Molecular dynamics in the membranes of helper T cells. *Proc Natl Acad Sci U S A* 85:8216.
145. Underhill, D.M., M. Bassetti, A. Rudensky, and A. Aderem. 1999. Dynamic interactions of macrophages with T cells during antigen presentation. *J Exp Med* 190:1909.
146. Gunzer, M., A. Schafer, S. Borgmann, S. Grabbe, K.S. Zanker, E.B. Brocker, E. Kampgen, and P. Friedl. 2000. Antigen presentation in extracellular matrix:

interactions of T cells with dendritic cells are dynamic, short lived, and sequential. *Immunity* 13:323.

147. Lorber, M.I., M.R. Loken, A.M. Stall, and F.W. Fitch. 1982. I-A antigens on cloned alloreactive murine T lymphocytes are acquired passively. *J Immunol* 128:2798.

148. Huang, J.F., Y. Yang, H. Sepulveda, W. Shi, I. Hwang, P.A. Peterson, M.R. Jackson, J. Sprent, and Z. Cai. 1999. TCR-Mediated internalization of peptide-MHC complexes acquired by T cells. *Science* 286:952.

149. Patel, D.M., P.Y. Arnold, G.A. White, J.P. Nardella, and M.D. Mannie. 1999. Class II MHC/peptide complexes are released from APC and are acquired by T cell responders during specific antigen recognition. *J Immunol* 163:5201.

150. Hwang, I., J.F. Huang, H. Kishimoto, A. Brunmark, P.A. Peterson, M.R. Jackson, C.D. Surh, Z. Cai, and J. Sprent. 2000. T cells can use either T cell receptor or CD28 receptors to absorb and internalize cell surface molecules derived from antigen-presenting cells. *J Exp Med* 191:1137.

151. Sabzevari, H., J. Kantor, A. Jaigirdar, Y. Tagaya, M. Naramura, J. Hodge, J. Bernon, and J. Schlom. 2001. Acquisition of CD80 (B7-1) by T cells. *J Immunol* 166:2505.

152. Schwartz, R.H. 1997. T cell clonal anergy. *Curr Opin Immunol* 9:351.

153. Schwartz, R.H. 1993. T cell anergy. *Sci Am* 269:62.

154. Kundig, T.M., A. Shahinian, K. Kawai, H.W. Mittrucker, E. Sebzda, M.F. Bachmann, T.W. Mak, and P.S. Ohashi. 1996. Duration of TCR stimulation determines costimulatory requirement of T cells. *Immunity* 5:41.

155. Kenworthy, A.K., N. Petranova, and M. Edidin. 2000. High-resolution FRET microscopy of cholera toxin B-subunit and GPI-anchored proteins in call plasma cell membranes. *Mol Cell Biol* 11:1645.
156. Krawczyk, C., K. Bachmaier, T. Sasaki, G.R. Jones, B.S. Snapper, D. Bouchard, I. Kozieradzki, S.P. Ohashi, W.F. Alt, and M.J. Penninger. 2000. Cbl-b is a negative regulator of receptor clustering and raft aggregation in T cells. *Immunity* 13:463.
157. Boussiotis, V.A., G.J. Freeman, A. Berezovskaya, D.L. Barber, and L.M. Nadler. 1997. Maintenance of human T cell anergy: blocking of IL-2 gene transcription by activated Rap1. *Science* 278:124.
158. Carey, K.D., T.J. Dillon, J.M. Schmitt, A.M. Baird, A.D. Holdorf, D.B. Straus, A.S. Shaw, and P.J. Stork. 2000. CD28 and the tyrosine kinase Ick stimulate mitogen-activated protein kinase activity in T cells via inhibition of the small G protein Rap1. *Mol Cell Biol* 20:8409.
159. Mochizuki, N., S. Yamashita, K. Kurokawa, Y. Ohba, T. Nagai, A. Miyawaki, and M. Matsuda. 2001. Spatio-temporal images of growth-factor-induced activation of Ras and Rap1. *Nature* 411:1065.
160. McClosky, M.A., and M.M. Poo. 1986. Contact-induced redistribution of specific membrane components: local accumulation and development of adhesion. *J Cell Biol* 102:2185.
161. Davis, D.M., I. Chiu, M. Fassett, G.B. Cohen, O. Mandelboim, and J.L. Strominger. 1999. The human natural killer cell immune synapse. *Proc Natl Acad Sci U S A* 96:15062.
162. Batista, F.D., D. Iber, and M.S. Neuberger. 2001. B cells acquire antigen from target cells after synapse formation. *Nature* 411:489 .

163. Wilson, N.A., P. Wolf, H. Ploegh, L. Ignatowicz, J. Kappler, and P. Marrack. 1998. Invariant chain can bind MHC class II at a site other than the peptide binding groove. *J Immunol* 161:4777.
164. Gunzer, M., P. Friedl, B. Niggemann, E.B. Brocker, E. Kampgen, and K.S. Zanker. 2000. Migration of dendritic cells within 3-D collagen lattices is dependent on tissue origin, state of maturation, and matrix structure and is maintained by proinflammatory cytokines. *J Leukoc Biol* 67:622.
165. Sharrow, S.O., B.J. Mathieson, and A. Singer. 1981. Cell surface appearance of unexpected host MHC determinants on thymocytes from radiation bone marrow chimeras. *J Immunol* 126:1327.
166. Nepom, J.T., B. Benacerraf, and R.N. Germain. 1981. Acquisition of syngeneic I-A determinants by T cells proliferating in response to poly (Gly⁶⁰Ala³⁰, Tyr¹⁰). *J Immunol* 127:888.
167. Hudrisier, D., J. Riond, H. Mazarguil, J.E. Gairin, and E. Joly. 2001. Cutting edge: CTLs rapidly capture membrane fragments from target cells in a TCR signaling-dependent manner. *J Immunol* 166:3645.
168. Hwang, I., and J. Sprent. 2001. Role of actin cytoskeleton in T cell absorption and internalization of ligands from APC. *J Immunol* 166:5099.
169. Merckenschlager, M. 1996. Tracing interactions of thymocytes with individual stromal cell partners. *Eur J Immunol* 26:892.
170. Carlin, L.M., K. Eleme, F.E. McCann, and D.M. Davis. 2001. Intercellular transfer and supramolecular organization of human leukocyte antigen C at inhibitory natural killer cell immune synapses. *J Exp Med* 194:1507.
171. Sjöström, A., M. Eriksson, C. Cerboni, M.H. Johansson, C.L. Sentman, K. Karre, and P. Hoglund. 2001. Acquisition of external major histocompatibility

- complex class I molecules by natural killer cells expressing inhibitory Ly49 receptors. *J Exp Med* 194:1519.
172. Zimmer, J., V. Ioannidis, and W. Held. 2001. H-2D Ligand Expression by Ly49A⁺ Natural Killer (NK) Cells Precludes Ligand Uptake from Environmental Cells: Implications for NK Cell Function. *J Exp Med* 194:1531.
173. Mannie, M.D., J.M. Rosser, and G.A. White. 1995. Autologous rat myelin basic protein is a partial agonist that is converted into a full antagonist upon blockade of CD4. Evidence for the integration of efficacious and nonefficacious signals during T cell antigen recognition. *J Immunol* 154:2642.
174. Mannie, M.D., J.P. Nardella, G.A. White, P.Y. Arnold, and D.K. Davidian. 1998. Class II MHC/peptide complexes on T cell antigen-presenting cells: agonistic antigen recognition inhibits subsequent antigen presentation. *Cell Immunol* 186:111.
175. Mannie, M.D., G.A. White, J.P. Nardella, D.K. Davidian, and P.Y. Arnold. 1998. Partial agonism elicits an enduring phase of T-cell-mediated antigen presentation. *Cell Immunol* 186:83.
176. Mannie, M.D., S.K. Rendall, P.Y. Arnold, J.P. Nardella, and G.A. White. 1996. Anergy-associated T cell antigen presentation. A mechanism of infectious tolerance in experimental autoimmune encephalomyelitis. *J Immunol* 157:1062.
177. Potter, T.A., K. Grebe, B. Freiberg, and A. Kupfer. 2001. Formation of supramolecular activation clusters on fresh ex vivo CD8⁺ T cells after engagement of the T cell antigen receptor and CD8 by antigen-presenting cells. *Proc Natl Acad Sci U S A* 98:12624.
178. Zagury, D., J. Bernard, P. Jeannesson, N. Thiernesse, and J.C. Cerottini. 1979. Studies on the mechanism of T cell-mediated lysis at the single effector cell level. I. Kinetic analysis of lethal hits and target cell lysis in multicellular conjugates. *J Immunol* 123:1604.

179. Rothstein, T.L., M. Mage, G. Jones, and L.L. McHugh. 1978. Cytotoxic T lymphocyte sequential killing of immobilized allogeneic tumor target cells measured by time-lapse microcinematography. *J Immunol* 121:1652.
180. Delon, J., and R.N. Germain. 2000. Information transfer at the immunological synapse. *Current biology* 10:R923.
181. Lanzavecchia, A., and F. Sallusto. 2000. From synapses to immunological memory: the role of sustained T cell stimulation. *Curr Opin Immunol* 12:92.
182. Acuto, O., and D. Cantrell. 2000. T cell activation and the cytoskeleton. *Annu Rev Immunol* 18:165.
183. Lowin-Kropf, B., V.S. Shapiro, and A. Weiss. 1998. Cytoskeletal polarization of T cells is regulated by an immunoreceptor tyrosine-based activation motif-dependent mechanism. *J Cell Biol* 140:861.
184. Røtnes, J.S., and B. Bogen. 1994. Ca²⁺ mobilization in physiologically stimulated single T cells gradually increases with peptide concentration (analog signaling). *European Journal of Immunology* 24:851.
185. Weiss, A., T. Kadlecik, M. Iwashima, A. Chan, and N. Van Oers. 1995. Molecular and genetic insights into T-cell antigen receptor signaling. *Ann N Y Acad Sci* 766:149.
186. Qian, D., and A. Weiss. 1997. T cell antigen receptor signal transduction. *Curr Opin Cell Biol* 9:205.
187. Germain, R.N. 2001. The T Cell Receptor for Antigen: Signaling and Ligand Discrimination. *J Biol Chem* 276:35223.
188. Weber, K.S.C., G. Osterman, A. Zerneck, A. Schröder, L.B. Klickstein, and C. Weber. 2001. Dual Role of H-Ras in Regulation of Lymphocyte Function

Antigen-1 Activity by Stromal Cell-derived Factor 1 α : Implications for Leukocyte Transmigration. *Molecular Biology of the Cell* 12.

189. Yoon, S.T., U. Dianzani, K. Bottomly, and C.A. Janeway, Jr. 1994. Both high and low avidity antibodies to the T cell receptor can have agonist or antagonist activity. *Immunity* 1:563.
190. Itoh, Y., B. Hemmer, R. Martin, and R.N. Germain. 1999. Serial TCR engagement and down-modulation by peptide:MHC molecule ligands: relationship to the quality of individual TCR signaling events. *J Immunol* 162:2073.
191. Bachmann, M.F., M. Salzman, A. Oxenius, and P.S. Ohashi. 1998. Formation of TCR dimers/trimers as a crucial step for T cell activation. *Eur J Immunol* 28:2571.
192. Salzman, M., and M.F. Bachmann. 1998. The role of T cell receptor dimidiation for T cell antagonism and T cell specificity. *Mol Immunol* 35:271.
193. Reich, Z., J.J. Boniface, D.S. Lyons, N. Brooch, E.J. Wattle, and M.M. Davis. 1997. Ligand-specific oligomerization of T-cell receptor molecules. *Nature* 387:617.
194. Boniface, J.J., J.D. Rabinowitz, C. Wulfig, J. Hampl, Z. Reich, J.D. Altman, R.M. Kantor, C. Beeson, H.M. McConnell, and M.M. Davis. 1998. Initiation of signal transduction through the T cell receptor requires the multivalent engagement of peptide/MHC ligands. *Immunity* 9:459.
195. Takeda, S., H.R. Ropewalk, H. Arakawa, H. Bluethmann, and T. Shimizu. 1996. MHC class II molecules are not required for survival of newly generated CD4⁺ T cells, but affect their long-term life span. *Immunity* 5:217.

196. Brocker, T. 1997. Survival of mature CD4 T lymphocytes is dependent upon major histocompatibility complex class II-expressing dendritic cells. *J Exp Med* 186:1223 .
197. Kirberg, J., A. Berns, and H. von Boehmer. 1997. Peripheral T cell survival requires continual ligation of the T cell receptor to major histocompatibility complex-encoded molecules. *J Exp Med* 186:1269 .
198. Beutner, U., and H.R. MacDonald. 1998. TCR-MHC class II interaction is required for peripheral expansion of CD4 cells in a T cell-deficient host. *Int Immunol* 10:305 .
199. Wong, P., G.M. Barton, K.A. Forbush, and A.Y. Rudensky. 2001. Dynamic tuning of T cell reactivity by self-peptide-major histocompatibility complex ligands. *J Exp Med* 193:1179.
200. Clarke, S.R.M., and A.Y. Rudensky. 2000. Survival and homeostatic proliferation of naive peripheral CD4⁺ T cells in the absence of self peptide:MHC complexes. *J Immunol* 165:2458.
201. Periasamy, A. 2001. Fluorescence resonance energy transfer microscopy: a mini review. *J Biomed Opt* 6:287.
202. Kenworthy, A.K. 2001. Imaging protein-protein interactions using fluorescence resonance energy transfer microscopy. *Methods* 24:289.
203. Abraham, C., J. Griffith, and J. Miller. 1999. The dependence for leukocyte function-associated antigen-1/ICAM-1 interactions in T cell activation cannot be overcome by expression of high density TCR ligand. *J Immunol* 162:4399.
204. Bachmann, M.F., K. McKall-Faienza, R. Schmits, D. Bouchard, J. Beach, D.E. Speiser, T.W. Mak, and P.S. Ohashi. 1997. Distinct roles for LFA-1 and CD28 during activation of naive T cells: adhesion versus costimulation. *Immunity* 7:549.

205. Salio, M., S. Valitutti, and A. Lanzavecchia. 1997. Agonist-induced T cell receptor down-regulation: molecular requirements and dissociation from T cell activation. *Eur J Immunol* 27:1769.
206. San José, E., A. Borroto, F. Niedergang, A. Alcover, and B. Alarcón. 2000. Triggering the TCR complex causes the downregulation of nonengaged receptors by a signal transduction-dependent mechanism. *Immunity* 12:161.
207. Kishimoto, H., R.T. Kubo, H. Yorifuji, T. Nakayama, Y. Asano, and T. Tada. 1995. Physical dissociation of the TCR-CD3 complex accompanies receptor ligation. *J Exp Med* 182:1997.
208. Gallego, M.D., M. Santamaria, J. Peña, and I.J. Molina. 1997. Defective actin reorganization and polymerization of Wiskott-Aldrich T cells in response to CD3-mediated stimulation. *Blood* 90:3089.
209. Snapper, S.B., F.S. Rosen, E. Mizoguchi, P. Cohen, W. Khan, C.-H. Liy, T.L. Hagemann, S.-P. Kwan, R. Ferrini, and L. Davidson. 1998. Wiskott-Aldrich syndrome protein-deficient mice reveal a role for WASP in T but not B cell activation. *Immunity* 9:81.
210. Prehoda, K.E., J.A. Scott, R. Dyche Mullins, and W.A. Lim. 2000. Integration of multiple signals through cooperative regulation of the N- WASP-Arp2/3 complex. *Science* 290:801.
211. Villalba, M., N. Coudronniere, M. Deckert, E. Teixeira, P. Mas, and A. Altman. 2000. A novel functional interaction between Vav and PKC θ is required for TCR-induced T cell activation. *Immunity* 12:151.
212. Harder, T., and K. Simons. 1997. Caveolae, DIGs, and the dynamics of sphingolipid-cholesterol microdomains. *Curr Opin Cell Biol* 9:534.

213. Harder, T., and K. Simons. 1999. Clusters of glycolipid and glycosylphosphatidylinositol-anchored proteins in lymphoid cells: accumulation of actin regulated by local tyrosine phosphorylation. *Eur J Immunol* 29:556.
214. Horejsí, V., K. Drbal, M. Cebecauer, J. Cerny, T. Brdicka, P. Angelisova, and H. Stockinger. 1999. GPI-microdomains: a role in signalling via immunoreceptors. *Immunol Today* 20:356.
215. Carrie Miceli, M., M. Moran, C.D. Chung, V.P. Patel, T. Low, and W. Zinnanti. 2000. Co-stimulation and counter-stimulation: lipid raft clustering controls TCR signaling and functional outcomes. *Seminars in Immunology* 13:115.
216. Dustin, M.L., and A.S. Shaw. 1999. Costimulation: building an immunological synapse. *Science* 283:649.
217. Mueller, D.L., M.K. Jenkins, and R.H. Schwartz. 1989. Clonal expansion versus functional clonal inactivation: a costimulatory signaling pathway determines the outcome of T cell antigen receptor occupancy. *Ann Rev Immunol* 7:445.
218. Gimmi, C.D., G.J. Freeman, J.G. Gribben, G. Gray, and L.M. Nadler. 1993. Human T cell clonal anergy is induced by antigen presentation in the absence of B7 costimulation. *Proc Natl Acad Sci U S A* 90:6586 .
219. Schwartz, R.H. 1996. Models of T cell anergy: is there a common molecular mechanism? *J Exp Med* 184:1.
220. Kang, S.M., B. Beverly, A.C. Tran, K. Brorson, R.H. Schwartz, and M.J. Lenardo. 1992. Transactivation by AP-1 is a molecular target of T cell clonal anergy. *Science* 257:1134.
221. Jackson, S.K., A. DeLoose, and K.M. Gilbert. 2001. Induction of anergy in Th1 cells associated with increased levels of cyclin-dependent kinase inhibitors P21^{Cip1} and p27^{Kip1}. *J Immunol* 166:952.

222. Eisenbraun, M.D., A. Tamir, and R.A. Miller. 2000. Altered Composition of the Immunological Synapse in an Anergic, Age- Dependent Memory T Cell Subset. *J Immunol* 164:6105.
223. Kirberg, J., H. von Boehmer, T. Brocker, H.R. Rodewald, and S. Takeda. 2001. Class II essential for CD4 survival. *Nat Immunol* 2:136.
224. Al-Alwan, M.M., G. Rowden, T.D. Lee, and K.A. West. 2001. The dendritic cell cytoskeleton is critical for the formation of the immunological synapse. *J Immunol* 166:1452.
225. Kondo, T., I. Cortese, S. Markovic-Plese, K.P. Wandinger, C. Carter, M. Brown, S. Leitman, and R. Martin. 2001. Dendritic cells signal T cells in the absence of exogenous antigen. *Nat Immunol* 2:932.
226. Murphy, M.A., R.G. Schnall, D.J. Venter, L. Barnett, I. Bertocello, C.B. Thein, W.Y. Langdon, and D.D. Bowtell. 1998. Tissue hyperplasia and enhanced T-cell signaling via ZAP-70 in c-Cbl deficient mice. *Mol Cell Biol* 18:4872.
227. Leo, A., and B. Schraven. 2001. Adapters in lymphocyte signaling. *Curr Opin Immunol* 13:307